

Response to reviewers for the paper “Secondary Organic Aerosol (SOA) yields from NO₃ radical + isoprene based on nighttime aircraft power plant plume transects” by J.L. Fry et al.

We thank the reviewers for their careful reading of and thoughtful comments on our paper. To guide the review process we have copied the reviewer comments in black text. Our responses are in regular blue font. We have responded to all the referee comments and made alterations to our paper (**in bold text**).

Overall response to reviews:

Taken together, these three reviews suggest that the referees struggled with many of the same issues that we did as we worked through the data analysis and wrote this paper. With the help of reviewer suggestions, we have attempted to further clarify how we have ruled out some potential confounding effects and how we can constrain the likely impact of others on our results, to ensure a clear discussion of the strengths and limitations of this yield analysis. We do remain convinced that despite the limits of this small dataset, its unique strength as a direct measurement of NO₃ + isoprene SOA yields under conditions of atmospherically relevant peroxy radical lifetime merits publication and will make a useful contribution to our field. We hope that with these responses the reviewers and editor will support our reporting these results as SOA yields, with clear discussion of the attendant uncertainties. We do understand the reviewers' concerns about the small number of measurements and large uncertainties in these yields, so we have proposed edits to the figures and discussion to emphasize this further. While the number of data are limited and the uncertainties substantial, it is the case that chamber-derived yields may also have large uncertainties due to instrument uncertainties, unaccounted for gas losses to Teflon chamber walls, RO₂ fate relevance, etc. -- and there are also quite limited chamber data available on this reaction. Thus, we feel that this paper adds a valuable contribution to the literature. We believe that as revised, this manuscript will not prematurely induce modelers to substitute uncertain yields into their models, but instead this report of higher yield values than those previously observed will pique other researchers' interest, and thus spur valuable follow-up studies.

Anonymous Referee #1

The manuscript is original and very interesting to read. The authors tried to get the optimum out of the data, but still addressed openly the limitations of their approach.

From the viewpoint of raising interesting questions regarding the role of isoprene chemistry and isoprene NO₃ chemistry for SOA formation and interesting approaches to address these questions, the paper could be published after some minor revisions (most of it of formal character, e.g. references in text and supplement, see below).

However the manuscript fails clearly short behind its title claim and from this point of view, I

suggest to reject the manuscript, due to the major concerns following below. Since the authors have already done the best with their data in a positive sense, I guess major revisions would not make sense.

A way out could be a reformulation of the title of the manuscript away from “providing yields” (reliable numbers) to a more procedural character of “addressing an important issue with interesting approaches and possibly important findings”.

The basic observation we report in this paper is a change in particulate nitrate for a change in isoprene ($\Delta p\text{RONO}_2/\Delta\text{Isop}$). As long as the $\Delta p\text{RONO}_2$ is attributable to organic nitrate (with uncertainties clearly acknowledged), and as long as the association is plausibly the result of the isoprene lost, then this number can only be called a yield. Therefore, we argue that the term yield should be retained in the title, but that, as described below, we provide clear accounting of the uncertainties.

We propose to update Figure 5 with error bars to more clearly emphasize the uncertainties (see response R2.2. below) and adjust wording (see abstract text change below) to ensure that the reliability of our derived yields is appropriately discussed. This way, the yield numbers will not be taken to be an update from previous chamber studies, but rather, this will spur valuable further work to better constrain these yields under atmospherically relevant conditions.

The last sentence of the abstract has been edited to emphasize this goal: **“More in-depth studies are needed to better understand the aerosol yield and oxidation mechanism of NO₃ radical + isoprene, a coupled anthropogenic – biogenic source of SOA that may be regionally significant.”**

Major:

R1.1. The authors convinced me that $p\text{RONO}_2$ and thus organic nitrate in plumes is enhanced and that may indeed relate to enhanced NO₃ concentrations (Figure 6). However, the paper does not really show that that increase of $p\text{RONO}_2$ is related to isoprene oxidation alone (Figure 5). While the reasoning of a single -ONO₂ group per organic nitrate molecules is an acceptable approach to derive molar yields, the scatter in Figure 5 casts doubts, if the increase of $p\text{RONO}_2$ is really related solely to isoprene oxidation. Herein the weak point is the limited number of data points. I don't say the authors are wrong, but one would need more observations to strengthen the case. I concede that the authors revealed an interesting phenomenon, interesting enough to pursue the ideas and go out and get more/better proof.

We agree that there are not many data points in Figure 5, although the paper describes in detail how many power plant plume intercepts were available and how many were suitable for analysis. Thus the data set is by its nature unavoidably limited. Nevertheless, the increase in $p\text{RONO}_2$ associated with each isoprene depletion is clear and repeatable, such that there is not another, more plausible explanation for the observation of $p\text{RONO}_2$ enhancement caused by

rapid NO₃ oxidation of isoprene. When these points are displayed in the format of Figure 5, they produce considerable scatter, indicating that the same yield is not necessarily obtained for each plume, or that the uncertainty in the determination is large. One potential reason for scatter in the data is that the plumes are not all of the same age, as the color code indicates. To clearly show the uncertainty in yields, we have modified Figure 5 to show the error bars that are associated with the yield determination.

R1.2. L: 651: In going from the molar yield to the mass yield the uncertainty - and speculations clearly indicated as such, though - become even larger. On one hand obviously two oxidation steps are needed to achieve condensable isoprene oxidation products, on the other hand NO₃ seems to be the only available oxidant. Oxidation of both double bonds should thus lead to dinitrates.

Two oxidation steps are needed only if auto-oxidation is an unimportant mechanism.

If pOrgNO₃ would really isoprene dinitrates the estimated yield would drop from 27% to 18%, not so far away from the referenced value by Rollins of 14%. I can follow the authors that it is likely that pRONO₂ dinitrates could be hydrolysed, but why should hydrolysis stop after one group, why not hydrolysing every second -ONO₂ group or even both ONO₂ groups? Moreover, as far as I understand, Rollin's value is based in parts on observations of several hours in a large chamber. So reaction time cannot be an issue?!

We agree with the reviewer's comment that the mass or molar yield would be different by a factor of two in the case of both double bonds oxidized by NO₃ and retention of both nitrate groups on the isoprene backbone. We do not understand the statement that reaction time cannot then be an issue. Especially in the case of a two step oxidation, with a slower rate constant anticipated for the second step, additional reaction time would be required, as stated in the manuscript.

I agree that wall losses could be an issue, though, but wall losses are also less important in large chambers.

Wall losses are not unimportant in large chambers. Cited references show that partitioning of semivolatile organic compounds to walls is an important effect in any chamber study.

There for with the same right I could argue that Rollin's yield of 14% is correct and then ask where could the rest of organic nitrate come from. I follow the authors that inorganic nitrate can be excluded as source. Could it be that the organic nitrates arise from liquid phase or heterogeneous processes via NO₂, NO₃? Is anything known about such heterogeneous nitration processes? NO_x and NO₃ were by definition high in the plumes. Actually if I really think about it the mass yield analysis adds not much beyond the molar yield considerations and an analogous plot would just reproduce Figure 5 with slopes of 18% or 27%, depending only on the assumption if the isoprene nitrates bring in two or three times the molecular weight of isoprene itself.

We concur that the mass yield estimate is subject to substantial additional uncertainties beyond the molar yield, which we have endeavored to describe clearly here. Because it took the author team quite some time and discussions to come up with all of these considerations, we thought it could be helpful to readers to have them collected here in one place. Because of the noted uncertainties, however, we choose not to emphasize these mass yields with a figure, instead showing molar yields in Figure 5. This way a future reader with additional information about likely reaction mechanisms or SOA composition could do exactly the calculation this reviewer does to determine refined mass yield estimates based on that new information.

In response to the suggestion to consider heterogeneous uptake of NO_3 onto organic particles, we make an estimate of the rate of that process to determine whether it might contribute to observed organic nitrate aerosol. Based on available literature, the maximum NO_3 uptake coefficient would be 0.1, and this condition would only occur if there are a significant number of double bonds remaining in the newly formed organic aerosol [Ng review paper, p. 2114]. Given this uptake coefficient and the observed in-plume wet aerosol surface of on average $300 \text{ um}^2 \text{ cm}^{-3}$ ($=3 \times 10^{-4} \text{ m}^{-1}$), the kinetic molecular theory predicted uptake rate constant is $k = \{\gamma\} * v * SA/4 = 0.0024 \text{ s}^{-1}$. At average in-plume $[\text{NO}_3]$ of 20 pptv, this would correspond to an uptake of 0.17 ppb NO_3 per hour. This means that a 5 to 6-hour old plume could have up to ~ 1 ppb of nitrate functional groups produced by this heterogeneous process if this high uptake coefficient is true. However, because the aerosol surface area is not exclusively alkene nor even exclusively organic aerosol (indeed, it is calculated to be partially aqueous), we expect that a much smaller uptake coefficient, on the order of 0.001, is more realistic, and thus heterogeneous NO_3 uptake is not likely to contribute significantly. (Brown & Stutz 2012).

We have added the following line to the revised manuscript at line 733: **“We have not corrected the calculated yields for the possibility of NO_3 heterogeneous uptake, which could add a nitrate functionality to existing aerosol. Such a process could be rapid if the uptake coefficient for NO_3 were 0.1, a value characteristics of unsaturated substrates (Ng et al, 3016), but would not contribute measurably at more conventional NO_3 uptake coefficients of 0.001 (Brown & Stutz 2012).”**

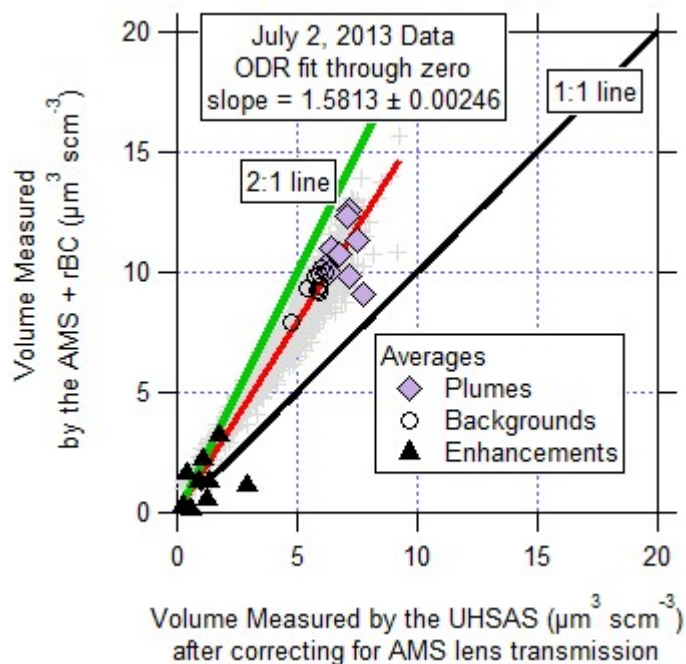
R1.3. L483/ Fig. 2: What also concerns me and this is again related to small number of cases: There are indeed correlations between PNO_3 and pRONO_2 and anti-correlation with isoprene, but pOrgNO_3 sometimes increases by the same amount in the absence of plumes (2:17.30AM, 2:22.00AM) and some plumes do not create OrgNO_3 despite lower isoprene (ca. 2:21.20AM).

We again concur that this study would be stronger with a larger number of observed plume transects, however we reassert that our screening methodology and error limits have all been stated in the manuscript. We have considered the variations in the background in making estimates of the organic nitrate increases in plumes. We average as many points as possible in each of multiple plumes.

Minor:

R1.4. I315, Fig.S1: If I compare the SENEX data with actual data in the range of plumes and background the difference is more a factor of 2 than 1.6. Moreover, two of the plumes fall off line while all the background measurements correlate as all other data. Unfortunately, the exception of AMS performance(?) or UHSAS performance(?) for "just that flight" in addition weakens the case.

The right-hand panel of Figure S1 is reproduced below with a 2:1 line shown, to illustrate that the slope of 1.6 is correct for this flight.



As far as the scatter in the plume enhancements and the contribution of this volume related uncertainty -- we now cite forward to Figure 4, where the enhancements are shown with complete propagated error on pRONO2, showing that while there are uncertainties due to (among other things) the uncertainty in the volume comparison, the enhancements are always positive. These same error bars are now also shown on Figure 5, so that the full uncertainties are available for the reader to evaluate.

We also noted in the process of updating this that the uncertainties in the yield tables had not incorporated these additional uncertainties -- these have all been updated to include the full error propagation. (Note: this did not change yields and increased errors on only some plumes)

Changed text to: "This does not change the conclusions of this work **because this has been incorporated into the error in aerosol organic nitrate, which still show positive enhancements in pRONO2 for these plumes (see Figure 4 below). These complete error estimates are also used in Figure 5 to clearly show the uncertainties in the yields.** The volume comparison is discussed further in the Supplemental Information and shown for the plumes of interest in Fig. S1

R1.5. I suggest listing also PNO₃ in Table 1; that would help to link quickly oxidation strength and observed effect

This has been added to Table 1.

R1.6. Main text: references not in ACP format Replace “author et al. (author et al., year)” by “author et al. (year)”

Fixed.

R1.7. Supplement: the literature is not assessable and given in bracketed format

Fixed.

R1.8. I59: review

This appears to be an editor's note.

I172: Xu et al. (2015)

Fixed.

I339: Fry et al. [47]

Fixed.

I657: no “N” in the formula, it is not clear that refer only to organic rest of the trihydroxynitrate

Thank you, clarified: “e.g. a tri-hydroxynitrate (**with organic portion of formula** C₅H₁₁O₃, 119 g mol⁻¹)”

I418: I suggest to replace “number densities” with “concentration” in context of gases I

Done.

Anonymous Referee #2

Summary: The manuscript by Fry et al. addresses, for the first time, the potential to measure in-situ secondary organic aerosol (SOA) yields from isoprene oxidation in a power plant plume by aircraft. This is a completely original and timely study that aims to assess SOA yields in the ambient environment without the competing effects of wall loss, which has hampered most laboratory (reaction chamber) studies in the past. In this view, the paper is highly suitable for Atmospheric Chemistry and Physics. The authors determine isoprene-derived SOA yields from NO₃ oxidation in the plume based on measured enhancements in aerosol organic nitrate and

isoprene loss in the plume relative to aerosol organic nitrate and isoprene concentrations outside of the plume. The authors find that isoprene-derived molar SOA yields from reaction with NO₃ is on the order of 9%, and mass-based SOA yields are 27%, larger than those measured previously in the laboratory (12-14%). The authors conclude that the relatively larger SOA mass yield is due to the longer plume age and processing (forming more nitrates) compared to apparently shorter processing time in chamber studies. While I thought the paper was creative, well written, and well supported by the literature, before I can fully support publication, I encourage the authors to address my points of concern in a revised manuscript as stated below.

Major comments:

R2.1a. Although I thought the authors did their due diligence by addressing several of the caveats in this study, I have a couple of additional concerns (but possible solutions) with the calculation of SOA yield that I encourage the authors to address in a revised manuscript. First, the authors use isoprene measured outside of the plume as the initial (starting) concentration and from that derive the SOA yield based on the difference in isoprene concentrations measured inside and outside of the plume. Ideally, I think you would want to use isoprene measured from the point of plume emission as the starting concentration of isoprene, i.e., measure the isoprene concentration in the plume near the point source, and then measure isoprene in the plume at a distance further downwind of the point source, because then you know how much of the initial isoprene in the plume (same air mass) was consumed. My main concern with using isoprene outside of the plume as the starting concentration is that it does not necessarily represent the isoprene that has undergone processing in the plume. According to the isoprene time series shown in Fig. 2, in the span of 5 minutes, isoprene outside of the plume can be 700 ppt, 500 ppt, and 300 ppt, for example. Thus, the SOA yields reported in this work depend critically on the choice of concentration measured outside of the plume. While I am not suggesting the authors are wrong in their approach, it might be helpful if the authors could identify a case where they sampled the same plume twice at different locations downwind of the point source and calculate the SOA yield based on the difference in isoprene/nitrate measured in the first transect and a later transect. This would at least strengthen/validate the approach. Alternatively, it may help to show that “background” isoprene measured outside of the plume does not vary significantly near and further downwind of the plume source.

We thank the reviewer for these suggestions. For each plume point, we used an iterative box model to calculate the isoprene that would have been present at sunset at that location outside of the NO_x plume. This enables an alternate Δ isoprene calculation based on in-plume isoprene minus modeled sunset isoprene, for comparison to the calculation used in the yield calculations, based on in-plume minus background isoprene. The similarity between these two values for most points suggests that the isoprene just outside of each plume transect was largely unperturbed from the sunset initial value. We have added these values to Table S3, with explanatory text:

“Also shown are the plume changes in isoprene used in the present analysis (Δ isop, the

difference between in-plume and background isoprene concentration, reproduced from Table 1), alongside for comparison the Δ isop determined as the difference between in-plume isoprene and the modeled sunset (initial) concentration of isoprene present at that location outside of the plume, determined using an iterative box model (ref). The similarity between these two values for most points suggests that the isoprene just outside of each plume transect was largely unperturbed from the sunset initial value.”

plume number [#isop/#AMS]	7/2/1 3 plume time (UTC)	Δ ORG _{aero} ($\mu\text{g m}^{-3}$)	Δ NH _{4,aero} ($\mu\text{g m}^{-3}$)	Δ SO _{4,aero} ($\mu\text{g m}^{-3}$)	Tem p (C)	%R H	Δ iso p (pptv)	Δ isop from mode l (pptv)	Isop:M T Mole Ratio
Typical variability ($\mu\text{g m}^{-3}$):		0.75	0.1	0.5					
1 [2/3]	2:18	0.35	0	0	23.6	66.5	-335	-327	36.5
2 [*]	2:20	0.89	0.3	1.91	23.6	65	-404	-453	71.4
3 [4/5]	2:21	1.25	1.05	5.14	23.6	65.2	-228	-337	16.6
4 [*]	3:03	0.16	0.08	0.7	21.2	68.1	-453	-391	50.6
5 [3/4]	3:55	0.32	0.26	6.07	21.9	65.5	-255	-376	34.2
6 [2/2]	4:34	0.57	0.3	1.12	19.9	74.6	-713	-233	17.3
7 [5/6]	4:37	1.05	0.22	0.65	19.7	76.2	-298	-221	14.2
8 [2/3]	4:39	1.26	0.44	1.18	18.3	82.2	-443	-353	11.0
9 [7/8]	5:04	1.45	0.35	1.9	17.2	84.8	-293	-434	17.8

This will allow the reader to assess the general robustness of the isoprene background values. However, we don't believe that it would be appropriate to calculate yields based on these values, because we don't have analogous pre-plume values for pRONO₂. Thus, for the yield calculations we think it's best to use in-plume and plume-adjacent background isoprene values even though there is noise in the background. We do account for this noise in the standard deviation error bars on the Δ isop values.

We appreciate the second suggestion to use multiple, successive downwind plume transects. While this approach has worked in previous analysis of nighttime power plant plumes (e.g., Brown et al. 2012), identifying such plumes is difficult. In the present case, there were not two easily identifiable successive Lagrangian plumes intercepts. Rather, we encountered a range of plumes, often at different altitudes, with different transport times but not in a successive manner.

R2.1b. Second, what is the impact of O₃ (and other oxidants) on isoprene loss in the plume? I thought there would be more discussion of this – while the reaction rate of O₃ with isoprene is several orders of magnitude less than NO₃, the concentration of O₃ can be several orders of magnitude greater than NO₃, and therefore may rival NO₃ in regards to isoprene consumption in the plume at night. In the Edwards, et al. [2017] study referenced by the authors, O₃ accounts for 45% of the BVOC consumption at night. In this study, the SOA yield is based on the premise that VOC consumption is controlled entirely by NO₃. If other reactants that consume isoprene (e.g., O₃ and OH) are present in sufficient quantities, the calculated yields might overestimate the contribution from NO₃. I encourage the authors to address this more explicitly, e.g., by calculating the relative loss rates of isoprene at night by NO₃, O₃, and OH.

We have added to the supplemental information the below plot (new Figure S9) showing isoprene loss in the plume model simulation (black) and stacked plot showing the contributions to this from the NO₃, O₃, and OH. As described in the model description, the modelled plume was emitted at sunset so these are all nocturnal processes. As is clear from this figure, in the power plant plumes, the isoprene loss is not entirely, but approximately 90% via NO₃ radical.

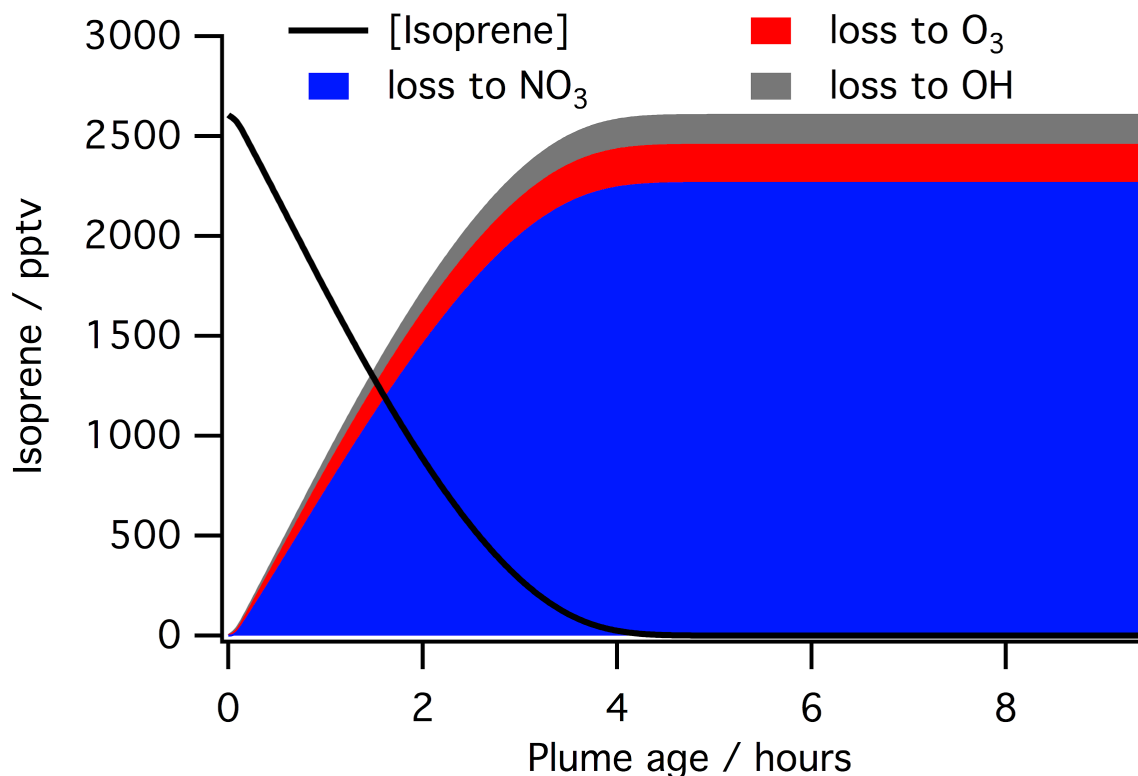
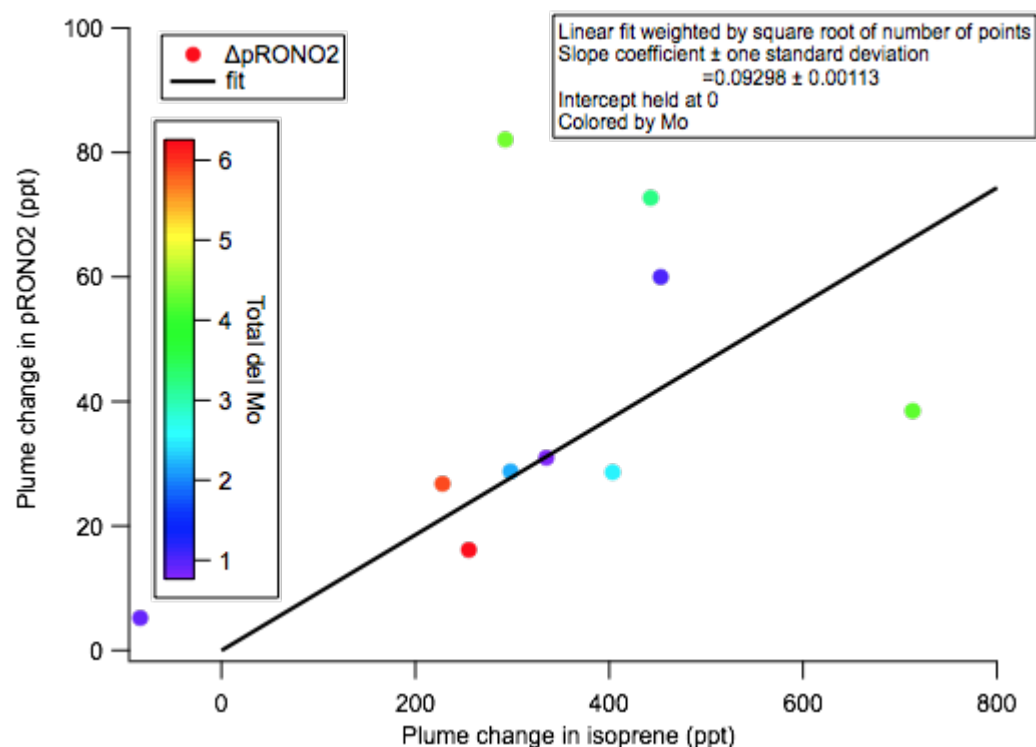


Figure S9. Model simulation of typical in-plume consumption of isoprene (black line), and stacked plot showing the contributions to this from the NO₃, O₃, and OH. Modeled plume was emitted at sunset, so this represents nocturnal processing under power plant plume conditions.

R2.2. The scatter and limited number of observations used to calculate the average yield as shown in Fig. 5 may be a point of concern. Uncertainty bars on the data would certainly help to convey how far off from the fit the measurements truly are. Often, SOA mass yields are expressed as a function of the change in particle mass (ΔM); if the authors were to instead plot plume change in pRONO₂ mass as a function of plume change in isoprene mass, could it be that the larger/smaller enhancements in aerosol organic nitrate mass simply result from a shift in equilibrium partitioning more/less to the particle phase owing to a larger/smaller ΔM ? I encourage the authors to show the effects of ΔM in some capacity, e.g., by normalizing each point in Fig. 5 by the measured ΔM (i.e., difference in M between inside and outside of plume) and/or making a separate figure to show mass yield as a function of ΔM . Alternatively, instead of using \sqrt{n} as the bubble size in Fig. 5, scale bubble size by ΔM .

We thank the reviewer for these insightful suggestions. We tried re-plotting Figure 5 with points colored by ΔM , and don't see a clear dependence that explains the high points (see figure below, not added to manuscript). Given this, we believe the colorbar in the manuscript shows a more likely contributing factor: plume age. The highest pRONO₂ values occur for the longest plume ages, which would allow for several routes to more pRONO₂: (1) more molecules in with

the second double bond has been oxidized, (2) more time for intramolecular H-rearrangement reactions, or (3) more time for contribution of (slower) heterogeneous uptake of NO₃ on organic aerosol.



We have added uncertainty error bars, thank you for that nudge. The new Figure 5 and updated caption are:

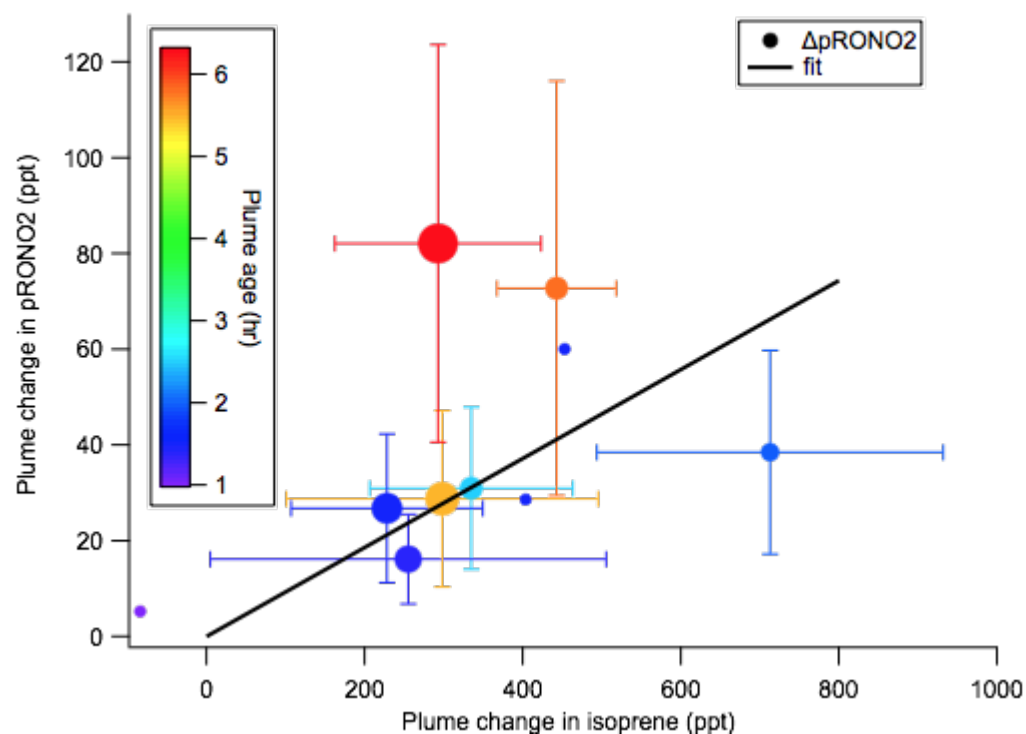


Figure 5. SOA molar yield can be determined as the slope of $\Delta p\text{RONO}_2$ vs. Δ isoprene, both in mixing ratio units. The linear fit is weighted by square root of number of points used to determine each in-plume $p\text{RONO}_2$, with intercept held at zero. The slope coefficient \pm one standard deviation is 0.0930 ± 0.0011 . Points are colored by plume age (red = longest), and size scaled by square root of number of points (the point weight used in linear fit). This plot and fit includes the nine plumes listed in Tables 1 and 2, as well as the 03:14 “unreacted” plume (at Δ isoprene = -84 ppt). **Error bars on isoprene are the propagated standard deviations of the (in plume - out plume) differences, for plumes in which multi-point averages were possible. Error bars on $p\text{RONO}_2$ are the same as in Figure 4. The points without error bars are single-point plumes.**

These error bars are the propagated standard deviations of the {in plume - out plume} differences for plumes in which multi-point averages were possible (the points without error bars are single-point plumes). This responds also to Reviewer 1’s concern about clearly demonstrating the uncertainties in the derived yields, and the x error bars respond to comment R2.1a. above about the variability of isoprene around these plumes.

Minor comments

R2.3. In the SOA molar yield calculation, the authors first convert the aerosol nitrate from mass concentration units to equivalent ppt assuming the aerosol organic nitrate has a molar mass of 62 g mol^{-1} . This seems far too small a molar mass expected for isoprene+ NO_3 oxidation products. Why not assume a molar mass consistent with the first generation carbonyl nitrate produced from isoprene+ NO_3 ($\text{MW}=145 \text{ g mol}^{-1}$) (Jenkin et al., 2015) or another suitable organic compound as done later with the SOA mass yield calculation?

The nitrate measurement by the AMS is calibrated to be the mass of the nitrate (NO_3) moiety alone, hence, 62 g mol^{-1} , and we use these masses, converted to mixing ratio, in order to determine molar yields. Using the nitrate component alone avoids needing to make any assumption about the molecular weight of the organic mass that accompanies the NO_3 in the produced SOA. We thus can make these assumptions separately to estimate a mass yield (see equations 3 and 4 and discussion thereof). To ensure clarity in the text, added this text:

“we convert the aerosol organic nitrate mass loading differences to mixing ratio differences (ppt) using the NO_3 molecular weight of 62 g mol^{-1} **(the AMS organic nitrate mass is the mass only of the $-\text{ONO}_2$ portion of the organonitrate aerosol).**”

R2.4. Page 2, line 52: “review”

This appears to be an editor’s note.

R2.5. Page 3, lines 92-94: Please include reference.

Added reference to: D'Ambro, E. L., K. H. Møller, F. D. Lopez-Hilfiker, S. Schobesberger, J. Liu, J. E. Shilling, B. H. Lee, H. G. Kjaergaard and J. A. Thornton (2017). "Isomerization of Second-Generation Isoprene Peroxy Radicals: Epoxide Formation and Implications for Secondary Organic Aerosol Yields." [Environmental Science & Technology](#) **51**(9): 4978-4987.

R2.6. Page 9, Eq. 1 (lines 367-371): Equation (1) has k_1 , whereas text states k_2 .

Thank you! Corrected.

R2.5. Page 14, lines 500-502: It's probably more correct to write the production rate of isoprene oxidation products by NO_3 reaction is greater than for monoterpenes.

As suggested we modified this line to read: "At these relative concentrations, even if all of the monoterpene is oxidized, **the production rate of oxidation products** will be much larger for isoprene."

R2.6. Figure 5: It would be helpful to the readers if in the legend, the symbol for $\Delta p\text{RONO}_2$ were black with a color scale next to the current legend (the red color of the symbol is confusing with some of the points being red). A separate legend for marker/bubble size would also be helpful.

Thank you, done, and color bar legend added (see new version of figure above in response to R2.2).

Anonymous Referee #3

Fry et al use airborne observations from the SENEX campaign to infer SOA yields for the reaction of isoprene with NO_3 radicals. Specifically they show that night time transects through power plant plumes capture conditions in which the loss of NO_3 is dominated by the reaction with isoprene. Comparisons of out of plume isoprene and particle phase nitrate measurements with values observed in the seconds to minutes long in-plume parts of the flight, are used to calculate SOA molar and mass yields. While the approach of using field data to evaluate SOA yields in "wall free" environments is interesting, the data analysis is based on highly speculative assumptions and the SOA yields can therefore not be taken as reliable real world reference. The paper needs major modifications before it can be published.

Major Points

R3.1. The particulate organic nitrate mass concentration is evaluated according to an established method using AMS observed $\text{NO}_2^+/\text{NO}^+$ ion ratios. While this method has been used before for high resolution data sets, the authors have to apply corrections for unknown organic interferences to their C-TOF-AMS dataset, subtracting 55% and 33% of the total measured signal on m/z 30 and 46, respectively. As shown in Figure S2 e (lower panel), the thus derived UMR corrected $\text{NO}_2^+/\text{NO}^+$ ratio agrees relatively well with the HR ratio, except for periods in which the total nitrate signal is low. The authors should have a look into this feature

and derive from it a threshold total nitrate mass concentration below which no reliable analysis of organic nitrate is possible.

Detection limits (DL) for nitrate using HR-ToF-AMS (HR data shown in Fig. S2) are ~ 10 ng/m³. As either NO_x^+ ion approaches their DL (and zero), the uncertainty in the NO_x^+ ratio determinations will blow up. This effect is clearly visible in both the HR and UMR -derived NO_x^+ ratios in Fig. S2. The DLs for NO_2^+ and NO^+ are similar to the nitrate DL. Depending on the instrument-specific response and the proportions of inorganic/organic nitrate, the $\text{NO}_2^+/\text{NO}^+$ ratio can vary between ~ 1 and ~ 0.1 . Therefore, the NO_x^+ ratio detection limit is typically dominated by the NO_2^+ ion DL, especially when the nitrate is dominated by pRONO₂. So for HR-ToF AMS that would be equivalent to a total nitrate concentration of ~ 50 ng/m³. Importantly, when the NO_x^+ ratio is below DL, discarding pRONO₂ and ammonium nitrate concentration data is not necessarily warranted or desired, since despite that apportionment may be indeterminate, the concentration of both are still constrained to the nitrate concentration (if above the total nitrate DL) or the nitrate DL (if below the total nitrate DL) which is often valuable information and places quantitative constraints on concentrations. Given these considerations, we do not think there is a “threshold total nitrate mass concentration below which no reliable analysis of organic nitrate is possible”.

For this study, the nitrate DLs (3-sigma) reported here for the native 10-second CToF data were 50 ng/m³ (L305) which for the upper limit of pure pRONO₂, where only $\sim 20\%$ of the NO_x^+ ions are NO_2^+ , would correspond to a nitrate DL of 250 ng/m³ for the NO_x^+ ratio. As seen in Fig. 6, all the plume pRONO₂ concentrations were between 200-600 ng/m³ (and total nitrate was similar or higher) and additionally the AMS plume averages typically consisted of several points (1-8) for which the combined DL should scale down as $1/\sqrt{n}$. Therefore, for the plume analysis used in this manuscript, the pRONO₂ concentration determination should be near or well above expected 3-sigma DLs.

Note that the values for R ammonium nitrate and R organic nitrate indicated in Figure S2 do not match with the values of 0.49 and 0.175 reported in the paper and in Figure 3.

That is correct, the NO_x^+ ratios for ammonium nitrate in Fig. S2 are from calibrations conducted during that campaign (SEAC⁴RS) while those in Fig. 3 are from the campaign investigated in this manuscript (SENEX). For both cases, the pRONO₂ ratio was estimated as 2.8 times lower $\text{NO}_2^+/\text{NO}^+$ ratio than measured for ammonium nitrate (see details in manuscript and below).

The use of a value $R=0.175$ of $\text{NO}_2^+/\text{NO}^+$ for organic nitrates is justified with reference to Day et al 2017, a paper in preparation. As the R-value directly affects the calculated mass concentration of organic nitrates, basing its justification on unpublished work is not acceptable. In a more conservative approach the authors should instead use the organic nitrate R-value of 0.1, which will lead to a lower estimate of organic nitrate mass concentration. Implementing this value for the data set in Table 2 would lead to a reduction of organic nitrate mass concentration by $\sim 25\%$, directly reducing the SOA molar and mass yields by the same percentage.

Noteworthy, the use of $R=0.1$ for organic nitrates would also increase slightly the mass concentration of ammonium nitrate. As for many plumes the authors calculate negative ammonium nitrate mass concentration, this negative bias for the ammonium nitrate would be overcome, further supporting the use of $R=0.1$ instead of $R=0.175$. As mentioned above, the use of $R=0.1$ would reduce organic nitrate mass concentration and therefore the SOA mass yield would be reduced to $\sim 20\%$ instead of the current 27% . Accounting for the $2/3$ organic mass the SOA mass yield presented here would translate into an organic mass yield of 13% , well comparable to the literature data cited by the authors.

We agree that the $p\text{RONO}_2/\text{NO}_x^+$ ratio affects $p\text{RONO}_2$ quantification. However, we disagree with the proposed value, which is not consistent with the average of the published literature.

As for the “negative ammonium nitrate mass concentration” when calculating the plume enhancements, these cannot be simply prescribed to a bias in the $p\text{RONO}_2/\text{NO}_x^+$ ratio. Note that those values are differences between in/out of plume. As shown in Fig. 4, they are statistically zero when considering the uncertainties derived from the variability associated with in/out plume subtraction and measurement uncertainties (as clearly shown in the error bars on that plot). Therefore this does not provide any evidence that a $p\text{RONO}_2/\text{NO}_x^+$ ratio of 0.1 is more appropriate.

We have replaced the text in question describing the $p\text{RONO}_2$ ratio used with the following text, and removed all references to Day et al. from the manuscript:

This factor was determined as the average of several literature studies (Fry et al., 2009; Rollins et al., 2009; Farmer et al., 2010; Sato et al., 2010; Fry et al., 2011; Boyd et al., 2015) and applied according to the “ratio of ratios” method (Fry et al., 2013).

R3.2. The discussion on urban plumes, although acknowledging uncertainties, is far too speculative and should be removed from the manuscript.

We agree that the urban plume cases are more difficult to analyze due to variability in the background that is on the same scale as the enhancements. Therefore, we have moved this figure and discussion to the supplement to make this observation available, with only a qualitative analysis that organic nitrate aerosol is also enhanced in these urban plumes but is superimposed on an apparently large background variability.

Other points (in order of appearance in the manuscript)

R3.3. Page 5, line 172, 174: “ $0.7\mu\text{g m}^{-3}$. . . a factor of three lower than . . . $1.7\mu\text{g m}^{-3}$ ” the numbers don’t match up, check for consistency.

Edited to: “Xu et al. predict only $0.7\mu\text{g m}^{-3}$ of SOA would be produced, **substantially lower than** the measured nighttime LO-OOA production of $1.7\mu\text{g m}^{-3}$.”

R3.4. Page 13, line 469: the nitrate radical production rate that was used to identify in-plume parts of the flight needs justification

Added text to explain: **“This threshold was chosen to be above background noise and large enough to isolate only true plumes (see Fig. 1a). The value is thus subjectively chosen, but was consistently applied across the dataset.”**

R3.5. Page 16, line 567 and following: To justify the statement, the authors need to show calibration data for deriving RIE of NH₄ and show the precision of ion balance in the calibration aerosol.

The values for the relative ionization efficiencies for ammonium are mentioned in the experimental section on page 9 in lines 357-358: “Note that the relative ionization efficiency for ammonium was 3.91 and 3.87 for the two bracketing calibrations and an average value of 3.9 was used for the flight analyzed here.”

The ion balance for the plume enhancements is now plotted with the ion balance for the ammonium nitrate calibration data along with uncertainty bands and error bars (new Figure S5b shown below & added to manuscript).

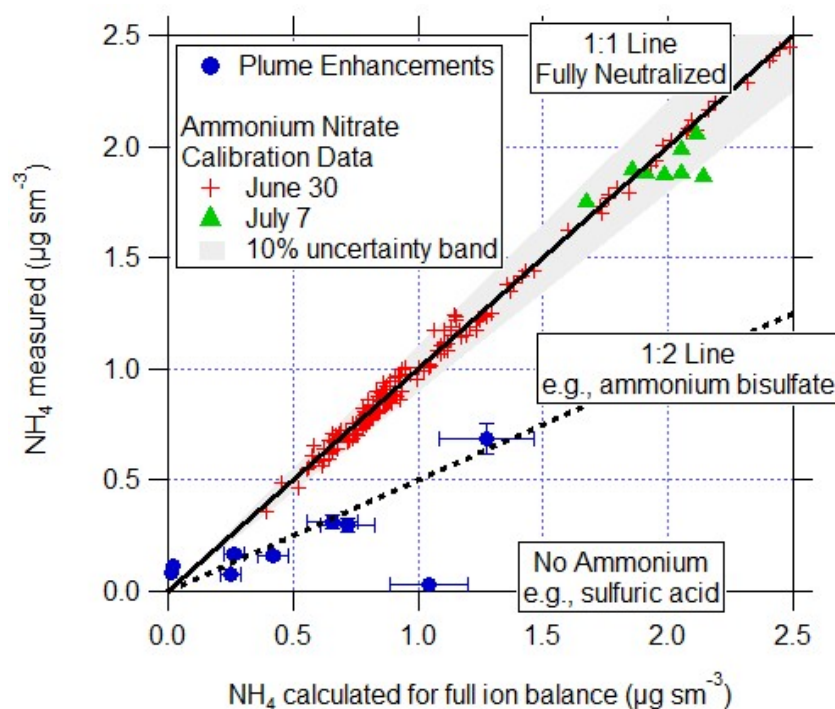


Figure 5. ... (b) Measured vs. calculated (ion balanced) NH₄ for calibration data and plume enhancements. This also shows that plumes are acidic than ammonium sulfate, ruling out the possibility of inorganic nitrate formation.

Added at line 647 to describe the ion balance precision:

“The ion balance for the ammonium nitrate calibration particles and the plume enhancements are shown in Fig. S5b. Complete neutralization of the calibration aerosols is nearly always within the gray 10% uncertainty band for the relative ionization efficiency of ammonium (Bahreini et al., 2009). In contrast, many of the plume enhancements are near the 1:2 line (as primarily ammonium bisulfate) within the combined 10% ammonium and 15% sulfate uncertainty error bars or without ammonium (sulfuric acid).”

R3.6. Although the authors cite, that NO₃ loss is dominated by reaction with isoprene, they could use the calculated potential for inorganic nitrate formation from N₂O₅ uptake to support the interpretation of most in-plume particulate nitrate formation having organic sources.

The contribution of N₂O₅ uptake to overall NO₃ losses was considered in detail in Edwards, et al. (2017). The results reported in Figure S4 show N₂O₅ heterogeneous uptake contributing negligibly, with the exception of 2 brief periods, which do not correspond to plumes analyzed in this work. The authors further argue that even this small contribution of N₂O₅ heterogeneous uptake is likely overestimated.

Added this line to the text at line 561 to clarify this:

“Inorganic nitrate can also be produced by the heterogeneous uptake of N₂O₅ onto aqueous aerosol; Edwards et al. (2017) demonstrated that this process is negligible relative to NO₃ + BVOC for the July 2 SENEX night flight considered here.”

References for these responses:

S.S. Brown and J. Stutz, “Nighttime radical observations and chemistry,” *Chem. Soc. Rev.*, 2012, 41, 6405-6447.

Brown, S.S., W.P. Dubé, P. Karamchandari, G. Yarwood, J. Peischl, T.B. Ryerson, J.A. Neuman, J.B. Nowak, J.S. Holloway, R.A. Washenfelder, C.A. Brock, G.J. Frost, M. Trainer, D.D. Parrish, F.C. Fehsenfeld, and A.R. Ravishankara, The effects of NO_x control and plume mixing on nighttime chemical processing of plumes from coal-fired power plants. *J. Geophys. Res.*, 2012. 117: p. D07304.

1 Secondary Organic Aerosol (SOA) yields from NO₃ radical 2 + isoprene based on nighttime aircraft power plant plume 3 transects

4
5 Juliane L. Fry¹, Steven S. Brown^{2,5}, Ann M. Middlebrook², Peter M. Edwards^{2,3,4}, Pedro
6 Campuzano-Jost^{3,5}, Douglas A. Day^{3,5}, José L. Jimenez^{3,5}, Hannah M. Allen⁶, Thomas B.
7 Ryerson², Ilana Pollack^{2,3,a}, Martin Graus^{3,b}, Carsten Warneke^{2,3}, Joost A. deGouw^{3,5}, Charles A.
8 Brock², Jessica Gilman^{2,3}, Brian M. Lerner^{2,3,c}, William P. Dubé^{2,3}, Jin Liao^{2,3,d}, André Welti^{2,3,e}

9
10 ¹Chemistry Department, Reed College, Portland, OR, USA

11 ²Chemical Sciences Division, Earth System Research Laboratory, National Oceanic and Atmospheric
12 Administration, Boulder, CO, USA

13 ³Cooperative Institute for Research in Environmental Sciences, University of Colorado, Boulder, CO, USA

14 ⁴Wolfson Atmospheric Chemistry Laboratories, Department of Chemistry, University of York, York, UK

15 ⁵Department of Chemistry, University of Colorado, Boulder, CO, USA

16 ⁶Division of Chemistry and Chemical Engineering, California Institute of Technology, Pasadena, CA, USA

17 ^anow at Department of Atmospheric Science, Colorado State University, Fort Collins, CO, USA

18 ^bnow at Institute of Atmospheric and Cryospheric Sciences, University of Innsbruck, Austria.

19 ^cnow at Aerodyne Research, Inc., Billerica, MA, USA

20 ^dnow at Universities Space Research Association, Columbia, MD, USA and NASA Goddard Space Flight
21 Center, Atmospheric Chemistry and Dynamic Laboratory, Greenbelt, MD, USA

22 ^enow at Leibniz Institute for Tropospheric Research, Department of Physics, Leipzig, Germany

23

24 Abstract

25 Nighttime reaction of nitrate radicals (NO₃) with biogenic volatile organic compounds (BVOC)
26 has been proposed as a potentially important but also highly uncertain source of secondary
27 organic aerosol (SOA). The southeast United States has both high BVOC and nitrogen oxide
28 (NO_x) emissions, resulting in a large model-predicted NO₃-BVOC source of SOA. Coal-fired
29 power plants in this region constitute substantial NO_x emissions point sources into a nighttime
30 atmosphere characterized by high regionally widespread concentrations of isoprene. In this
31 paper, we exploit nighttime aircraft observations of these power plant plumes, in which NO₃
32 radicals rapidly remove isoprene, to obtain field-based estimates of the secondary organic
33 aerosol yield from NO₃ + isoprene. Observed in-plume increases in nitrate aerosol are
34 consistent with organic nitrate aerosol production from NO₃ + isoprene, and these are used to
35 determine molar SOA yields, for which the average over 9 plumes is 9%. Corresponding mass
36 yields depend on the assumed molecular formula for isoprene-NO₃-SOA, but the average over
37 9 plumes is 27%, larger than those previously measured in chamber studies (12 – 14% after
38 oxidation of both double bonds). Yields are larger for longer plume ages. This suggests that
39 ambient aging processes lead more effectively to condensable material than typical chamber
40 conditions allow. We discuss potential mechanistic explanations for this difference, including
41 [longer](#) ambient peroxy radical lifetimes and heterogeneous reactions of NO₃-isoprene gas
42 [phase products](#). [More in-depth](#) studies are needed to better understand the [aerosol yield and](#)

Juliane Fry 5/15/2018 6:29 PM

~~Deleted:~~ Future

Juliane Fry 5/15/2018 6:30 PM

~~Deleted:~~ of aerosol composition from NO₃
radical + isoprene

46 | oxidation mechanism of NO₃ radical + isoprene, a coupled anthropogenic – biogenic source of
47 | SOA that may be regionally significant.

48 | 1 Introduction

49 | Organic aerosol (OA) is increasingly recognized as a globally important component of the fine
50 | particulate matter that exerts a large but uncertain negative radiative forcing on Earth's climate
51 | (Myhre et al., 2013) and adversely affects human health around the world (Lelieveld et al.,
52 | 2015). This global importance is complicated by large regional differences in OA concentrations
53 | relative to other sources of aerosol such as black carbon, sulfate, nitrate and sea salt. OA
54 | comprises 20 – 50% of total fine aerosol mass at continental mid-latitudes, but more in urban
55 | environments and biomass burning plumes, and up to 90% over tropical forests (Kanakidou et
56 | al., 2005, Zhang et al., 2007). Outside of urban centers and fresh biomass burning plumes, the
57 | majority of this OA is secondary organic aerosol (SOA) (Jimenez et al., 2009), produced by
58 | oxidation of directly emitted volatile organic compounds followed by partitioning into the aerosol
59 | phase. Forests are strong biogenic VOC emitters, in the form of isoprene (C₅H₈), monoterpenes
60 | (C₁₀H₁₆), and sesquiterpenes (C₁₅H₂₄), all of which are readily oxidized by the three major
61 | atmospheric oxidants, OH, NO₃, and O₃. The total global source of biogenic SOA from such
62 | reactions remains highly uncertain, with a review estimating it at 90 +/- 90 Tg C yr⁻¹ (Hallquist et
63 | al., 2009), a large fraction of which may be anthropogenically controlled (Goldstein et al., 2009,
64 | Carlton et al., 2010, Hoyle et al., 2011, Spracklen et al., 2011). As most NO₃ arises from
65 | anthropogenic emissions, OA production from NO₃ + isoprene is one mechanism that could
66 | allow for the anthropogenic control of biogenic SOA mass loading.

67 |
68 | Isoprene constitutes nearly half of all global VOC emissions to the atmosphere, with a flux of
69 | ~600 Tg yr⁻¹ (Guenther et al., 2006). As a result, accurate global biogenic SOA budgets depend
70 | strongly on yields from isoprene oxidation. Recent global modeling efforts find that isoprene
71 | SOA is produced at rates from 14 (Henze and Seinfeld 2006, Hoyle et al., 2007) to 19 TgC yr⁻¹
72 | (Heald et al., 2008), which implies that it could constitute 27% (Hoyle et al., 2007) to 48%
73 | (Henze and Seinfeld 2006) to 78% (Heald et al., 2008) of total SOA (based also on varying
74 | estimates of total SOA burden in each study). More recent observational constraints on SOA
75 | yield from isoprene find complex temperature-dependent mechanisms that could affect vertical
76 | distributions (Worton et al., 2013) and suggest that isoprene SOA constitutes from 17% (Hu et
77 | al., 2015) to 40% (Kim et al., 2015) up to 48% (Marais et al., 2016) of total OA in the
78 | southeastern United States. This large significance comes despite isoprene's low SOA mass
79 | yields – two recent observational studies estimated the total isoprene SOA mass yield to be
80 | ~3% (Kim et al., 2015, Marais et al., 2016), and modeling studies typically estimate isoprene
81 | SOA yields to be 4 to 10%, depending on the oxidant, in contrast to monoterpenes' yields of 10
82 | to 20% and sesquiterpenes' yields of >40% (Pye et al., 2010). Furthermore, laboratory studies
83 | of SOA mass yields may have a tendency to underestimate these yields, if they cannot access
84 | the longer timescales of later-generation chemistry, or are otherwise run under conditions that
85 | limit oxidative aging of first-generation products (Carlton et al., 2009).

86 |

Juliane Fry 5/15/2018 6:31 PM

Deleted: chemistry

Juliane Fry 5/15/2018 6:32 PM

Deleted: producing

Juliane Fry 5/15/2018 6:32 PM

Deleted: this potentially important

90 Laboratory chamber studies of SOA mass yield at OA loadings of $\sim 10 \mu\text{g m}^{-3}$ from isoprene
91 have typically found low yields from O_3 (1% (Kleindienst et al., 2007)) and OH (2% at low NO_x to
92 5% at high NO_x (Kroll et al., 2006, Dommen et al., 2009); 1.3% at low NO_x and neutral seed
93 aerosol pH but rising to 29% in the presence of acidic sulfate seed aerosol due to reactive
94 uptake of epoxydiols of isoprene (IEPOX) (Surratt et al., 2010)). One recent chamber study on
95 OH-initiated isoprene SOA formation focused on the fate of second-generation RO_2 radical
96 found significantly higher yields, up to 15% at low NO_x (Liu et al., 2016), suggesting that omitting
97 later-generation oxidation chemistry could be an important limitation of early chamber
98 determinations of isoprene SOA yields. Another found an increase in SOA formed with
99 increasing HO_2 to RO_2 ratios, suggesting that RO_2 fate could also play a role in the variability of
100 | previously reported SOA yields (D'Ambro et al., 2017).

101
102 For NO_3 oxidation of isoprene, early chamber experiments already pointed to higher yields (e.g.,
103 12% (Ng et al., 2008)) than for OH oxidation. Ng et al. (Ng et al., 2008) also observed chemical
104 regime differences: SOA yields were approximately two times larger when chamber conditions
105 were tuned such that first-generation peroxy radical fate was RO_2+RO_2 dominated than when it
106 was RO_2+NO_3 dominated. In addition, Rollins et al. (Rollins et al., 2009) observed a significantly
107 higher SOA yield (14%) from second-generation NO_3 oxidation than that when only one double
108 bond was oxidized (0.7%). This points to the possibility that later-generation, RO_2+RO_2
109 dominated isoprene + NO_3 chemistry may be an even more substantial source of SOA than
110 what current chamber studies have captured. Schwantes et al. (Schwantes et al., 2015)
111 investigated the gas-phase products of NO_3 + isoprene in the RO_2+HO_2 dominated regime and
112 found the major product to be isoprene nitrooxy hydroperoxide (INP, 75-78% molar yield), which
113 can photochemically convert to isoprene nitrooxy hydroxyepoxide (INHE), a molecule that might
114 contribute to SOA formation via heterogeneous uptake similar to IEPOX. Here again, multiple
115 generations of chemistry are required to produce products that may contribute to SOA.

116
117 Because the SOA yield appears to be highest for NO_3 radical oxidation, and isoprene is such an
118 abundantly emitted BVOC, oxidation of isoprene by NO_3 may be an important source of OA in
119 areas with regional NO_x pollution. Since the SOA yield with neutral aerosol seed appears to be
120 an order of magnitude larger than that from other oxidants, even if only 10% of isoprene is
121 oxidized by NO_3 , it will produce comparable SOA to daytime photo-oxidation. For example,
122 Brown et al. (Brown et al., 2009) concluded that NO_3 contributed more SOA from isoprene than
123 OH over New England, where $> 20\%$ of isoprene emitted during the previous day was available
124 at sunset to undergo dark oxidation by either NO_3 or O_3 . The corresponding contribution to total
125 SOA mass loading was 1 – 17% based on laboratory yields (Ng et al., 2017). Rollins et al.
126 (Rollins et al., 2012) concluded that multi-generational NO_3 oxidation of biogenic precursors was
127 responsible for one-third of nighttime organic aerosol increases during the CalNex-2010
128 experiment in Bakersfield, CA. In an aircraft study near Houston, TX, Brown et al. (Brown et al.,
129 2013) observed elevated organic aerosol in the nighttime boundary layer, and correlated vertical
130 profiles of organic and nitrate aerosol in regions with rapid surface level NO_3 radical production
131 and BVOC emissions. From these observations, the authors estimated an SOA source from
132 NO_3 + BVOCs within the nocturnal boundary layer of $0.05 - 1 \mu\text{g m}^{-3} \text{h}^{-1}$. Carlton et al. (Carlton
133 et al., 2009) note the large scatter in chamber-measured SOA yields from isoprene

134 photooxidation and point throughout their review of SOA formation from isoprene to the likely
135 importance of poorly understood later generations of chemistry in explaining field observations.
136 We suggest that similar differences in multi-generational chemistry could explain the variation
137 among the (sparse) chamber and field observations of NO_3 + isoprene yields described in the
138 previous paragraph, and summarized in a recent review of NO_3 + BVOC oxidation mechanisms
139 and SOA formation (Ng et al., 2017).

140
141 The initial products of NO_3 + isoprene include organic nitrates, some of which will partially
142 partition to the aerosol phase. Organic nitrates in the particle phase (pRONO_2) are challenging
143 to quantify with online methods, due to both interferences and their often overall low
144 concentrations in ambient aerosol. Hence, field datasets to constrain modeled pRONO_2 are
145 sparse (Fisher et al., 2016, Ng et al., 2017). One of the most used methods in recent studies,
146 used also here, is quantification with the Aerodyne Aerosol Mass Spectrometer (AMS). Organic
147 nitrates thermally decompose in the AMS vaporizer and different approaches have been used to
148 apportion the organic fraction contributing to the total nitrate signal. Allan et al. (Allan et al.,
149 2004) first proposed the use of nitrate peaks at m/z 30 and 46 to distinguish various nitrate
150 species with the AMS. Marcolli et al. (Marcolli et al., 2006), in the first reported tentative
151 assignment of aerosol organic nitrate using AMS data, used cluster analysis to analyze data
152 from the 2002 New England Air Quality Study. In that study, cluster analysis identified two
153 categories with high m/z 30 contributions. One of these peaked in the morning when NO_x was
154 abundant and was more prevalent in plumes with lowest photochemical ages, potentially from
155 isoprene oxidation products. The second was observed throughout the diurnal cycle in both
156 fresh and aged plumes, and contained substantial m/z 44 contribution (highly oxidized OA). A
157 subsequent AMS laboratory and field study discussed and further developed methods for
158 separate quantification of organic nitrate (in contrast to inorganic nitrate) (Farmer et al., 2010). A
159 refined version of one of these separation methods, based on the differing $\text{NO}_2^+/\text{NO}^+$
160 fragmentation ratio for organic vs. inorganic nitrate, was later employed to quantify organic
161 nitrate aerosol at two forested rural field sites where strong biogenic VOC emissions and
162 relatively low NO_x combined to make substantial organic nitrate aerosol concentrations ((Fry et
163 al., 2013, Ayres et al., 2015)). Most recently, Kiendler-Scharr et al. (Kiendler-Scharr et al., 2016)
164 used a variant of this method to conclude that across Europe, organic nitrates comprise ~40%
165 of submicron organic aerosol. Modeling analysis concluded that a substantial fraction of this
166 organic nitrate aerosol is produced via NO_3 radical initiated chemistry. Chamber studies have
167 employed this fragmentation ratio method to quantify organic nitrates (Fry et al., 2009, Rollins et
168 al., 2009, Bruns et al., 2010, Fry et al., 2011, Boyd et al., 2015), providing the beginnings of a
169 database of typical organonitrate fragmentation ratios from various BVOC precursors.

170
171 Measurements conducted at the SOAS ground site in Centreville, Alabama in 2013 found
172 evidence of significant organonitrate contribution to SOA mass loading. Xu et al. (Xu et al.,
173 2015) reported that organic nitrates constituted 5 to 12% of total organic aerosol mass from
174 AMS data applying a variant of the $\text{NO}_2^+/\text{NO}^+$ ratio method. They identify a nighttime-peaking
175 "LO-OOA" AMS factor which they attribute to mostly NO_3 oxidation of BVOC (in addition to O_3 +
176 BVOC). They estimated that the NO_3 radical oxidizes 17% of isoprene, 20% of α -pinene, and
177 38% of β -pinene in the nocturnal boundary layer at this site. However, applying laboratory-

Juliane Fry 5/15/2018 9:01 PM

Comment [1]: fix format & below.

Juliane Fry 5/26/2018 6:00 PM

Deleted: Xu et al. (Xu et al., 2015)

179 based SOA yields to model the predicted increase in OA, Xu et al. predict only $0.7 \mu\text{g m}^{-3}$ of
180 SOA would be produced, **substantially** lower than the measured nighttime LO-OOA production
181 of $1.7 \mu\text{g m}^{-3}$. The more recent analysis of Zhang et al. (Zhang et al., 2018) found a strong
182 correlation of monoterpene SOA with the fraction of monoterpene oxidation attributed to NO_3 ,
183 even for non-nitrate containing aerosol, suggesting an influence of NO_3 even in pathways that
184 ultimately eliminate the nitrate functionality from the SOA, such as hydrolysis or NO_2
185 regeneration. Ayres et al. (Ayres et al., 2015) used a correlation of overnight organonitrate
186 aerosol buildup with calculated net NO_3 + monoterpene and isoprene reactions to estimate an
187 overall NO_3 + monoterpene SOA mass yield of 40 – 80%. The factor of two range in this
188 analysis was based on two different measurements of aerosol-phase organic nitrates. These
189 authors used similar correlations to identify specific CIMS-derived molecular formulae that are
190 likely to be NO_3 radical chemistry products of isoprene and monoterpenes, and found minimal
191 contribution of identified first-generation NO_3 + isoprene products to the aerosol phase (as
192 expected based on their volatility). Lee et al. (Lee et al., 2016) detected abundant highly
193 functionalized particle-phase organic nitrates at the same site, with apparent origin both from
194 isoprene and monoterpenes, and both daytime and nighttime oxidation, and estimated their
195 average contribution to submicron organic aerosol mass to be between 3 – 8 %. For the same
196 ground campaign, Romer et al. (Romer et al., 2016) found evidence of rapid conversion from
197 alkyl nitrates to HNO_3 , with total alkyl nitrates having an average daytime lifetime of 1.7 hours.
198
199 Xie et al. (Xie et al., 2013) used a model constrained by observed alkyl nitrate correlations with
200 O_3 from the INTEX-NA/ICARTT 2004 field campaign to determine a range of isoprene nitrate
201 lifetimes between 4 and 6 hours, with 40-50% of isoprene nitrates formed by NO_3 + isoprene
202 reactions. Laboratory studies show that not all organic nitrates hydrolyze to HNO_3 equally
203 rapidly: primary and secondary organic nitrates were found to be less prone to aqueous
204 hydrolysis than tertiary organic nitrates (Darer et al., 2011, Hu et al., 2011, Boyd et al., 2015,
205 Fisher et al., 2016). This suggests that field-based estimates of the contribution of organic
206 nitrates to SOA formation could be a lower limit, if they are based on measurement of those
207 aerosol-phase nitrates. This is because if hydrolysis is rapid, releasing HNO_3 but leaving behind
208 the organic fraction in the aerosol phase, then that organic mass would not be accurately
209 accounted for as arising from nitrate chemistry. This was addressed in a recent modeling study
210 of SOAS (Pye et al., 2015) in which modeled hydrolysis products of particulate organic nitrates
211 of up to $0.8 \mu\text{g m}^{-3}$ additional aerosol mass loading in the southeast U.S. were included in the
212 estimate of change in OA due to changes in NO_x . Another recent GEOS-Chem modeling study
213 using of gas- and particle-phase organic nitrates observed during the SEAC⁴RS and SOAS
214 campaigns similarly finds RONO_2 to be a major sink of NO_x across the SEUS region (Fisher et
215 al., 2016, Lee et al., 2016).
216
217 Complementing these SOAS ground site measurements, the NOAA-led SENEX (Southeast
218 Nexus) aircraft campaign conducted 18 research flights focused in part on studying the
219 interactions between biogenic and anthropogenic emissions that form secondary pollutants
220 between 3 June and 10 July 2013 (Warneke et al., 2016). Flight instrumentation focused on
221 measurement of aerosol precursors and composition enable the present investigation of SOA
222 yields using this aircraft data set. Edwards et al. (Edwards et al., 2017) used data from the

Juliane Fry 5/15/2018 10:12 PM

Deleted: a factor of three

224 SENEX night flights to evaluate the nighttime oxidation of BVOC, observing high nighttime
225 isoprene mixing ratios in the residual layer that can undergo rapid NO₃ oxidation when sufficient
226 NO_x is present. These authors suggest that past NO_x reductions may have been uncoupled
227 from OA trends due to NO_x not having been the limiting chemical species for OA production, but
228 that future reductions in NO_x may decrease OA if NO₃ oxidation of BVOC is a substantial
229 regional SOA source. Because isoprene is ubiquitous in the nighttime residual layer over the
230 southeastern United States and the NO₃ + isoprene reaction is rapid, NO₃ reaction will be
231 dominant relative to O₃ in places with anthropogenic inputs of NO_x (Edwards et al. (Edwards et
232 al., 2017) concludes that when NO₂/BVOC > 0.5, NO₃ oxidation will be dominant). Hence, a
233 modest NO₃ + isoprene SOA yield may constitute a regionally important OA source.

234
235 Several modeling studies have investigated the effects of changing NO_x on global and SEUS
236 SOA. Hoyle et al. (Hoyle et al., 2007) found an increase in global SOA production from 35 Tg yr⁻¹
237 to 53 Tg yr⁻¹ since preindustrial times, resulting in an increase in global annual mean SOA
238 mass loading of 51%, attributable in part to changing NO_x emissions. Zheng et al. (Zheng et al.,
239 2015) found only moderate SOA reductions from a 50% reduction in NO emissions: 0.9 – 5.6 %
240 for global NO_x or 6.4 – 12.0% for southeast US NO_x, which they attributed to buffering by
241 alternate chemical pathways and offsetting tendencies in the biogenic vs. anthropogenic SOA
242 components. In contrast, Pye et al. (Pye et al., 2015) find a 9% reduction in total organic aerosol
243 in Centreville, AL for only 25% reduction in NO_x emissions. A simple limiting-reagent analysis of
244 NO₃ + monoterpene SOA from power plant plumes across the United States found that between
245 2008 and 2011, based on EPA-reported NO_x emissions inventories, some American power
246 plants shifted to the NO_x-limited regime (from 3.5% to 11% of the power plants), and showed
247 that these newly NO_x-limited power plants were primarily in the southeastern United States (Fry
248 et al., 2015). The effect of changing NO_x on SOA burden is clearly still in need of further study.

249
250 Here, we present aircraft transects of spatially discrete NO_x plumes from electric generating
251 units (EGU), or power plants (PP), as a method to specifically isolate the influence of NO₃
252 oxidation. These plumes are concentrated and highly enriched in NO_x over a scale of only a
253 few km (Brown et al., 2012), and have nitrate radical production rates ($P(\text{NO}_3)$) 10 – 100 times
254 greater than those of background air. The rapid shift in $P(\text{NO}_3)$ allows direct comparison of air
255 masses with slow and rapid oxidation rates attributable to the nitrate radical, effectively isolating
256 the influence of this single chemical pathway in producing SOA and other oxidation products.
257 Changes in organic nitrate aerosol (pRONO₂) concentration and accompanying isoprene
258 titration enable a direct field determination of the SOA yield from NO₃ + isoprene.

259 **2 Field campaign and experimental and modeling methods**

260 The Southeast Nexus (SENEX: <http://esrl.noaa.gov/csd/projects/senex/>) campaign took place 3
261 June through 10 July 2013 as the NOAA WP-3D aircraft contribution to the larger Southeast
262 Atmospheric Study (SAS: http://www.eol.ucar.edu/field_projects/sas/), a large, coordinated
263 research effort focused on understanding natural and anthropogenic emissions, oxidation
264 chemistry and production of aerosol in the summertime atmosphere in the southeastern United
265 States. The NOAA WP-3D aircraft operated 18 research flights out of Smyrna, Tennessee,

266 carrying an instrument payload oriented towards elucidating emissions inventories and reactions
267 of atmospheric trace gases, and aerosol composition and optical properties (Warneke et al.,
268 2016). One of the major goals of the larger SAS study is to quantify the fraction of organic
269 aerosol that is anthropogenically controlled, with a particular focus on understanding how OA
270 may change in the future in response to changing anthropogenic emissions.
271

272 The subset of aircraft instrumentation employed for the present analysis of nighttime NO_3 +
273 isoprene initiated SOA production includes measurements used to determine NO_3 radical
274 production rate ($P(\text{NO}_3) = k_{\text{NO}_2+\text{O}_3}(\text{T}) [\text{NO}_2] [\text{O}_3]$), isoprene and monoterpene concentrations,
275 other trace gases for plume screening and identification, aerosol size distributions, and aerosol
276 composition. The details on the individual measurements and the overall aircraft deployment
277 goals and strategy are described in Warneke et al. (Warneke et al., 2016). Briefly, NO_2 was
278 measured by UV photolysis and gas-phase chemiluminescence (P-CL) and by cavity ringdown
279 spectroscopy, (CRDS), which agreed within 6%. O_3 was also measured by both gas-phase
280 chemiluminescence and CRDS and agreed within 8%, within the combined measurement
281 uncertainties of the instruments. Various volatile organic compounds were measured with
282 several techniques, including for the isoprene and monoterpenes of interest here, proton
283 reaction transfer mass spectrometry (PTR-MS) and canister whole air samples and post-flight
284 GC-MS analysis (iWAS/GCMS). A comparison of PTR-MS and iWAS/GCMS measurements of
285 isoprene during SENEX has high scatter due to imperfect time alignment and isoprene's high
286 variability in the boundary layer, but the slope of the intercomparison is 1.04 ((Warneke et al.,
287 2016); for more details on the VOC intercomparisons, see also Lerner et al., (Lerner et al.,
288 2017)). Acetonitrile from the PTRMS was used to screen for the influence of biomass burning.
289 Sulfur dioxide (SO_2) was used to identify emissions from coal-fired power plants. All gas-phase
290 instruments used dedicated inlets, described in detail in the supplemental information for
291 Warneke et al. (Warneke et al., 2016).
292

293 Aerosol particles were sampled downstream of a low turbulence inlet (Wilson et al., 2004), after
294 which they were dried by ram heating, size-selected by an impactor with 1 μm aerodynamic
295 diameter size cut-off, and measured by various aerosol instruments (Warneke et al., 2016). An
296 ultra-high-sensitivity aerosol sizing spectrometer (UHSAS, Particle Metrics, Inc., Boulder, CO
297 (Cai et al., 2008, Brock et al., 2011)) was used to measure the dry submicron aerosol size
298 distribution down to about 70 nm. Data for the UHSAS are reported at 1 Hz whereas AMS data
299 were recorded roughly every 10 seconds. The ambient (wet) surface areas were calculated
300 according to the procedures described in Brock et al., 2016 (Brock et al., 2016). A pressure-
301 controlled inlet (Bahreini et al., 2008) was employed to ensure that a constant mass flow rate
302 was sampled by a compact time-of-flight aerosol mass spectrometer (C-ToF-AMS) which
303 measured the non-refractory aerosol composition (Drewnick et al., 2005). The aerosol volume
304 transmitted into the AMS was calculated by applying the measured AMS lens transmission
305 curve (Bahreini et al., 2008) to the measured particle volume distributions from the UHSAS. For
306 the entire SENEX study, the mean, calculated fraction of aerosol volume behind the 1 micron
307 impactor that was transmitted through the lens into the AMS instrument was 97% (with $\pm 4\%$
308 standard deviation), indicating that most of the submicron aerosol volume measured by the
309 sizing instruments was sampled by the AMS.

310

311 After applying calibrations and the composition-dependent collection efficiency following
312 Middlebrook et al. (Middlebrook et al., 2012), the limits of detection for the flight analyzed here
313 were $0.05 \mu\text{g m}^{-3}$ for nitrate, $0.26 \mu\text{g m}^{-3}$ for organic mass, $0.21 \mu\text{g m}^{-3}$ for ammonium, and 0.05
314 $\mu\text{g m}^{-3}$ for sulfate, determined as three times the standard deviation of 10-second filtered air
315 measurements obtained for 10 minutes during preflight and 10 minutes during postflight (110
316 datapoints). Note that the relative ionization efficiency for ammonium was 3.91 and 3.87 for the
317 two bracketing calibrations and an average value of 3.9 was used for the flight analyzed here.
318 An orthogonal distance regression (ODR-2) of the volume from composition data (AMS mass
319 plus refractory black carbon) using a mass weighted density as described by Bahreini et al.
320 (Bahreini et al., 2009) versus the volume based on the sizing instruments (after correcting for
321 AMS lens transmission as above) had a slope of 1.06 for the entire SENEX study and 72% of
322 the data points were within the measurements' combined uncertainties of $\pm 45\%$ (Bahreini et al.,
323 2008). For the flight analyzed here, however, the same regression slope was 1.58, which is
324 slightly higher than the combined uncertainties. It is unclear why the two types of volume
325 measurements disagree more for this flight. This does not change the conclusions of this work,
326 because this has been incorporated into the error in aerosol organic nitrate, which still show
327 positive enhancements in pRONO₂ for these plumes (see Figure 4 below). These complete
328 error estimates are also used in Figure 5 to clearly show the uncertainties in the yields. The
329 volume comparison is discussed further in the Supplemental Information and shown for the
330 plumes of interest in Fig. S1.

331

332 The C-ToF-AMS is a unit mass resolution (UMR) instrument and the mass spectral signals that
333 are characteristic of aerosol nitrate at m/z 30 and 46 (NO^+ and NO_2^+) often contain interferences
334 from organic species such as CH_2O^+ and CH_2O_2^+ , respectively. Here, the m/z 30 and 46 signals
335 have been corrected for these interferences by using correlated organic signals at m/z 29, 42,
336 43, and 45 that were derived from high-resolution AMS measurements during the NASA
337 SEAC⁴RS campaign that took place in the same regions of the SE US shortly after SENEX (see
338 Supplemental Information and Fig. S2). The corrections were applied to the individual flight
339 analyzed here from July 2. All of the corrections were well correlated with each other for the
340 SEAC⁴RS dataset and we used the organic peak at m/z 29 (from CHO^+) and the peak at m/z 45
341 (from CHO_2^+), respectively, since those corrections were from peaks closest (in m/z) to those
342 being corrected. Once corrected, the nitrate mass concentrations in the final data archive for
343 this flight were reduced by 0-0.24 $\mu\text{g sm}^{-3}$, an average reduction of $0.11 \mu\text{g sm}^{-3}$ or 32% from
344 the initial nitrate mass concentrations. The organic interferences removed from the m/z 30 and
345 m/z 46 signals are linearly correlated with the total organic mass concentrations, corresponding
346 to an average 1.3% increase in the total organic mass.

347

348 The ratio of the corrected $\text{NO}_2^+/\text{NO}^+$ signals was then used to calculate the fraction of aerosol
349 nitrate that was organic (pRONO₂) or inorganic (ammonium nitrate) based on the method
350 described first in (Fry et al., 2013). Here we used an organic $\text{NO}_2^+/\text{NO}^+$ ratio that was equal to
351 the ammonium nitrate $\text{NO}_2^+/\text{NO}^+$ ratio from our calibrations divided by 2.8. This factor was
352 determined from multiple datasets (see discussion in Supplemental Information). The
353 ammonium nitrate $\text{NO}_2^+/\text{NO}^+$ ratio was obtained from the two calibrations on 30 June and 7 July

Juliane Fry 5/31/2018 5:01 PM

Deleted: , since other flights during this field project compared better;

Juliane Fry 5/31/2018 5:01 PM

Deleted: t

Juliane Fry 5/31/2018 5:47 PM

Deleted: ,

Juliane Fry 5/31/2018 5:10 PM

Deleted: but

Juliane Fry 5/31/2018 5:10 PM

Deleted: comparisons are

Juliane Fry 5/26/2018 6:02 PM

Deleted: Fry et al. [27]

Juliane Fry 5/26/2018 10:18 PM

Deleted: compiled by Day et al (Day et al., 2017)

Juliane Fry 5/26/2018 10:19 PM

Deleted: , who discuss the uncertainties of this approach in detail

365 that bracketed the flight on 2 July, which is analyzed here. It was 0.514 and 0.488, respectively,
366 and for all of the data from both calibrations it averaged 0.490. Hence, the organic nitrate
367 $\text{NO}_2^*/\text{NO}^*$ ratio was estimated to be 0.175. This is the first time, to our knowledge, that UMR
368 measurements of aerosol nitrate have been corrected with HR correlations and used to
369 apportion the corrected nitrate into inorganic or organic nitrate species.

370

371 The time since emission of intercepted power plant plumes was estimated from the slope of a
372 plot of O_3 against NO_2 . For nighttime emitted NO_x plumes that consist primarily of NO (Peischl
373 et al., 2010), O_3 is negatively correlated with NO_2 due to the rapid reaction of NO with O_3 that
374 produces NO_2 in a 1:1 ratio:

375



377

378 Reaction R1 goes rapidly (NO pseudo first order loss rate coefficient of 0.03 s^{-1} at 60 ppb O_3) to
379 completion, so that all NO_x is present as NO_2 , as long as the plume NO does not exceed
380 background O_3 after initial mixing of the plume into background air. Subsequent oxidation of
381 NO_2 via reaction (R2) leads to an increasingly negative slope of O_3 vs NO_2 :

382



384

385 Equation (1) then gives plume age subsequent to the completion of (R1) in terms of the
386 observed slope, m , of O_3 vs NO_2 (Brown et al., 2006).

387

$$t_{\text{plume}} = \frac{\ln[1-S(m+1)]}{sk_1\bar{\text{O}}_3} \quad (1)$$

389

390 Here S is a stoichiometric factor that is chosen for this analysis to be 1 based on agreement of
391 plume age with elapsed time in a box model run initialized with SENEX flight conditions (see
392 below); k_1 is the temperature dependent bimolecular rate constant for $\text{NO}_2 + \text{O}_3$ (R2) and $\bar{\text{O}}_3$ is
393 the average O_3 within the plume.

394

395 We calculate plume ages using both a stoichiometric factor of 1 (loss of NO_3 and N_2O_5
396 dominated by NO_3 reactions) and 2 (loss dominated by N_2O_5 reactions), although we note that
397 the chemical regime for $\text{NO}_3+\text{N}_2\text{O}_5$ loss may change over the lifetime of the plume, progressing
398 from 1 to 2 as the BVOC is consumed. We use $S=1$ values in the analysis that follows. Because
399 the more aged plumes are more likely to have S approach 2, this means that some of the older
400 plumes may have overestimated ages. Fig. S3 in the Supplemental Information shows the
401 plume age calculated by Eq. 1 using modeled NO_x , NO_y and O_3 concentrations for $S=1$ and
402 $S=2$, from nighttime simulations of plume evolution using an observationally constrained box
403 model. This confirms that for nighttime plumes, $S=1$ plume ages match modeled elapsed time
404 well. The model used for this calculation, and those used to assess peroxy radical lifetimes and
405 fates in Section 4.3, was the Dynamically Simple Model of Atmospheric Chemical Complexity
406 (DSMACC (Emmerson and Evans 2009)) containing the Master Chemical Mechanism v3.3.1
407 chemistry scheme (Jenkin et al., 2015). More details on the model approach are provided in the
408 SI.

Juliane Fry 5/15/2018 9:54 PM

Deleted: 2

Juliane Fry 6/1/2018 8:11 AM

Deleted: .

411 3 Nighttime flight selection

412 There were three nighttime flights (takeoffs on the evenings of 19 June, 2 July, and 3 July,
413 2013, local time) conducted during SENEX, of which one (2 July) surveyed regions surrounding
414 Birmingham, Alabama, including multiple urban and power plant plume transects. As described
415 in the introduction, these plume transects are the focus of the current analysis since they
416 correspond to injections of concentrated NO (and subsequently high $P(\text{NO}_3)$) into the regionally
417 widespread residual layer isoprene. The nighttime flight on 3 July, over Missouri, Tennessee
418 and Arkansas sampled air more heavily influenced by biomass burning than biogenic emissions.
419 The 19 June night flight sampled earlier in the evening, in the few hours immediately after
420 sunset, and sampled more diffuse urban plume transects that had less contrast with background
421 air. Therefore, this paper uses data exclusively from the 2 July flight, in which 9 transects of
422 well-defined NO_x plumes from power plants emitted during darkness can be analyzed to obtain
423 independent yields measurements.

424
425 A map of the 2 July flight track is shown in Fig. 1a. After takeoff at 8:08 pm local Central
426 Daylight Time on 2 July, 2013 (1:08 am UTC 3 July, 2016), the flight proceeded towards the
427 southwest until due west of Montgomery, AL, after which it conducted a series of east-west
428 running tracks while working successively north toward Birmingham, AL. Toward the east of
429 Birmingham, the aircraft executed overlapping north-south tracks at six elevations to sample the
430 E. C. Gaston power plant. During the course of the flight, concentrated NO_x plumes from the
431 Gaston, Gorgas, Miller and Greene City power plants were sampled. Around 1:30 and 2:30 AM
432 Central Daylight Time (5:30 and 6:30 am UTC), two transects of the Birmingham, AL urban
433 plume were measured prior to returning to the Smyrna, TN airport base.

434
435 The flight track is shown colored by the nitrate radical production rate, $P(\text{NO}_3)$, to show the
436 points of urban and/or power plant plume influence:

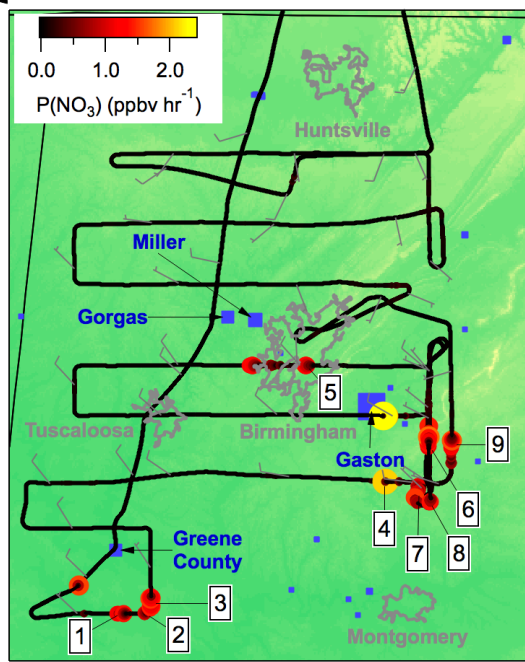
$$437 \quad P(\text{NO}_3) = k_2(T) [\text{NO}_2][\text{O}_3] \quad (2)$$

438
439 Here, k_2 is again the temperature-dependent rate coefficient for reaction of $\text{NO}_2 + \text{O}_3$ (Atkinson
440 et al., 2004), and the square brackets indicate **concentrations**. Fig. 1b further illustrates the
441 selection of power plants plumes: sharp peaks in $P(\text{NO}_3)$ are indicative of power plant plume
442 transects, during which isoprene mixing ratios also are observed to drop from the typical
443 regional residual layer background values of ~ 1 ppb, indicative of loss by NO_3 oxidation (an
444 individual transect is shown in more detail below in Fig. 2). Also shown in Fig. 1b are measured
445 concentrations of isoprene and monoterpenes throughout the flight, showing substantial residual
446 layer isoprene and supporting the assumption that effectively all NO_3 reactivity is via isoprene
447 (see calculation in next section). Residual layer concentrations of other VOCs that could
448 produce SOA (e.g., aromatics) are always below 100 pptv, and their reaction rates with NO_3 are
449 slow. Edwards *et al.* (Edwards et al., 2017) have shown that NO_3 and isoprene mixing ratios for
450 this and other SENEX night flights exhibit a strong and characteristic anticorrelation that is
451 consistent with nighttime residual layer oxidation chemistry.

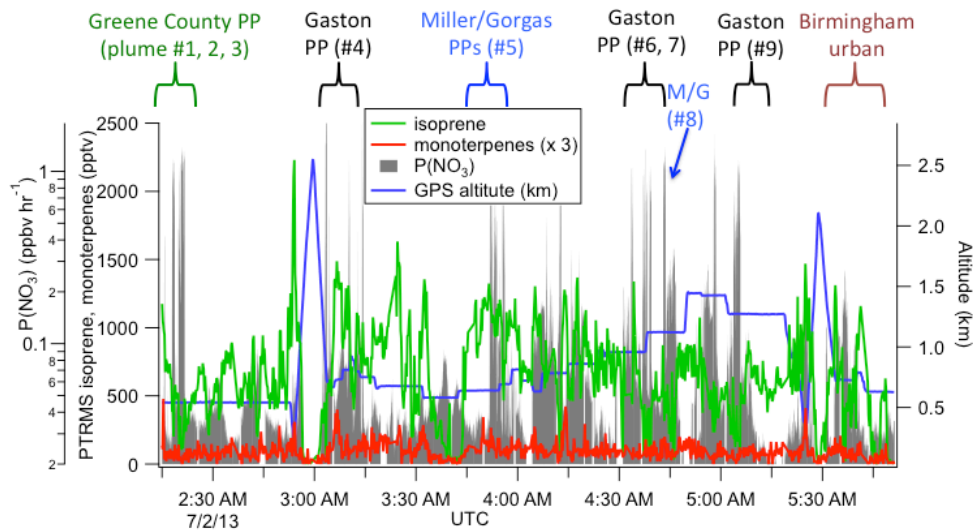
452
453

Juliane Fry 5/15/2018 9:06 PM

Deleted: number densities



455 1a
456 1b



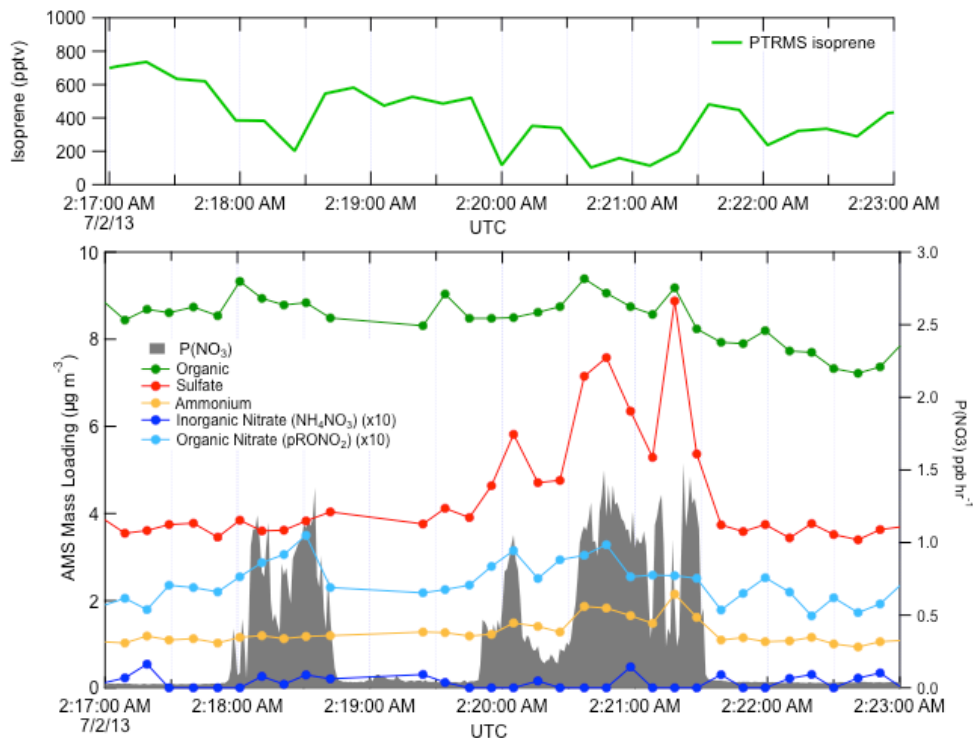
457
458 **Figure 1a.** Map of northern Alabama, showing the location of the flight track of the 2 July 2013
459 night flight used in the present analysis, with plume numbers labeled and wind direction shown.
460 Although the wind direction changed throughout the night, these measurements enable us to

461 attribute each plume to a power plant source (see labels in Figure 1b and Table 2). Color scale
462 shows $P(\text{NO}_3)$ based on aircraft-measured $[\text{NO}_2]$ and $[\text{O}_3]$, while power plants discussed in the
463 text are indicated in blue squares with marker size scaled to annual NO_x emissions for 2013
464 (scale not shown). Isoprene emissions are widespread in the region (Edwards et al., 2017).
465 **Figure 1b** shows time series data from the same flight, with plume origins and numbers labeled,
466 showing aircraft-measured isoprene and monoterpene concentrations, altitude, and $P(\text{NO}_3)$
467 determined according to Eq. 2 (log scale), showing that the isoprene was uniformly distributed
468 (mixing ratios often in excess of 1 ppbv), while the more reactive monoterpenes were present at
469 mixing ratios below 100 ppt except at the lowest few hundred meters above ground in the
470 vertical profiles (not used in the present analysis). Figure 1b also shows that sharp peaks in
471 nitrate radical production rate occur both at the lowest points of these vertical profiles, when the
472 aircraft approached the surface, but also frequently during periods of level flight in the residual
473 layer, which correspond to the power plant plume transects analyzed in this paper.

474 **4 Results**

475 **4.1 Selection of plumes**

476 Figure 2 shows a subset of the July 2 flight time series data, illustrating three NO_x plumes used
477 for analysis. The large NO_3 source and isoprene loss was accompanied by an increase in
478 organic nitrate aerosol mass, which we attribute to the $\text{NO}_3 + \text{isoprene}$ reaction based on prior
479 arguments. We observed each plume as a rapid and brief perturbation to background
480 conditions, of order 10 – 50 sec., or 1 – 5 km in spatial scale. Each plume's perturbed
481 conditions can correspond to different plume ages, depending on how far downwind of the
482 power plant the plume transect occurred.



484
 485 **Figure 2.** Three representative plume transect observations from the 2 July 2013 flight (plumes
 486 are identified by the peaks in $P(\text{NO}_3)$, listed in Table 1 at times 02:18, 02:20, and 02:21 UTC).
 487 Note the difference in sulfate enhancement in the three plumes, which is largest in the third
 488 plume, and is accompanied by increases in ammonium. In all three cases, the isoprene
 489 concentration drops in the plumes, accompanied by a clear increase in organic nitrate, no
 490 changes in the inorganic nitrate, and a modest changes in organic aerosol mass concentrations.
 491

492 Candidate plumes were initially identified by scanning the time series flight data for any period
 493 where the production rate of nitrate radical ($P(\text{NO}_3)$) rose above 0.5 ppbv hr^{-1} . This threshold
 494 was chosen to be above background noise and large enough to isolate only true plumes (see
 495 Fig. 1a). The value is thus subjectively chosen, but was consistently applied across the dataset.
 496 For each such period, a first screening removed any of these candidate plumes that occurred
 497 during missed approaches or other periods where radar altitude above ground level (AGL) was
 498 changing, because in the stratified nighttime boundary layer structure, variations in altitude may
 499 result in sampling different air-masses, rendering the adjacent out of plume background not
 500 necessarily comparable to in-plume conditions. A second criterion for rejection of a plume was
 501 missing isoprene or AMS data during brief plume intercepts. No selected plumes on July 2
 502 showed enhanced acetonitrile or refractory black carbon, indicating no significant biomass

503 burning influence. Finally, two plumes downwind of the Gaston power plant (at 03:10 and
504 03:14) were removed from the present analysis, because (03:10) the background isoprene was
505 changing rapidly, preventing a good baseline measurement, and (03:14) there was no observed
506 decrease in isoprene concentration in-plume (as well as no increase in nitrate aerosol). The
507 03:14 plume was apparently too recently emitted to have undergone significant nighttime
508 reaction; its O_3/NO_2 slope was unity to within the combined measurement error of O_3 and NO_2
509 (Eq. 1). After this filtering, there are 9 individual plume observations for determination of NO_3 +
510 isoprene SOA yields (see Table 1). The rapid increases in $P(NO_3)$ appeared simultaneously with
511 significant decreases in isoprene and increases in aerosol nitrate. The aerosol and isoprene
512 measurements (taken at data acquisition rates < 1 Hz) were not exactly coincident in time which
513 leads to some uncertainty in the yield analysis below.

514

515 Derivation of SOA yields from observed changes in isoprene and aerosol mass in plumes
516 depends on two conditions, and has several caveats that will be discussed in the text that
517 follows (see Table 3 below for a summary of these caveats). The two conditions are: (1) that the
518 majority of VOC mass consumed by NO_3 in plumes is isoprene (rather than monoterpenes or
519 other VOC), and then either or both (2a) that the change in aerosol organic mass concentration
520 during these plumes is due to NO_3 + isoprene reactions, and/or (2b) that the change in aerosol
521 nitrate mass concentration is due to NO_3 + isoprene reactions. There are separate
522 considerations for each of these conditions.

523

524 For the first condition, we note that the isoprene to monoterpenes ratio just outside each plume
525 transect was always high (a factor of 10 to 70, on average 26). With the 298 K NO_3 rate
526 constants of $\sim 5 \times 10^{-12} \text{ cm}^3 \text{ molec}^{-1} \text{ s}^{-1}$ for monoterpenes and $6.5 \times 10^{-13} \text{ cm}^3 \text{ molec}^{-1} \text{ s}^{-1}$ for
527 isoprene (Calvert et al., 2000), isoprene (~ 2 ppb) will always react faster with nitrate than
528 monoterpenes (~ 0.04 ppbv). At these relative concentrations, even if all of the monoterpene is
529 oxidized, the **production rate of oxidation products will** be much larger for isoprene. Contribution
530 to aerosol by N_2O_5 uptake is also not important in these plumes. Edwards et al. (Edwards et al.,
531 2017) calculated the sum of NO_3 and N_2O_5 loss throughout this flight and showed that it is
532 consistently NO_3 +BVOC dominated (Fig. S4 of that paper). As isoprene depletes, N_2O_5 uptake
533 will increasingly contribute to NO_3 loss, but as shown below, we are able to rule out a
534 substantial source of inorganic nitrate for most plumes. We also know that despite increased
535 OH production in-plume, the isoprene loss is still overwhelming dominated by NO_3 (Fig. S5 in
536 Edwards, et al. (Edwards et al., 2017)).

537

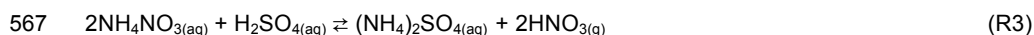
538 The second condition requires that we can find an aerosol signal that is attributable exclusively
539 to NO_3 + isoprene reaction products, whether it be organic aerosol (OA) or organic nitrate
540 aerosol ($pRONO_2$) mass loading, or both. We note that the ratio of in-plume aerosol organic
541 mass increase to $pRONO_2$ mass increase is noisy (see discussion below at Fig. 6), but indicates
542 an average in-plume ΔOA to $\Delta pRONO_2$ ratio of about 5. The large variability is primarily due to
543 the fact that the variability in organic aerosol mass between successive 10-second data points
544 for the entire flight is quite large (of order $0.75 \mu\text{g m}^{-3}$) and comparable to many of the individual
545 plume ΔOA increases, far exceeding the expected organonitrate driven increases in OA, which
546 are roughly twice the $pRONO_2$ mass increases. It is also possible that in these plumes, where

Juliane Fry 5/15/2018 9:56 PM

Deleted: mass of hydrocarbon conversion will

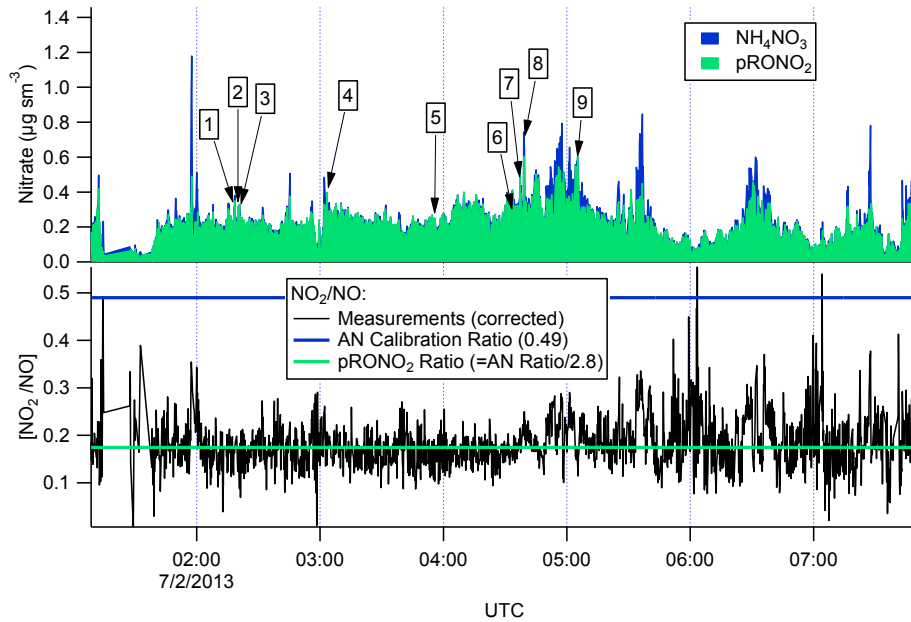
549 total aerosol mass is elevated, semivolatile organic compounds may re-partition to the aerosol
550 phase, contributing a non-pRONO₂ driven variability in ΔOA. For example, if some gas phase
551 IEPOX is present in the residual layer, it may be taken up into the highly acidic aerosol from the
552 power plants. Alternatively, very polar gas-phase compounds could partition further into the
553 higher liquid water associated with the sulfate in the plume. Therefore, in-plume organic aerosol
554 increases cannot be attributed clearly to NO₃ + isoprene SOA production, so we do not use
555 them in the SOA yield calculations.

556
557 This leaves consideration 2b, whether all increase in nitrate mass is due to NO₃ + isoprene
558 reactions. Here we must evaluate the possibility of inorganic nitrate aerosol production in these
559 high-NO_x plumes. Fine-mode aerosol inorganic nitrate can be formed by the (reversible)
560 dissolution of HNO_{3(g)} into aqueous aerosol. In dry aerosol samples, inorganic nitrate is typically
561 in the form of ammonium nitrate (NH₄NO₃), when excess ammonium is available after
562 neutralization of sulfate as (NH₄)₂SO₄ and NH₄(HSO₄). Because of the greater stability of
563 ammonium sulfate salt relative to ammonium nitrate, in high-sulfate plumes with limited
564 ammonium, inorganic nitrate aerosol will typically evaporate as HNO_{3(g)} (Guo et al., 2015)
565 (reaction R3):



567
568 Inorganic nitrate can also form when crustal dust (e.g. CaCO₃) or seasalt (NaCl) are available.
569 Uptake of HNO₃ is rendered favorable by the higher stability of nitrate mineral salts, evaporating
570 CO₂ or HCl. [Inorganic nitrate can also be produced by the heterogeneous uptake of N₂O₅ onto](#)
571 [aqueous aerosol; Edwards et al. \(2017\) demonstrated that this process is negligible relative to](#)
572 [NO₃ + BVOC for the July 2 SENEX night flight considered here.](#)

573
574 There are several lines of evidence that the observed nitrate aerosol is organic and not
575 inorganic. First, examination of the NO₂⁺/NO⁺ (interference-corrected *m/z* 46:*m/z* 30) ratio
576 measured by the aircraft AMS (Fig. 3) shows a ratio throughout the July 2 flight, including the
577 selected plumes, that is substantially lower than that from the bracketing ammonium nitrate
578 calibrations. This lower AMS measured NO₂⁺/NO⁺ ratio has been observed for organic nitrates
579 (Farmer et al., 2010), and some mineral nitrates (e.g. Ca(NO₃)₂ and NaNO₃, (Hayes et al.,
580 2013)), which are not important in this case because aerosol was dominantly submicron. As
581 described above, we can separate the observed AMS nitrate signal into pRONO₂ and inorganic
582 nitrate contributions. These mass loadings are also shown in Fig. 3, indicating dominance of
583 pRONO₂ throughout the flight.
584



586

587 **Figure 3.** For the flight under consideration, the estimated relative contributions of ammonium
 588 and organic nitrate to the total corrected nitrate signal (top panel) was calculated from the ratios
 589 of the corrected peaks at m/z 30 and 46 (lower panel). Each of the plumes is identified here by
 590 plume number. The ratios of $\text{NO}_2^+/\text{NO}^+$ (black data in the lower panel) from the corrected peaks
 591 at m/z 46 and 30, respectively, are compared to the ratios expected for ammonium nitrate (AN
 592 Calibration Ratio, blue horizontal line at 0.49) or organic nitrate (pRONO₂ Ratio, green
 593 horizontal line at 0.175 which is estimated from the AN calibration ratio using multiple data sets
 594 (see discussion in Supplemental Information). The measured ratio for most of the flight is more
 595 characteristic of organic nitrate than ammonium nitrate.
 596

597 We can also employ the comparison of other AMS-measured aerosol components during the
 598 individual plumes to assess the possibility of an inorganic nitrate contribution to total measured
 599 nitrate. Fig. S5a shows that the in-plume increases in sulfate are correlated with increases in
 600 ammonium with an R^2 of 0.4. The observed slope of 5.4 is characteristic of primarily $(\text{NH}_4)\text{HSO}_4$,
 601 which indicates that the sulfate mass is not fully neutralized by ammonium. We note, however,
 602 that if the largest observed aerosol nitrate increase is due solely to ammonium nitrate, the
 603 ammonium increase would be only $0.11 \mu\text{g m}^{-3}$, which would be difficult to discern from the NH_4
 604 variability of order $0.11 \mu\text{g m}^{-3}$. However, the slope is consistent with incomplete neutralization
 605 of the sulfate by ammonium, which would make $\text{HNO}_{3(g)}$ the more thermodynamically favorable
 606 form of inorganic nitrate. The ion balance for the ammonium nitrate calibration particles and the
 607 plume enhancements are shown in Fig. S5b. Complete neutralization of the calibration aerosols
 608 is nearly always within the gray 10% uncertainty band for the relative ionization efficiency of

Juliane Fry 5/26/2018 9:56 PM
 Deleted: by Day et al. (Day et al., 2017)

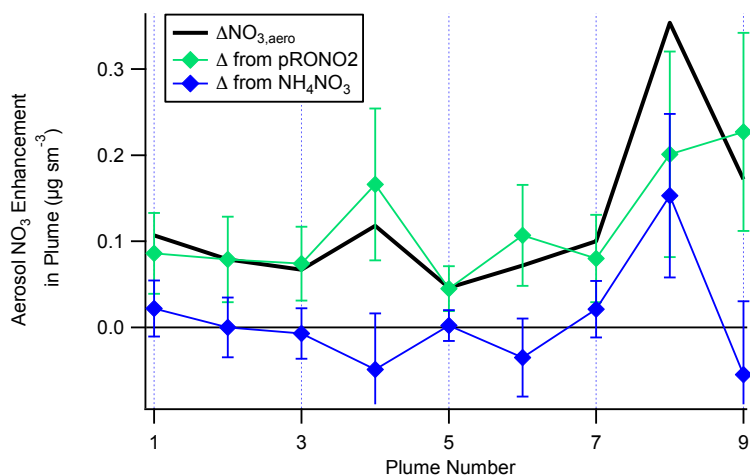
Juliane Fry 6/1/2018 8:39 AM
 Formatted: Normal

Juliane Fry 6/1/2018 8:39 AM
 Formatted: Font color: Auto

Juliane Fry 6/1/2018 8:39 AM
 Formatted: Font:Not Bold, Font color:
 Auto

610 ammonium (Bahreini et al., 2009). In contrast, many of the plume enhancements are near the
611 1:2 line (as primarily ammonium bisulfate) within the combined 10% ammonium and 15%
612 sulfate uncertainty error bars or without ammonium (sulfuric acid). Thus, NH_4NO_3 is unlikely to
613 be stable in the aerosol phase under the conditions of these plumes, consistent with the AMS
614 observations.

615
616 A plot of the calculated plume enhancements from the derived apportionment into organic
617 (pRONO₂) and inorganic (ammonium) nitrate is shown in Fig. 4. The increases in aerosol nitrate
618 for nearly all of the plumes appear to be mostly due to enhancements in pRONO₂. Based on
619 these considerations, we conclude that in-plume pRONO₂ mass increases are a consequence
620 (and thus a robust measure) of organic nitrate aerosol produced from NO₃ + isoprene. Since
621 each isoprene molecule condensing will have one nitrate group, the ratio of these increases to
622 isoprene loss is a direct measure of the molar organic aerosol yield from NO₃-isoprene
623 oxidation.



624

625

626 **Figure 4.** The contribution of each species to the nitrate enhancements in each of the plumes,
627 showing that the enhancements in most of the plumes are mainly due to enhancements in
628 organic nitrate, with the exception of Plume 8 which had enhancements in both organic and
629 ammonium nitrate. Error bars are estimated from the measurement variability, the UMR
630 corrections to the nitrate signals, apportionment between organic and inorganic nitrate, and the
631 total nitrate uncertainty (see Supplemental Information).

632

633 Table 1 shows the selected plumes to be used for yield analysis. Wherever possible, multiple
634 points have been averaged for in-plume and background isoprene and nitrate aerosol
635 concentrations; in each case the number of points used is indicated and the corresponding
636 standard deviations are reported. In two cases (2:20 and 3:03 plumes), the plumes were so
637 narrow that only a single point was measured in-plume at the 10 s time resolution of the PTR-

Juliane Fry 6/1/2018 8:39 AM

Formatted: Font:(Default) Times, 10 pt,
Font color: Auto

638 MS and AMS; for these “single-point” plumes it is not possible to calculate error bars. Error bars
639 were determined using the standard deviations calculated for in-plume and background
640 isoprene and nitrate aerosol concentrations, [accounting also for the additional uncertainty in the](#)
641 [AMS measurement described in the caption to Figure 4](#), and propagated through the yield
642 formula detailed in the following section.
643

644 **Table 1.** List of plumes used in this NO₃ + isoprene SOA yield analysis. For each plume, the
 645 delta-values listed indicate the difference between in-plume and outside-plume background in
 646 average observed concentration, and the standard deviations (SD) are the propagated error
 647 from this subtraction. (For ΔNO₃ from pRONO₂, the standard deviations also include error
 648 propagated from the uncertainties in the nitrate apportionment and aerosol volume, as
 649 described in the caption for Figure 4) After each plume number, the numbers of points averaged
 650 for isoprene (10 s resolution) and AMS (10 s resolution), respectively, are listed. Because the
 651 isoprene data were reported at a lower frequency, these numbers are typically lower to cover
 652 the same period of time. Plume numbers annotated with * indicate brief plumes for which only
 653 single-point measurements of in-plume aerosol composition were possible. Additional AMS and
 654 auxiliary data from each plume is included in the Supplemental Information, Table S3.

plume number [#isop/#AMS]	7/2/13 plume time (UTC)	P(NO ₃) (ppbv hr ⁻¹)	ΔISOP (ppt) [± SD]	ΔNO _{3,aero} (μg m ⁻³) [± SD]	ΔNO ₃ from pRONO ₂ (μg m ⁻³) [± SD]	ΔNO ₃ from NH ₄ NO ₃ (μg m ⁻³) [± SD]
Typical variability (μg m ⁻³):				0.05	0.05	0.05
1 [2/3]	2:18	0.9 _v	-335 [128]	0.107 [0.039]	0.086 [0.047]	0.022 [0.012]
2 [*]	2:20	0.8 _v	-404	0.079	0.079	0
3 [4/5]	2:21	1.2 _v	-228 [121]	0.067 [0.039]	0.074 [0.043]	-0.007 [0.027]
4 [*]	3:03	1.4 _v	-453	0.118	0.166	-0.049
5** [3/4]	3:55	1.0 _v	-255 [251]	0.046 [0.019]	0.045 [0.026]	0.002 [0.015]
6 [2/2]	4:34	0.6 _v	-713 [219]	0.072 [0.031]	0.107 [0.059]	-0.035 [0.029]
7 [5/6]	4:37	0.8 _v	-298 [197]	0.100 [0.082]	0.080 [0.051]	0.021 [0.034]
8*** [2/3]	4:39	0.9 _v	-443 [75]	0.354 [0.058]	0.201 [0.12]	0.153 [0.057]
9 [7/8]	5:04	0.6 _v	-293 [131]	0.172 [0.048]	0.227 [0.115]	-0.055 [0.042]

655 **Plume 5 has the smallest ΔNO_{3,aero} and may be affected by background pRONO₂ variability.

656 ***Plume 8 has a measurable increase in inorganic nitrate as well as organic.

657 4.2 SOA yield analysis

658 A molar SOA yield refers to the number of molecules of aerosol organic nitrate produced per
 659 molecule of isoprene consumed. In order to determine molar SOA yields from the data
 660 presented in Table 1, we convert the aerosol organic nitrate mass loading differences to mixing
 661 ratio differences (ppt) using the NO₃ molecular weight of 62 g mol⁻¹ (the AMS organic nitrate

Juliane Fry 5/15/2018 8:52 PM
 Comment [2]: add P(NO₃) to table

Juliane Fry 6/1/2018 3:35 PM
 Formatted: Subscript

Juliane Fry 6/1/2018 3:35 PM
 Formatted: Subscript

Juliane Fry 5/26/2018 5:28 PM
 Formatted Table

Juliane Fry 5/26/2018 5:18 PM
 Formatted: Superscript

Juliane Fry 5/26/2018 5:14 PM
 Deleted: ΔISOP (ppt) ... [1]

Juliane Fry 5/26/2018 5:14 PM
 Deleted: -335 ... [2]

Juliane Fry 6/1/2018 3:25 PM
 Deleted: 33

Juliane Fry 5/26/2018 5:14 PM
 Deleted: -404

Juliane Fry 5/26/2018 5:14 PM
 Deleted: -228 ... [3]

Juliane Fry 6/1/2018 3:25 PM
 Deleted: 8

Juliane Fry 5/26/2018 5:14 PM
 Deleted: -453

Juliane Fry 5/26/2018 5:14 PM
 Deleted: -255 ... [4]

Juliane Fry 5/26/2018 5:14 PM
 Deleted: -713 ... [5]

Juliane Fry 6/1/2018 3:25 PM
 Deleted: 34

Juliane Fry 5/26/2018 5:14 PM
 Deleted: -298 ... [6]

Juliane Fry 6/1/2018 3:25 PM
 Deleted: 077

Juliane Fry 5/26/2018 5:14 PM
 Deleted: -443 ... [7]

Juliane Fry 6/1/2018 3:27 PM
 Deleted: 12

Juliane Fry 5/26/2018 5:14 PM
 Deleted: -293 ... [8]

Juliane Fry 6/1/2018 3:27 PM
 Deleted: 056

686 | **mass is the mass only of the $-ONO_2$ portion of the organonitrate aerosol**). At standard
687 conditions of 273 K and 1 atm (all aerosol data are reported with this STP definition), 1000 ppt
688 $NO_3 = 2.77 \mu g m^{-3}$, so each ΔM_{pRONO_2} is multiplied by $361 ppt (\mu g m^{-3})^{-1}$ to determine this molar
689 yield:

691
$$Y_{SOA,molar} = \frac{(pRONO2_{plume} \pm SD_{pRONO2plume}) - (pRONO2_{bkg} \pm SD_{pRONO2bkg})}{-[(isop_{plume} \pm SD_{isopplume}) - (isop_{bkg} \pm SD_{isopbkg})]} \times \frac{361 ppt NO_3}{\mu g m^{-3}} \quad (3)$$

692 The SOA molar yields resulting from this calculation are shown in Table 2, spanning a range of
693 5-28%, with uncertainties indicated based on the SDs in measured AMS and isoprene
694 concentrations. In addition to this uncertainty based on measurement precision and ambient
695 variability, there is an uncertainty of 50% in the AMS derived-organic nitrate mass loadings (see
696 SI) and 25% in the PTR-MS isoprene concentrations (Warneke et al., 2016). The average molar
697 pRONO₂ yield across all plumes, with each point weighed by the inverse of its standard
698 deviation and assuming SD = 0.1 for single point plumes, is 9%. (As noted below, the yield
699 appears to increase with plume age, so this average obscures that trend.) An alternate
700 graphical analysis of molar SOA yield from all nine plumes plus one 'null' plume (03:14, in which
701 no isoprene had yet reacted and thus not included in Tables 1 and 2) obtains the same average
702 molar yield of 9% (Fig. 5). Here, the molar yield is the slope of a plot of plume change in
703 pRONO₂ vs plume change in isoprene. The slope is determined by a linear fit with points
704 weighted by the square root of the number of AMS data points used to determine in-plume
705 pRONO₂ in each case. **We have not corrected the calculated yields for the possibility of NO_3
706 heterogeneous uptake, which could add a nitrate functionality to existing aerosol. Such a
707 process could be rapid if the uptake coefficient for NO_3 were 0.1, a value characteristics of
708 unsaturated substrates (Ng et al., 2017), but would not contribute measurably at more
709 conventional NO_3 uptake coefficients of 0.001 (Brown and Stutz 2012).**

710
711
712

Juliane Fry 5/26/2018 9:16 PM
Formatted: Subscript

Juliane Fry 6/1/2018 8:21 AM
Formatted: Font:Not Bold, Font color: Auto

Juliane Fry 6/1/2018 8:21 AM
Formatted: Font:11 pt, Not Bold, Font color: Auto

Juliane Fry 6/1/2018 8:21 AM
Formatted: Font:Not Bold, Font color: Auto

Juliane Fry 6/1/2018 8:21 AM
Formatted: Font:11 pt, Not Bold, Font color: Auto

Juliane Fry 6/1/2018 8:21 AM
Formatted: Font:Not Bold, Font color: Auto

Juliane Fry 6/1/2018 8:21 AM
Formatted: Font color: Auto

Juliane Fry 6/1/2018 8:21 AM
Formatted: Font:Not Bold, Font color: Auto

Juliane Fry 6/1/2018 8:21 AM
Formatted: Font:11 pt, Not Bold, Font color: Auto

Juliane Fry 6/1/2018 8:21 AM
Formatted: Font:Not Bold, Font color: Auto

Juliane Fry 6/1/2018 8:21 AM
Formatted: Font color: Auto

Juliane Fry 6/1/2018 8:21 AM
Formatted: Font color: Auto

Juliane Fry 6/1/2018 8:21 AM
Formatted: Font:Not Bold, Font color: Auto

Juliane Fry 6/1/2018 8:21 AM
Formatted: Font:11 pt

713

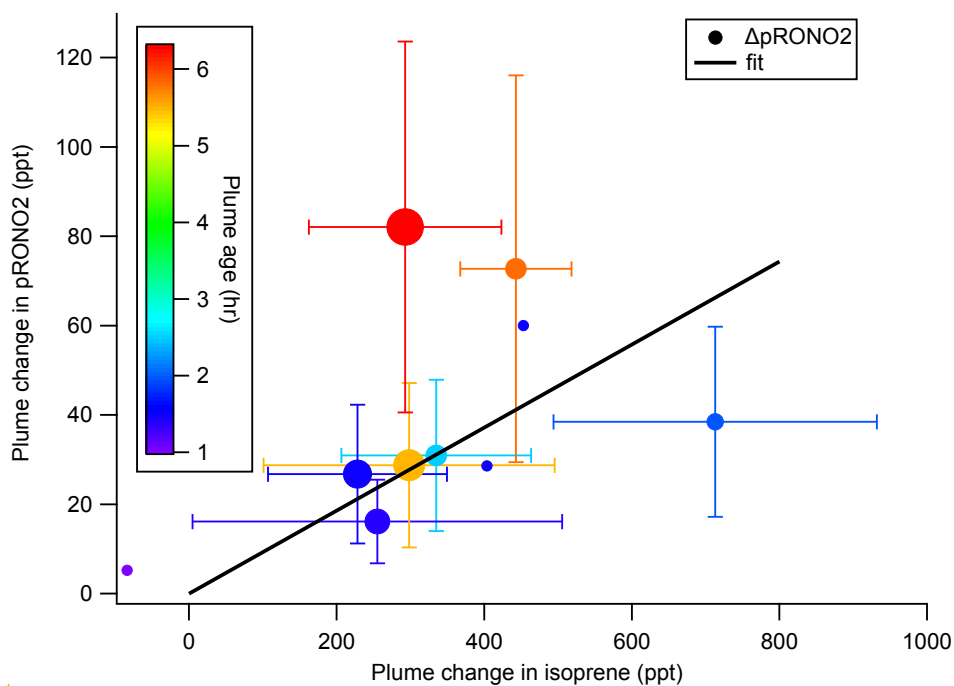
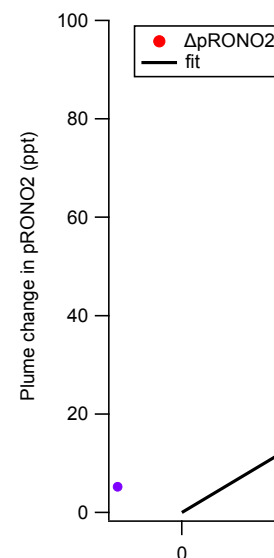
714
715

Figure 5. SOA molar yield can be determined as the slope of $\Delta p\text{RONO}_2$ vs. Δ isoprene, both in mixing ratio units. The linear fit is weighted by square root of number of points used to determine each in-plume $p\text{RONO}_2$, with intercept held at zero. The slope coefficient \pm one standard deviation is 0.0930 ± 0.0011 . Points are colored by plume age, and size scaled by square root of number of points (the point weight used in linear fit). This plot and fit includes the nine plumes listed in Tables 1 and 2, as well as the 03:14 “unreacted” plume (at Δ isoprene = -84 ppt). Error bars on isoprene are the propagated standard deviations of the (in plume - out plume) differences, for plumes in which multi-point averages were possible. Error bars on $p\text{RONO}_2$ are the same as in Figure 4. The points without error bars are single-point plumes.

To estimate SOA mass yields, we need to make some assumption about the mass of the organic molecules containing the nitrate groups that lead to the observed nitrate aerosol mass increase. The observed changes in organic aerosol are too variable to be simply interpreted as the organic portion of the aerosol organic nitrate molecules. We conservatively assume the organic mass to be approximately double the nitrate mass (62 g mol^{-1}), based on an “average” molecular structure of an isoprene nitrate with 3 additional oxygens: e.g. a tri-hydroxynitrate (with organic portion of formula $\text{C}_5\text{H}_{11}\text{O}_3$, 119 g mol^{-1}), consistent with 2nd-generation oxidation product structures suggested in Schwantes, et al. (Schwantes et al., 2015). Based on this assumed organic to nitrate ratio, all plumes’ expected organic mass increases would be less

Juliane Fry 5/26/2018 9:05 PM



Deleted:

Unknown

Formatted: Font:(Default) Times, 10 pt, Font color: Auto

Juliane Fry 5/26/2018 9:08 PM

Formatted: Normal

Juliane Fry 5/15/2018 7:09 PM

Deleted: 298

Juliane Fry 5/15/2018 7:09 PM

Deleted: 3

Juliane Fry 6/3/2018 5:53 PM

Deleted: (red = longest)

Juliane Fry 5/26/2018 5:28 PM

Deleted:

Juliane Fry 5/26/2018 9:07 PM

Formatted: Font color: Auto

Juliane Fry 5/26/2018 9:07 PM

Formatted: Font color: Auto

Juliane Fry 5/26/2018 9:07 PM

Formatted: Font color: Auto

Juliane Fry 5/26/2018 9:07 PM

Formatted: Font color: Auto

Juliane Fry 5/26/2018 9:07 PM

Formatted: Font color: Auto

Juliane Fry 5/26/2018 9:08 PM

Formatted: Font:(Default) Times, 10 pt, Font color: Auto

740 than the typical variability in organic of $0.75 \mu\text{g m}^{-3}$. This assumed structure is consistent with
 741 oxidation of both double bonds, which appears to be necessary for substantial condensation of
 742 isoprene products, and which structures would have calculated vapor pressures sufficiently low
 743 to partition to the aerosol phase (Rollins et al., 2009). Another possible route to low vapor
 744 pressure products is intramolecular H rearrangement reactions, discussed below in Section 4.3,
 745 which would not require oxidant reactions at both double bonds. In the case of oxidant reactions
 746 at both double bonds, it is difficult to understand how the second double bond would be oxidized
 747 unless by another nitrate radical, which would halve these assumed organic to nitrate ratios
 748 (assuming the nitrate is retained in the molecules). On the other hand, any organic nitrate
 749 aerosol may lose NO_3 moieties, increasing the organic to nitrate ratio. Given these uncertainties
 750 in both directions, we use the assumed “average” structure above to guess an associated
 751 organic mass of double the nitrate mass. Thus, to estimate SOA mass yield, we multiply the
 752 increase in organic nitrate aerosol mass concentration by three (i.e., $2 \times \Delta M_{\text{pRONO}_2} + \Delta M_{\text{pRONO}_2}$),
 753 and divide by the observed decrease in isoprene, converted to $\mu\text{g m}^{-3}$ by multiplying by 329 ppt
 754 ($\mu\text{g m}^{-3}$)⁻¹, the conversion factor based on isoprene’s molecular weight of 68.12 g mol^{-1} .

$$756 Y_{\text{SOA, mass}} = \frac{(\text{pRONO}_2_{\text{plume}} \pm \text{SD}_{\text{pRONO}_2\text{plume}}) - (\text{pRONO}_2_{\text{bkg}} \pm \text{SD}_{\text{pRONO}_2\text{bkg}})}{-[(\text{isop}_{\text{plume}} \pm \text{SD}_{\text{isop}_{\text{plume}}}) - (\text{isop}_{\text{bkg}} \pm \text{SD}_{\text{isop}_{\text{bkg}}})]} \times 3 \times \frac{329 \text{ ppt}}{\mu\text{g m}^{-3}} \quad (4)$$

757
 758 Note that the SOA mass yield reported here is based on the (assumed) mass of organic aerosol
 759 plus the (organo)nitrate aerosol formed in each plume. If instead the yield were calculated using
 760 only the assumed increase in **organic** mass (i.e., $2 \times \Delta M_{\text{pRONO}_2}$ instead of $3 \times \Delta M_{\text{pRONO}_2}$), which
 761 would be consistent with the method used in Rollins, et al. (Rollins et al., 2009) and Brown et al.
 762 (Brown et al., 2009), the mass yields would be 2/3 the values reported here. However, since
 763 SOA mass yield is typically defined based on the total increase in aerosol mass, we use the
 764 definition with the sum of the organic and nitrate mass here.

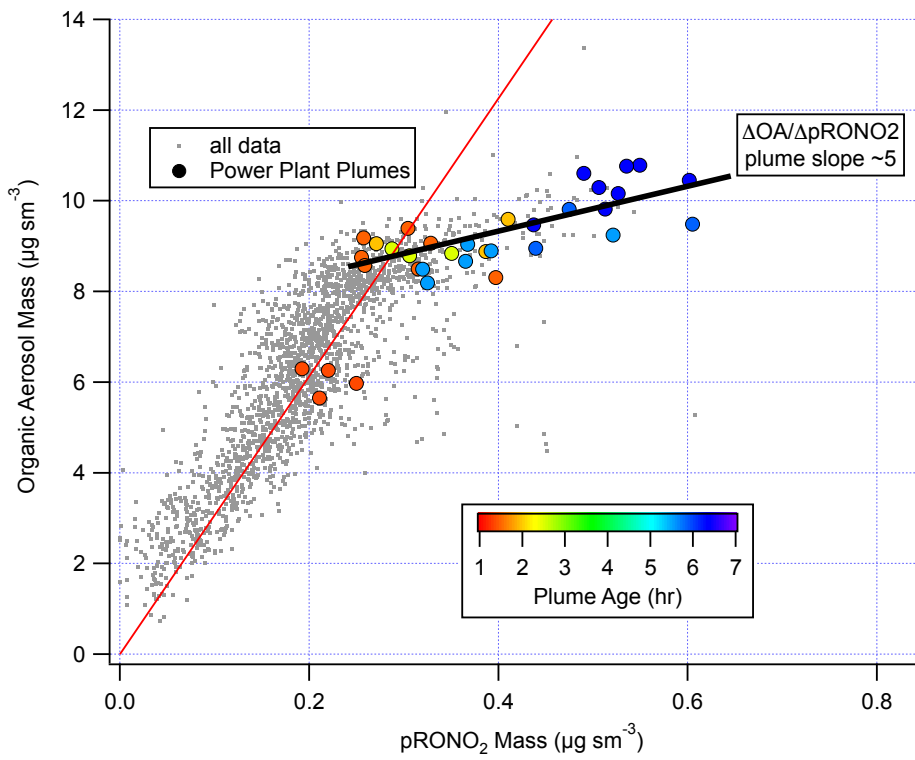
765
 766 We note also that correlation of in-plume increases in OA with pRONO_2 (Fig. 6) point to a
 767 substantially larger 5:1 organic-to-nitrate ratio; if this were interpreted as indicating that the
 768 average molecular formula of the condensing organic nitrate has 5 times the organic mass as
 769 nitrate, this would increase the SOA mass yields reported here. However, due to the
 770 aforementioned possibility of additional sources of co-condensing organic aerosol, which led us
 771 to avoid using ΔOA in determining SOA yields, we do not consider this to be a direct indication
 772 of the molecular formula of the condensing organic nitrate. Including OA in the SOA yield
 773 determination, based on this 5:1 slope rather than the assumed 2:1 OA: pRONO_2 , would give
 774 2.5 times larger SOA mass yields than reported here.

775

Juliane Fry 5/15/2018 8:20 PM
 Deleted: However

Juliane Fry 5/15/2018 8:17 PM
 Deleted: the

Juliane Fry 5/15/2018 8:17 PM
 Deleted: y



779

780 **Figure 6.** Correlation of organic aerosol mass concentration with pRONO₂ mass concentration

781 for the full 2 July flight (grey points and red fit line, fitted slope and thus average OA/pRONO₂

782 mass ratio of ~ 30) and for the points during the selected plumes (colored points, colored by

783 plume age, average OA/pRONO₂ mass ratio of ~ 5).

784

785

786 **Table 2.** SOA Yields for each plume observation, estimated plume age, and likely origin. See
 787 text for description of uncertainty estimates. For the mass yields, the calculated SOA mass
 788 increase includes both the organic and (organo)nitrate aerosol mass; the measurements for OA
 789 increases shown in Figure 6 do not include the nitrate mass.

plume number	plume time (UTC)	SOA molar yield (fraction) [± SD]	SOA mass yield (fraction) [± SD]	plume age from O ₃ / NO ₂ clock assuming S=1 (hours)	Likely NO _x origin & altitude (m)
1	7/2/13 2:18	0.09 [0.06]	0.25 [0.17]	2.5	Greene County @ 540 m
2	7/2/13 2:20	0.07	0.21	1.5	<i>ibid</i>
3	7/2/13 2:21	0.12 [0.10]	0.32 [0.25]	1.5	<i>ibid</i>
4	7/2/13 3:03	0.13	0.36	1.5	Gaston @ 720 m
5	7/2/13 3:55	0.06 [0.07]	0.17 [0.20]	1.4	Miller / Gorgas @ 690 m
6	7/2/13 4:34	0.05 [0.03]	0.15 [0.09]	2	<i>ibid</i>
7	7/2/13 4:37	0.10 [0.09]	0.26 [0.24]	5.5	<i>ibid</i>
8	7/2/13 4:39	0.16 [0.10]	0.45 [0.28]	5.8	Miller / Gorgas @ 1120 m
9	7/2/13 5:04	0.28 [0.19]	0.77 [0.52]	6.3	Gaston @ 1280 m

Juliane Fry 6/1/2018 3:38 PM

Deleted: 5

Juliane Fry 6/1/2018 3:38 PM

Deleted: 4

Juliane Fry 6/1/2018 3:38 PM

Deleted: 27

Juliane Fry 6/1/2018 3:38 PM

Deleted: 2

Juliane Fry 6/1/2018 3:39 PM

Deleted: 7

Juliane Fry 6/1/2018 3:39 PM

Deleted: 11

Juliane Fry 6/1/2018 3:39 PM

Deleted: 31

Juliane Fry 6/1/2018 3:39 PM

Deleted: 6

Juliane Fry 6/1/2018 3:39 PM

Deleted: 4

Juliane Fry 6/1/2018 3:39 PM

Deleted: 39

790
791

802 **Table 3.** Several caveats to the present SOA yields analysis are listed below, alongside the
 803 expected direction each would adjust the estimated yields. Because we do not know whether or
 804 how much each process may have occurred in the studied plumes, we cannot quantitatively
 805 assess the resulting uncertainties, so we simply list them here. See text above for more detailed
 806 discussion.

Process	Effect on determined SOA yield
Organic nitrate aerosol loses NO ₃ functional group	Larger, because the non-nitrate OA would not be counted in this analysis
Both double bonds in isoprene are oxidized by NO ₃ : two nitrates per condensing molecule	Smaller, because the assumed organic to nitrate mass ratio assumes one nitrate per molecule
NO ₃ oxidizes daytime isoprene oxidation products (e.g. ISOPOOH) to make new aerosol	Smaller, because this would produce organic nitrate aerosol without corresponding decrease in isoprene, so that some of existing SOA production is mis-attributed to isoprene + NO ₃
Assumed organic to nitrate mass ratio is incorrect	Unknown direction of effect, depends on whether assumed ratio is high or low
Daytime-produced IEPOX uptake onto acidic particles	No effect (only changes ΔOA, not nitrate)
Suppression of O ₃ + monoterpene or O ₃ + isoprene SOA in plumes	No effect (only changes ΔOA, not nitrate)

807
 808 Finally, the large range in observed yields can be interpreted by examining the relationship to
 809 estimated plume age. Using the slope of O₃ to NO₂ (Eq. 1) to estimate plume age as described
 810 above, a weak positive correlation is observed (Table 2, Fig. S4), suggesting that as the plume
 811 ages, later-generation chemistry results in greater partitioning to the condensed phase of NO₃ +
 812 isoprene organonitrate aerosol products. This is consistent with the observation by Rollins et al.
 813 (Rollins et al., 2009) that 2nd-generation oxidation produced substantially higher SOA yields
 814 than the oxidation of the first double bond alone, but we note that these mass yields (averaging
 815 27%, would be 18% using the organic mass only) are higher than even the largest yield found in
 816 that chamber study (14%, used organic mass only).

817
 818 We observe increasing SOA yield, from a molar yield of around 10% at 1.5 hours up to 30% at 6
 819 hours of aging. The lowest yields observed are found in the most recently emitted plumes,
 820 suggesting the interpretation of the higher yields as a consequence of longer aging timescales
 821 in the atmosphere.

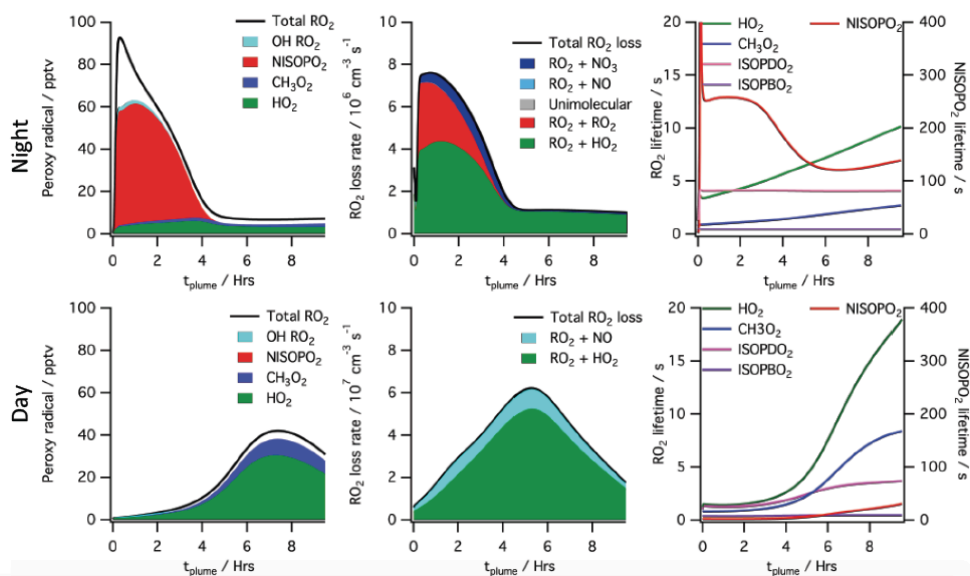
822 **4.3 Mechanistic considerations**

823
 824 These larger SOA mass yields from field determinations (average 27%) relative to chamber
 825 work (12 – 14%, see introduction) may arise for several reasons. We first assess the volatility of
 826 assumed first- and second-generation products using group contribution theory in order to
 827 predict partitioning. After a single oxidation step, with a representative product assumed to be a

828 C₅ hydroperoxynitrate, the saturation vapor pressure estimated by group contribution theory
829 (Pankow and Asher 2008) at 283 K would be 2.10×10^{-3} Torr ($C^* = 1.7 \times 10^4 \mu\text{g m}^{-3}$ for MW =
830 147 g mol^{-1}), while a double-oxidized isoprene molecule (assuming a C₅ dihydroxy dinitrate) has
831 an estimated vapor pressure of 7.95×10^{-8} Torr ($C^* = 1.01 \mu\text{g m}^{-3}$ for MW = 226 g mol^{-1}). This
832 supports the conclusion that while the first oxidation step produces compounds too volatile to
833 contribute appreciably to aerosol formation, oxidizing both double bonds of the isoprene
834 molecule is sufficient to produce substantial partitioning, consistent with Rollins et al. (Rollins et
835 al., 2009). This is also true if the second double bond is not oxidized by nitrate (group
836 contribution estimate P_{vap} for a C₅ tri-hydroxy nitrate is 7.7×10^{-8} Torr, $C^* = 0.79 \mu\text{g m}^{-3}$ for MW =
837 181 g mol^{-1}). These C^* saturation concentration values suggest that no dimer formation or
838 oligomerization is *required* to produce low-enough volatility products to condense to the aerosol
839 phase; however, such oligomerization would result in more efficient condensation. The fact that
840 Rollins et al. (Rollins et al., 2009) did not observe larger mass yields may indicate that it takes
841 longer than a typical chamber experiment timescale to reach equilibrium, or that this absorptive
842 partitioning model did not accurately capture those experiments, or that substantial loss of
843 semivolatiles to the chamber walls (e.g. (Krechmer et al., 2016)) suppressed apparent yields.
844

845 Determination of yields from ambient atmospheric data differs from chamber determinations in
846 several additional respects. First, ambient measurements do not suffer from wall loss effects,
847 such that no corrections are necessary for loss of aerosol or semi-volatile gases (Matsunaga
848 and Ziemann 2010, Krechmer et al., 2016). Second, ambient measurements take place on the
849 aging time scale of the atmosphere rather than a time scale imposed by the characteristics of
850 the chamber or the choice of oxidant addition. Third, the typical lifetime of the initially produced
851 nitrooxy-isoprene-RO₂ radical is more representative of the ambient atmosphere rather than a
852 chamber. The unique conditions of a high NO_x power plant plume affect lifetime and fates of
853 peroxy radicals, as described below.
854

855 To help interpret these in-plume peroxy radical lifetimes, a box model calculation using the
856 MCM v3.3.1 chemistry scheme was run (see details in Supplemental Information). This box
857 model shows substantially longer peroxy radical lifetimes during nighttime than daytime,
858 initializing with identical plume-observed conditions. These long peroxy radical lifetimes may
859 have consequences for comparison to chamber experiments: for example, in Schwantes'
860 (Schwantes et al., 2015) chamber experiment on the NO₃ + isoprene reaction mechanism, the
861 HO₂-limited nitrooxy-RO₂ lifetime was at maximum 30 s. In the plumes investigated in this study,
862 peroxy radical lifetimes are predicted to be substantially longer (>200 s early in the night, see
863 Fig. 7), allowing for the possibility of different bimolecular fates, or of unimolecular
864 transformations of the peroxy radicals that may result in lower-volatility products (e.g., auto-
865 oxidation to form highly oxidized molecules (Ehn et al., 2014)).
866
867



868
 869 **Figure 7.** Simulated peroxy radical concentration (left), loss rates (middle), and lifetime (right),
 870 using the MCM v3.3.1 chemical mechanism, for conditions typical of a nighttime intercepted
 871 power plant plume (top) and the same plume initial conditions run for daytime simulation
 872 (bottom, local noon occurs at 5 hrs). Included are total peroxy radical concentration and losses,
 873 as well as the highlighted subclasses HO₂, CH₃O₂, total nitrooxy-isoprene-RO₂, and the total
 874 hydroxy-isoprene-RO₂ produced from OH oxidation. The righthand panels show HO₂, CH₃O₂
 875 and the dominant hydroxy-isoprene-RO₂ ISOPBO₂ and ISOPDO₂ (β -hydroxy-peroxy radicals
 876 from OH attack at carbons 1 and 4 respectively) lifetime on the left axis and nitrooxy-isoprene-
 877 RO₂ on the right axis, showing nighttime lifetimes an order of magnitude longer than daytime for
 878 this NO₃ + isoprene derived RO₂ radical (NISOPO₂).
 879

880 The typically assumed major fate of nighttime RO₂ in the atmosphere is reaction with HO₂ to
 881 yield a hydroperoxide, NO₃-ROOH. This is shown in the model output above as the green
 882 reaction, and is responsible for half of early RO₂ losses in the MCM modeled plume. Schwantes
 883 *et al.* (Schwantes *et al.*, 2015) proposed reaction of these nighttime derived hydroperoxides with
 884 OH during the following day as a route to epoxides, which in turn can form SOA via reaction
 885 with acidic aerosol. Reaction of hydroperoxides with nighttime generated OH may similarly
 886 provide a route to SOA through epoxides, albeit more slowly than that due to photochemically
 887 generated OH.
 888

889 The predicted longer nighttime peroxy radical lifetimes may enable unique chemistry. For
 890 example, if nitrooxy-isoprene-RO₂ self-reactions are substantially faster than assumed in the
 891 MCM, as suggested by Schwantes *et al.* (Schwantes *et al.*, 2015), RO₂+RO₂ reactions may
 892 compete with the HO₂ reaction even more than shown in Fig. 7, and dimer formation may be
 893 favored at night, yielding lower volatility products. The 5:1 AMS Organic:Nitrate ratio observed in

894 the SOA formed in Rollins et al. (Rollins et al., 2009) , and consistent with aggregated
895 observations reported here, may suggest that in some isoprene units the nitrate is re-released
896 as NO₂ in such oligomerization reactions. We note that this larger organic to nitrate ratio would
897 mean higher SOA mass yields than estimated in Table 2.

898
899 Alternatively, longer nighttime peroxy radical lifetimes may allow sufficient time for
900 intramolecular reactions to produce condensable products. This unimolecular isomerization
901 (auto-oxidation) of initially formed peroxy radicals is a potentially efficient route to low-volatility,
902 highly functionalized products that could result in high aerosol yields. For OH-initiated oxidation
903 of isoprene, laboratory relative rate experiments found the fastest 1,6-H-shift isomerization
904 reaction to occur for the hydroxy-isoprene-RO₂ radical at a rate of 0.002 s⁻¹ (Crouse et al.,
905 2011), meaning that peroxy radicals must have an ambient lifetime of >500 s for this process to
906 be dominant. As shown in Fig. 7, the simulated power plant plume peroxy radical lifetimes are
907 long (>200 s), so an isomerization reaction at this rate may play a significant role. However, a
908 recent study has demonstrated that OH-initiated and NO₃-initiated RO₂ radicals from the same
909 precursor VOC can have very different unimolecular reactive fates due to highly structurally
910 sensitive varying rates of reactions of different product channels (Kurtén et al., 2017). A similar
911 theoretical study on the rate of unimolecular autooxidation reactions of nitrooxy-isoprene-RO₂
912 radicals would be valuable to help determine under what conditions such reactions might occur,
913 and this knowledge could be applied to comparing chamber and field SOA yields.

914 **4.4 Atmospheric implications and needs for future work**

915 Because this paper proposes higher SOA yield for the NO₃ + isoprene reaction than measured
916 in chamber studies, we conclude with some discussion of the implications for regional aerosol
917 burdens, and further needs for investigation in the NO₃ + isoprene system.

918
919 Using an isoprene + NO₃ yield parameterization that gave a 12% SOA mass yield at 10 µg m⁻³,
920 Pye et al. (2010) found that adding the NO₃ + isoprene oxidation pathway increased isoprene
921 SOA mass concentrations in the southeastern United States by about 30%, increases of 0.4 to
922 0.6 µg m⁻³. The larger NO₃ + isoprene SOA mass yields suggested in this paper, with average
923 value of 30%, could double this expected NO₃ radical enhancement of SOA production.
924 Edwards et al. (2017) concluded that the southeast U.S. is currently in transition between NO_x-
925 independent and NO_x-controlled nighttime BVOC oxidation regime. If NO₃-isoprene oxidation is
926 a larger aerosol source than currently understood, and if future NO_x reductions lead to a
927 stronger sensitivity in nighttime BVOC oxidation rates, regional SOA loadings could decrease by
928 a substantial fraction from the typical regional summertime OA loadings of 5 +/- 3 µg m⁻³ (Saha
929 et al., 2017).

930
931 Analysis of the degree of oxidation and chemical composition of NO₃ + isoprene SOA would
932 help to elucidate mechanistic reasons for the different field and lab SOA yields. For example,
933 the potential contribution of the uptake of morning-after OH + NISOPOOH produced epoxides,
934 discussed above in section 4.3, onto existing (acidic) aerosol could be quantified by
935 measurement of these intermediates or their products in the aerosol phase. Assessment of
936 degree of oxidation could help determine whether auto-oxidation mechanisms are active.

Juliane Fry 5/26/2018 10:23 PM

Deleted: 4.4 Two urban plume case studies

... [9]

Juliane Fry 5/26/2018 10:23 PM

Deleted: 5

941 Because of the potentially large effect on predicted SOA loading in regions of high isoprene
942 emissions, a better mechanistic understanding of these observed yields is crucial.

943

944 **Acknowledgements**

945 JLF gratefully acknowledges funding from the EPA STAR Program (no. RD-83539901) and from
946 the Fulbright U.S. Scholars Program in the Netherlands. PCJ, DAD, and JLJ were partially
947 supported by EPA STAR 83587701-0 and DOE (BER/ASR) DE-SC0016559. This paper has not
948 been formally reviewed by EPA. The views expressed in this document are solely those of the
949 authors, and do not necessarily reflect those of EPA. EPA does not endorse any products or
950 commercial services mentioned in this publication.

951 **5 References**

- 952 Allan, J. D., K. N. Bower, H. Coe, H. Boudries, J. T. Jayne, M. R. Canagaratna, D. B. Millet, A.
953 H. Goldstein, P. K. Quinn, R. J. Weber and D. R. Worsnop (2004). "Submicron aerosol
954 composition at Trinidad Head, California, during ITCT 2K2: Its relationship with gas phase
955 volatile organic carbon and assessment of instrument performance." *Journal of Geophysical*
956 *Research: Atmospheres* **109**(D23): n/a-n/a.
- 957 Allan, J. D., A. E. Delia, H. Coe, K. N. Bower, M. R. Alfarra, J. L. Jimenez, A. M. Middlebrook, F.
958 Drewnick, T. B. Onasch, M. R. Canagaratna, J. T. Jayne and D. R. Worsnop (2004). "A
959 generalised method for the extraction of chemically resolved mass spectra from Aerodyne
960 aerosol mass spectrometer data." *Journal of Aerosol Science* **35**(7): 909-922.
- 961 Atkinson, R., D. L. Baulch, R. A. Cox, J. N. Crowley, R. F. Hampson, R. G. Hynes, M. E. Jenkin,
962 M. J. Rossi and J. Troe (2004). "Evaluated kinetic and photochemical data for atmospheric
963 chemistry: Volume I - gas phase reactions of Ox, HOx, NOx and SOx species." *Atmos. Chem.*
964 *Phys.* **4**(6): 1461-1738.
- 965 Ayres, B. R., H. M. Allen, D. C. Draper, S. S. Brown, R. J. Wild, J. L. Jimenez, D. A. Day, P.
966 Campuzano-Jost, W. Hu, J. de Gouw, A. Koss, R. C. Cohen, K. C. Duffey, P. Romer, K.
967 Baumann, E. Edgerton, S. Takahama, J. A. Thornton, B. H. Lee, F. D. Lopez-Hilfiker, C. Mohr,
968 P. O. Wennberg, T. B. Nguyen, A. Teng, A. H. Goldstein, K. Olson and J. L. Fry (2015).
969 "Organic nitrate aerosol formation via NO₃ + biogenic volatile organic compounds
970 in the southeastern United States." *Atmos. Chem. Phys.* **15**(23): 13377-13392.
- 971 Bahreini, R., E. J. Dunlea, B. M. Matthew, C. Simons, K. S. Docherty, P. F. DeCarlo, J. L.
972 Jimenez, C. A. Brock and A. M. Middlebrook (2008). "Design and Operation of a Pressure-
973 Controlled Inlet for Airborne Sampling with an Aerodynamic Aerosol Lens." *Aerosol Science and*
974 *Technology* **42**(6): 465-471.
- 975 Bahreini, R., B. Ervens, A. M. Middlebrook, C. Warneke, J. A. de Gouw, P. F. DeCarlo, J. L.
976 Jimenez, C. A. Brock, J. A. Neuman, T. B. Ryerson, H. Stark, E. Atlas, J. Brioude, A. Fried, J. S.
977 Holloway, J. Peischl, D. Richter, J. Walega, P. Weibring, A. G. Wollny and F. C. Fehsenfeld
978 (2009). "Organic aerosol formation in urban and industrial plumes near Houston and Dallas,
979 Texas." *Journal of Geophysical Research: Atmospheres* **114**(D7): n/a-n/a.
- 980 Boyd, C. M., J. Sanchez, L. Xu, A. J. Eugene, T. Nah, W. Y. Tuet, M. I. Guzman and N. L. Ng
981 (2015). "Secondary organic aerosol formation from the β-pinene+NO₃ system: effect of humidity
982 and peroxy radical fate." *Atmos. Chem. Phys.* **15**(13): 7497-7522.
- 983 Brock, C. A., J. Cozic, R. Bahreini, K. D. Froyd, A. M. Middlebrook, A. McComiskey, J. Brioude,
984 O. R. Cooper, A. Stohl, K. C. Aikin, J. A. de Gouw, D. W. Fahey, R. A. Ferrare, R. S. Gao, W.
985 Gore, J. S. Holloway, G. Hübler, A. Jefferson, D. A. Lack, S. Lance, R. H. Moore, D. M. Murphy,
986 A. Nenes, P. C. Novelli, J. B. Nowak, J. A. Ogren, J. Peischl, R. B. Pierce, P. Pilewskie, P. K.
987 Quinn, T. B. Ryerson, K. S. Schmidt, J. P. Schwarz, H. Sodemann, J. R. Spackman, H. Stark,

988 D. S. Thomson, T. Thornberry, P. Veres, L. A. Watts, C. Warneke and A. G. Wollny (2011).
989 "Characteristics, sources, and transport of aerosols measured in spring 2008 during the aerosol,
990 radiation, and cloud processes affecting Arctic Climate (ARCPAC) Project." Atmos. Chem.
991 Phys. **11**(6): 2423-2453.
992 Brock, C. A., N. L. Wagner, B. E. Anderson, A. R. Attwood, A. Beyersdorf, P. Campuzano-Jost,
993 A. G. Carlton, D. A. Day, G. S. Diskin, T. D. Gordon, J. L. Jimenez, D. A. Lack, J. Liao, M. Z.
994 Markovic, A. M. Middlebrook, N. L. Ng, A. E. Perring, M. S. Richardson, J. P. Schwarz, R. A.
995 Washenfelder, A. Welti, L. Xu, L. D. Ziemba and D. M. Murphy (2016). "Aerosol optical
996 properties in the southeastern United States in summer – Part 1: Hygroscopic growth." Atmos.
997 Chem. Phys. **16**(8): 4987-5007.
998 Brown, S. S., J. A. deGouw, C. Warneke, T. B. Ryerson, W. P. Dubé, E. Atlas, R. J. Weber, R.
999 E. Peltier, J. A. Neuman, J. M. Roberts, A. Swanson, F. Flocke, S. A. McKeen, J. Brioude, R.
1000 Sommariva, M. Trainer, F. C. Fehsenfeld and A. R. Ravishankara (2009). "Nocturnal isoprene
1001 oxidation over the Northeast United States in summer and its impact on reactive nitrogen
1002 partitioning and secondary organic aerosol." Atmos. Chem. Phys. **9**(9): 3027-3042.
1003 Brown, S. S., W. P. Dubé, R. Bahreini, A. M. Middlebrook, C. A. Brock, C. Warneke, J. A. de
1004 Gouw, R. A. Washenfelder, E. Atlas, J. Peischl, T. B. Ryerson, J. S. Holloway, J. P. Schwarz, R.
1005 Spackman, M. Trainer, D. D. Parrish, F. C. Fehsenfeld and A. R. Ravishankara (2013).
1006 "Biogenic VOC oxidation and organic aerosol formation in an urban nocturnal boundary layer:
1007 aircraft vertical profiles in Houston, TX." Atmos. Chem. Phys. **13**(22): 11317-11337.
1008 Brown, S. S., W. P. Dubé, P. Karamchandani, G. Yarwood, J. Peischl, T. B. Ryerson, J. A.
1009 Neuman, J. B. Nowak, J. S. Holloway, R. A. Washenfelder, C. A. Brock, G. J. Frost, M. Trainer,
1010 D. D. Parrish, F. C. Fehsenfeld and A. R. Ravishankara (2012). "Effects of NO_x control and
1011 plume mixing on nighttime chemical processing of plumes from coal-fired power plants." Journal
1012 of Geophysical Research: Atmospheres **117**(D7): n/a-n/a.
1013 Brown, S. S., J. A. Neuman, T. B. Ryerson, M. Trainer, W. P. Dubé, J. S. Holloway, C.
1014 Warneke, J. A. de Gouw, S. G. Donnelly, E. Atlas, B. Matthew, A. M. Middlebrook, R. Peltier, R.
1015 J. Weber, A. Stohl, J. F. Meagher, F. C. Fehsenfeld and A. R. Ravishankara (2006). "Nocturnal
1016 odd-oxygen budget and its implications for ozone loss in the lower troposphere." Geophysical
1017 Research Letters **33**(8): n/a-n/a.
1018 Brown, S. S. and J. Stutz (2012). "Nighttime radical observations and chemistry." Chemical
1019 Society Reviews **41**(19): 6405-6447.
1020 Bruns, E. A., V. Perraud, A. Zelenyuk, M. J. Ezell, S. N. Johnson, Y. Yu, D. Imre, B. J.
1021 Finlayson-Pitts and M. L. Alexander (2010). "Comparison of FTIR and Particle Mass
1022 Spectrometry for the Measurement of Particulate Organic Nitrates." Environmental Science &
1023 Technology **44**(3): 1056-1061.
1024 Cai, Y., D. C. Montague, W. Mooiweer-Bryan and T. Deshler (2008). Performance
1025 characteristics of the ultra high sensitivity aerosol spectrometer for particles between 55 and
1026 800 nm: Laboratory and field studies.
1027 Calvert, J. G., J. A. Atkinson, J. A. Kerr, S. Madronich, G. K. Moortgat, T. J. Wallington and G.
1028 Yarwood (2000). Mechanisms of the atmospheric oxidation of the alkenes. New York, NY,
1029 Oxford University Press.
1030 Carlton, A. G., R. W. Pinder, P. V. Bhave and G. A. Pouliot (2010). "To What Extent Can
1031 Biogenic SOA be Controlled?" Environmental Science & Technology **44**(9): 3376-3380.
1032 Carlton, A. G., C. Wiedinmyer and J. H. Kroll (2009). "A review of Secondary Organic Aerosol
1033 (SOA) formation from isoprene." Atmos. Chem. Phys. **9**(14): 4987-5005.
1034 Crouse, J. D., F. Paulot, H. G. Kjaergaard and P. O. Wennberg (2011). "Peroxy radical
1035 isomerization in the oxidation of isoprene." Physical Chemistry Chemical Physics **13**(30): 13607-
1036 13613.
1037 D'Ambro, E. L., K. H. Møller, F. D. Lopez-Hilfiker, S. Schobesberger, J. Liu, J. E. Shilling, B. H.
1038 Lee, H. G. Kjaergaard and J. A. Thornton (2017). "Isomerization of Second-Generation Isoprene

1039 Peroxy Radicals: Epoxide Formation and Implications for Secondary Organic Aerosol Yields." Environmental Science & Technology **51**(9): 4978-4987.

1040

1041 Darer, A. I., N. C. Cole-Filipiak, A. E. O'Connor and M. J. Elrod (2011). "Formation and Stability

1042 of Atmospherically Relevant Isoprene-Derived Organosulfates and Organonitrates." Environmental Science & Technology **45**(5): 1895-1902.

1043

1044 Day, D. A., P. Campuzano-Jost, B. B. Palm, W. W. Hu, B. A. Nault, P. J. Wooldridge, R. C.

1045 Cohen, K. S. Docherty, J. A. Huffman and J. L. Jimenez (2017). "Evaluation of methods for

1046 quantification of bulk particle-phase organic nitrates using real-time aerosol mass spectrometry."

1047 in preparation.

1048 Dommen, J., H. Hellén, M. Saurer, M. Jaeggi, R. Siegwolf, A. Metzger, J. Duplissy, M. Fierz and

1049 U. Baltensperger (2009). "Determination of the Aerosol Yield of Isoprene in the Presence of an

1050 Organic Seed with Carbon Isotope Analysis." Environmental Science & Technology **43**(17):

1051 6697-6702.

1052 Drewnick, F., S. S. Hings, P. DeCarlo, J. T. Jayne, M. Gonin, K. Fuhrer, S. Weimer, J. L.

1053 Jimenez, K. L. Demerjian, S. Borrmann and D. R. Worsnop (2005). "A New Time-of-Flight

1054 Aerosol Mass Spectrometer (TOF-AMS)—Instrument Description and First Field Deployment." Aerosol Science and Technology **39**(7): 637-658.

1055

1056 Dunlea, E. J., P. F. DeCarlo, A. C. Aiken, J. R. Kimmel, R. E. Peltier, R. J. Weber, J. Tomlinson,

1057 D. R. Collins, Y. Shinozuka, C. S. McNaughton, S. G. Howell, A. D. Clarke, L. K. Emmons, E. C.

1058 Apel, G. G. Pfister, A. van Donkelaar, R. V. Martin, D. B. Millet, C. L. Heald and J. L. Jimenez

1059 (2009). "Evolution of Asian aerosols during transpacific transport in INTEX-B." Atmos. Chem.

1060 Phys. **9**(19): 7257-7287.

1061 Edwards, P. M., K. C. Aikin, W. P. Dube, J. L. Fry, J. B. Gilman, J. A. de Gouw, M. G. Graus, T.

1062 F. Hanisco, J. Holloway, G. Hubler, J. Kaiser, F. N. Keutsch, B. M. Lerner, J. A. Neuman, D. D.

1063 Parrish, J. Peischl, I. B. Pollack, A. R. Ravishankara, J. M. Roberts, T. B. Ryerson, M. Trainer,

1064 P. R. Veres, G. M. Wolfe, C. Warneke and S. S. Brown (2017). "Transition from high- to low-

1065 NOx control of night-time oxidation in the southeastern US." Nature Geosci **10**(7): 490-495.

1066 Ehn, M., J. A. Thornton, E. Kleist, M. Sipila, H. Junninen, I. Pullinen, M. Springer, F. Rubach, R.

1067 Tillmann, B. Lee, F. Lopez-Hilfiker, S. Andres, I.-H. Acir, M. Rissanen, T. Jokinen, S.

1068 Schobesberger, J. Kangasluoma, J. Kontkanen, T. Nieminen, T. Kurten, L. B. Nielsen, S.

1069 Jorgensen, H. G. Kjaergaard, M. Canagaratna, M. D. Maso, T. Berndt, T. Petaja, A. Wahner, V.-

1070 M. Kerminen, M. Kulmala, D. R. Worsnop, J. Wildt and T. F. Mentel (2014). "A large source of

1071 low-volatility secondary organic aerosol." Nature **506**(7489): 476-479.

1072 Emmerson, K. M. and M. J. Evans (2009). "Comparison of tropospheric gas-phase chemistry

1073 schemes for use within global models." Atmos. Chem. Phys. **9**(5): 1831-1845.

1074 Farmer, D. K., A. Matsunaga, K. S. Docherty, J. D. Surratt, J. H. Seinfeld, P. J. Ziemann and J.

1075 L. Jimenez (2010). "Response of an aerosol mass spectrometer to organonitrates and

1076 organosulfates and implications for atmospheric chemistry." Proceedings of the National

1077 Academy of Sciences **107**(15): 6670-6675.

1078 Fisher, J. A., D. J. Jacob, K. R. Travis, P. S. Kim, E. A. Marais, C. Chan Miller, K. Yu, L. Zhu, R.

1079 M. Yantosca, M. P. Sulprizio, J. Mao, P. O. Wennberg, J. D. Crouse, A. P. Teng, T. B. Nguyen,

1080 J. M. St. Clair, R. C. Cohen, P. Romer, B. A. Nault, P. J. Wooldridge, J. L. Jimenez, P.

1081 Campuzano-Jost, D. A. Day, W. Hu, P. B. Shepson, F. Xiong, D. R. Blake, A. H. Goldstein, P.

1082 K. Misztal, T. F. Hanisco, G. M. Wolfe, T. B. Ryerson, A. Wisthaler and T. Mikoviny (2016).

1083 "Organic nitrate chemistry and its implications for nitrogen budgets in an isoprene- and

1084 monoterpene-rich atmosphere: constraints from aircraft (SEAC4RS) and ground-based (SOAS)

1085 observations in the Southeast US." Atmos. Chem. Phys. **16**(9): 5969-5991.

1086 Fry, J. L., D. C. Draper, K. J. Zarzana, P. Campuzano-Jost, D. A. Day, J. L. Jimenez, S. S.

1087 Brown, R. C. Cohen, L. Kaser, A. Hansel, L. Cappellin, T. Karl, A. Hodzic Roux, A. Turnipseed,

1088 C. Cantrell, B. L. Lefer and N. Grossberg (2013). "Observations of gas- and aerosol-phase

1089 organic nitrates at BEACHON-RoMBAS 2011." Atmos. Chem. Phys. **13**(1): 8585-8605.

1090 Fry, J. L., A. Kiendler-Scharr, A. W. Rollins, T. Brauers, S. S. Brown, H.-P. Dorn, W. P. Dube, H.
1091 Fuchs, A. Mensah, F. Rohrer, R. Tillmann, A. Wahner, P. J. Wooldridge and R. C. Cohen
1092 (2011). "SOA from limonene: role of NO₃ in its generation and degradation." *Atmospheric*
1093 *Chemistry and Physics* **11**(8): 3879-3894.
1094 Fry, J. L., A. Kiendler-Scharr, A. W. Rollins, P. J. Wooldridge, S. S. Brown, H. Fuchs, W. Dube,
1095 A. Mensah, M. dal Maso, R. Tillmann, H. P. Dorn, T. Brauers and R. C. Cohen (2009). "Organic
1096 nitrate and secondary organic aerosol yield from NO₃ oxidation of beta-pinene evaluated using
1097 a gas-phase kinetics/aerosol partitioning model." *Atmospheric Chemistry and Physics* **9**(4):
1098 1431-1449.
1099 Fry, J. L., C. Koski, K. Bott, R. Hsu-Flanders and M. Hazell (2015). "Downwind particulate
1100 matters: Regulatory implications of secondary aerosol formation from the interaction of nitrogen
1101 oxides and tree emissions." *Environmental Science & Policy* **50**: 180-190.
1102 Goldstein, A. H., C. D. Koven, C. L. Heald and I. Y. Fung (2009). "Biogenic carbon and
1103 anthropogenic pollutants combine to form a cooling haze over the southeastern United States."
1104 *Proceedings of the National Academy of Sciences* **106**(22): 8835-8840.
1105 Guenther, A., T. Karl, P. Harley, C. Wiedinmyer, P. I. Palmer and C. Geron (2006). "Estimates
1106 of global terrestrial isoprene emissions using MEGAN (Model of Emissions of Gases and
1107 Aerosols from Nature)." *Atmos. Chem. Phys.* **6**: 3181-3210.
1108 Guo, H., L. Xu, A. Bougiatioti, K. M. Cerully, S. L. Capps, J. R. Hite Jr, A. G. Carlton, S. H. Lee,
1109 M. H. Bergin, N. L. Ng, A. Nenes and R. J. Weber (2015). "Fine-particle water and pH in the
1110 southeastern United States." *Atmos. Chem. Phys.* **15**(9): 5211-5228.
1111 Hallquist, M., J. C. Wenger, U. Baltensperger, Y. Rudich, D. Simpson, M. Claeys, J. Dommen,
1112 N. M. Donahue, C. George, A. H. Goldstein, J. F. Hamilton, H. Herrmann, T. Hoffmann, Y.
1113 Iinuma, M. Jang, M. E. Jenkin, J. L. Jimenez, A. Kiendler-Scharr, W. Maenhaut, G. McFiggans,
1114 T. F. Mentel, A. Monod, A. S. H. Prévôt, J. H. Seinfeld, J. D. Surratt, R. Szmigielski and J. Wildt
1115 (2009). "The formation, properties and impact of secondary organic aerosol: current and
1116 emerging issues." *Atmospheric Chemistry & Physics* **9**: 5155-5235.
1117 Hayes, P. L., A. M. Ortega, M. J. Cubison, K. D. Froyd, Y. Zhao, S. S. Cliff, W. W. Hu, D. W.
1118 Toohey, J. H. Flynn, B. L. Lefer, N. Grossberg, S. Alvarez, B. Rappenglück, J. W. Taylor, J. D.
1119 Allan, J. S. Holloway, J. B. Gilman, W. C. Kuster, J. A. de Gouw, P. Massoli, X. Zhang, J. Liu, R.
1120 J. Weber, A. L. Corrigan, L. M. Russell, G. Isaacman, D. R. Worton, N. M. Kreisberg, A. H.
1121 Goldstein, R. Thalman, E. M. Waxman, R. Volkamer, Y. H. Lin, J. D. Surratt, T. E. Kleindienst,
1122 J. H. Offenberg, S. Dusanter, S. Griffith, P. S. Stevens, J. Brioude, W. M. Angevine and J. L.
1123 Jimenez (2013). "Organic aerosol composition and sources in Pasadena, California, during the
1124 2010 CalNex campaign." *Journal of Geophysical Research: Atmospheres* **118**(16): 9233-9257.
1125 Heald, C. L., D. K. Henze, L. W. Horowitz, J. Feddema, J. F. Lamarque, A. Guenther, P. G.
1126 Hess, F. Vitt, J. H. Seinfeld, A. H. Goldstein and I. Fung (2008). "Predicted change in global
1127 secondary organic aerosol concentrations in response to future climate, emissions, and land
1128 use change." *Journal of Geophysical Research: Atmospheres* **113**(D5): n/a-n/a.
1129 Henze, D. K. and J. H. Seinfeld (2006). "Global secondary organic aerosol from isoprene
1130 oxidation." *Geophysical Research Letters* **33**(9).
1131 Hoyle, C., M. Boy, N. Donahue, J. Fry, M. Glasius, A. Guenther, A. Hallar, K. H. Hartz, M.
1132 Petters and T. Petaja (2011). "A review of the anthropogenic influence on biogenic secondary
1133 organic aerosol." *Atmospheric Chemistry and Physics* **11**(1): 321-343.
1134 Hoyle, C. R., T. Berntsen, G. Myhre and I. S. A. Isaksen (2007). "Secondary organic aerosol in
1135 the global aerosol - chemical transport model Oslo CTM2." *Atmospheric Chemistry and Physics*
1136 **7**(21): 5675-5694.
1137 Hu, K. S., A. I. Darer and M. J. Elrod (2011). "Thermodynamics and kinetics of the hydrolysis of
1138 atmospherically relevant organonitrates and organosulfates." *Atmos. Chem. Phys.* **11**(16):
1139 8307-8320.

1140 Hu, W. W., P. Campuzano-Jost, B. B. Palm, D. A. Day, A. M. Ortega, P. L. Hayes, J. E.
1141 Krechmer, Q. Chen, M. Kuwata, Y. J. Liu, S. S. de Sá, K. McKinney, S. T. Martin, M. Hu, S. H.
1142 Budisulistiorini, M. Riva, J. D. Surratt, J. M. St. Clair, G. Isaacman-Van Wertz, L. D. Yee, A. H.
1143 Goldstein, S. Carbone, J. Brito, P. Artaxo, J. A. de Gouw, A. Koss, A. Wisthaler, T. Mikoviny, T.
1144 Karl, L. Kaser, W. Jud, A. Hansel, K. S. Docherty, M. L. Alexander, N. H. Robinson, H. Coe, J.
1145 D. Allan, M. R. Canagaratna, F. Paulot and J. L. Jimenez (2015). "Characterization of a real-
1146 time tracer for isoprene epoxydiols-derived secondary organic aerosol (IEPOX-SOA) from
1147 aerosol mass spectrometer measurements." *Atmos. Chem. Phys.* **15**(20): 11807-11833.
1148 Jenkin, M. E., J. C. Young and A. R. Rickard (2015). "The MCM v3.3.1 degradation scheme for
1149 isoprene." *Atmos. Chem. Phys.* **15**(20): 11433-11459.
1150 Jimenez, J. L., M. R. Canagaratna, N. M. Donahue, A. S. H. Prevot, Q. Zhang, J. H. Kroll, P. F.
1151 DeCarlo, J. D. Allan, H. Coe, N. L. Ng, A. C. Aiken, K. S. Docherty, I. M. Ulbrich, A. P. Grieshop,
1152 A. L. Robinson, J. Duplissy, J. D. Smith, K. R. Wilson, V. A. Lanz, C. Hueglin, Y. L. Sun, J. Tian,
1153 A. Laaksonen, T. Raatikainen, J. Rautiainen, P. Vaattovaara, M. Ehn, M. Kulmala, J. M.
1154 Tomlinson, D. R. Collins, M. J. Cubison, E., J. Dunlea, J. A. Huffman, T. B. Onasch, M. R.
1155 Alfara, P. I. Williams, K. Bower, Y. Kondo, J. Schneider, F. Drewnick, S. Borrmann, S. Weimer,
1156 K. Demerjian, D. Salcedo, L. Cottrell, R. Griffin, A. Takami, T. Miyoshi, S. Hatakeyama, A.
1157 Shimono, J. Y. Sun, Y. M. Zhang, K. Dzepina, J. R. Kimmel, D. Sueper, J. T. Jayne, S. C.
1158 Herndon, A. M. Trimborn, L. R. Williams, E. C. Wood, A. M. Middlebrook, C. E. Kolb, U.
1159 Baltensperger and D. R. Worsnop (2009). "Evolution of Organic Aerosols in the Atmosphere."
1160 *Science*(5959): 1525-1529.
1161 Kanakidou, M., J. H. Seinfeld, S. N. Pandis, I. Barnes, F. J. Dentener, M. C. Facchini, R. Van
1162 Dingenen, B. Ervens, A. Nenes, C. J. Nielsen, E. Swietlicki, J. P. Putaud, Y. Balkanski, S. Fuzzi,
1163 J. Horth, G. K. Moortgat, R. Winterhalter, C. E. L. Myhre, K. Tsigaridis, E. Vignati, E. G.
1164 Stephanou and J. Wilson (2005). "Organic aerosol and global climate modelling: a review."
1165 *Atmospheric Chemistry and Physics* **5**: 1053-1123.
1166 Kiendler-Scharr, A., A. A. Mensah, E. Friese, D. Topping, E. Nemitz, A. S. H. Prevot, M. Äijälä,
1167 J. Allan, F. Canonaco, M. Canagaratna, S. Carbone, M. Crippa, M. Dall'Osto, D. A. Day, P. De
1168 Carlo, C. F. Di Marco, H. Elbern, A. Eriksson, E. Freney, L. Hao, H. Herrmann, L. Hildebrandt,
1169 R. Hillamo, J. L. Jimenez, A. Laaksonen, G. McFiggans, C. Mohr, C. O'Dowd, R. Otjes, J.
1170 Ovadnevaite, S. N. Pandis, L. Poulain, P. Schlag, K. Sellegri, E. Swietlicki, P. Tiitta, A.
1171 Vermeulen, A. Wahner, D. Worsnop and H. C. Wu (2016). "Ubiquity of organic nitrates from
1172 nighttime chemistry in the European submicron aerosol." *Geophysical Research Letters* **43**(14):
1173 7735-7744.
1174 Kim, P. S., D. J. Jacob, J. A. Fisher, K. Travis, K. Yu, L. Zhu, R. M. Yantosca, M. P. Sulprizio, J.
1175 L. Jimenez, P. Campuzano-Jost, K. D. Froyd, J. Liao, J. W. Hair, M. A. Fenn, C. F. Butler, N. L.
1176 Wagner, T. D. Gordon, A. Welti, P. O. Wennberg, J. D. Crouse, J. M. St. Clair, A. P. Teng, D.
1177 B. Millet, J. P. Schwarz, M. Z. Markovic and A. E. Perring (2015). "Sources, seasonality, and
1178 trends of southeast US aerosol: an integrated analysis of surface, aircraft, and satellite
1179 observations with the GEOS-Chem chemical transport model." *Atmos. Chem. Phys.* **15**(18):
1180 10411-10433.
1181 Kleindienst, T. E., M. Lewandowski, J. H. Offenberg, M. Jaoui and E. O. Edney (2007). "Ozone-
1182 isoprene reaction: Re-examination of the formation of secondary organic aerosol." *Geophysical*
1183 *Research Letters* **34**(1): n/a-n/a.
1184 Krechmer, J. E., D. Pagonis, P. J. Ziemann and J. L. Jimenez (2016). "Quantification of Gas-
1185 Wall Partitioning in Teflon Environmental Chambers Using Rapid Bursts of Low-Volatility
1186 Oxidized Species Generated in Situ." *Environmental Science & Technology* **50**(11): 5757-5765.
1187 Kroll, J. H., N. L. Ng, S. M. Murphy, R. C. Flagan and J. H. Seinfeld (2006). "Secondary Organic
1188 Aerosol Formation from Isoprene Photooxidation." *Environmental Science & Technology* **40**(6):
1189 1869-1877.

1190 Kurtén, T., K. H. Møller, T. B. Nguyen, R. H. Schwantes, P. K. Misztal, L. Su, P. O. Wennberg,
1191 J. L. Fry and H. G. Kjaergaard (2017). "Alkoxy Radical Bond Scissions Explain the Anomalously
1192 Low Secondary Organic Aerosol and Organonitrate Yields From α -Pinene + NO₃." The Journal
1193 of Physical Chemistry Letters: 2826-2834.
1194 Lee, B. H., C. Mohr, F. D. Lopez-Hilfiker, A. Lutz, M. Hallquist, L. Lee, P. Romer, R. C. Cohen,
1195 S. Iyer, T. Kurtén, W. Hu, D. A. Day, P. Campuzano-Jost, J. L. Jimenez, L. Xu, N. L. Ng, H.
1196 Guo, R. J. Weber, R. J. Wild, S. S. Brown, A. Koss, J. de Gouw, K. Olson, A. H. Goldstein, R.
1197 Seco, S. Kim, K. McAvey, P. B. Shepson, T. Starn, K. Baumann, E. S. Edgerton, J. Liu, J. E.
1198 Shilling, D. O. Miller, W. Brune, S. Schobesberger, E. L. D'Ambro and J. A. Thornton (2016).
1199 "Highly functionalized organic nitrates in the southeast United States: Contribution to secondary
1200 organic aerosol and reactive nitrogen budgets." Proceedings of the National Academy of
1201 Sciences **113**(6): 1516-1521.
1202 Lelieveld, J., J. S. Evans, M. Fnais, D. Giannadaki and A. Pozzer (2015). "The contribution of
1203 outdoor air pollution sources to premature mortality on a global scale." Nature **525**(7569): 367-
1204 371.
1205 Lerner, B. M., J. B. Gilman, K. C. Aikin, E. L. Atlas, P. D. Goldan, M. Graus, R. Hendershot, G.
1206 A. Isaacman-VanWertz, A. Koss, W. C. Kuster, R. A. Lueb, R. J. McLaughlin, J. Peischl, D.
1207 Sueper, T. B. Ryerson, T. W. Tokarek, C. Warneke, B. Yuan and J. A. de Gouw (2017). "An
1208 improved, automated whole air sampler and gas chromatography mass spectrometry analysis
1209 system for volatile organic compounds in the atmosphere." Atmos. Meas. Tech. **10**(1): 291-313.
1210 Liu, J., E. L. D'Ambro, B. H. Lee, F. D. Lopez-Hilfiker, R. A. Zaveri, J. C. Rivera-Rios, F. N.
1211 Keutsch, S. Iyer, T. Kurten, Z. Zhang, A. Gold, J. D. Surratt, J. E. Shilling and J. A. Thornton
1212 (2016). "Efficient Isoprene Secondary Organic Aerosol Formation from a Non-IEPOX Pathway."
1213 Environmental Science & Technology **50**(18): 9872-9880.
1214 Marais, E. A., D. J. Jacob, J. L. Jimenez, P. Campuzano-Jost, D. A. Day, W. Hu, J. Krechmer,
1215 L. Zhu, P. S. Kim, C. C. Miller, J. A. Fisher, K. Travis, K. Yu, T. F. Hanisco, G. M. Wolfe, H. L.
1216 Arkinson, H. O. T. Pye, K. D. Froyd, J. Liao and V. F. McNeill (2016). "Aqueous-phase
1217 mechanism for secondary organic aerosol formation from isoprene: application to the southeast
1218 United States and co-benefit of SO₂ emission controls." Atmos. Chem. Phys. **16**(3): 1603-1618.
1219 Marcolli, C., M. R. Canagaratna, D. R. Worsnop, R. Bahreini, J. A. de Gouw, C. Warneke, P. D.
1220 Goldan, W. C. Kuster, E. J. Williams, B. M. Lerner, J. M. Roberts, J. F. Meagher, F. C.
1221 Fehsenfeld, M. Marchewka, S. B. Bertman and A. M. Middlebrook (2006). "Cluster Analysis of
1222 the Organic Peaks in Bulk Mass Spectra Obtained During the 2002 New England Air Quality
1223 Study with an Aerodyne Aerosol Mass Spectrometer." Atmos. Chem. Phys. **6**(12): 5649-5666.
1224 Matsunaga, A. and P. J. Ziemann (2010). "Gas-Wall Partitioning of Organic Compounds in a
1225 Teflon Film Chamber and Potential Effects on Reaction Product and Aerosol Yield
1226 Measurements." Aerosol Science and Technology **44**(10): 881-892.
1227 Middlebrook, A. M., R. Bahreini, J. L. Jimenez and M. R. Canagaratna (2012). "Evaluation of
1228 Composition-Dependent Collection Efficiencies for the Aerodyne Aerosol Mass Spectrometer
1229 using Field Data." Aerosol Science and Technology **46**(3): 258-271.
1230 Myhre, G., D. Shindell, F.-M. Bréon, W. Collins, J. Fuglestedt, J. Huang, D. Koch, J.-F.
1231 Lamarque, D. Lee, B. Mendoza, T. Nakajima, A. Robock, G. Stephens, T. Takemura and H.
1232 Zhang (2013). Anthropogenic And Natural Radiative Forcing, in Climate Change 2013: The
1233 Physical Science Basis. Contribution of Working Group I to the Fifth Assessment Report of the
1234 Intergovernmental Panel on Climate Change. T. F. Stocker, D. Qin, G.-K. Plattner et al. New
1235 York, NY, USA, Cambridge University Press: 659-740.
1236 NASA. (2018). "SEAC4RS data site." from DOI: 10.5067/Aircraft/SEAC4RS/Aerosol-TraceGas-
1237 Cloud.
1238 Ng, N. L., S. S. Brown, A. T. Archibald, E. Atlas, R. C. Cohen, J. N. Crowley, D. A. Day, N. M.
1239 Donahue, J. L. Fry, H. Fuchs, R. J. Griffin, M. I. Guzman, H. Herrmann, A. Hodzic, Y. Iinuma, J.
1240 L. Jimenez, A. Kiendler-Scharr, B. H. Lee, D. J. Luecken, J. Mao, R. McLaren, A. Mutzel, H. D.

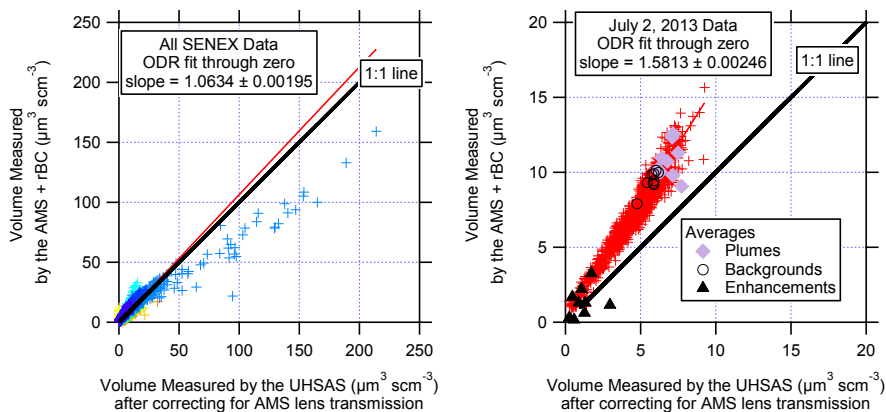
1241 Osthoff, B. Ouyang, B. Picquet-Varrault, U. Platt, H. O. T. Pye, Y. Rudich, R. H. Schwantes, M.
1242 Shiraiwa, J. Stutz, J. A. Thornton, A. Tilgner, B. J. Williams and R. A. Zaveri (2017). "Nitrate
1243 radicals and biogenic volatile organic compounds: oxidation, mechanisms, and organic aerosol."
1244 *Atmos. Chem. Phys.* **17**(3): 2103-2162.
1245 Ng, N. L., A. J. Kwan, J. D. Surratt, A. W. H. Chan, P. S. Chhabra, A. Sorooshian, H. O. T. Pye,
1246 J. D. Crouse, P. O. Wennberg, R. C. Flagan and J. H. Seinfeld (2008). "Secondary organic
1247 aerosol (SOA) formation from reaction of isoprene with nitrate radicals (NO₃)."
1248 *Atmos. Chem. Phys.* **8**: 4117-4140.
1249 Palm, B. B., P. Campuzano-Jost, D. A. Day, A. M. Ortega, J. L. Fry, S. S. Brown, K. J. Zarzana,
1250 W. Dube, N. L. Wagner, D. C. Draper, L. Kaser, W. Jud, T. Karl, A. Hansel, C. Gutiérrez-Montes
1251 and J. L. Jimenez (2017). "Secondary organic aerosol formation from in situ OH, O₃, and NO₃
1252 oxidation of ambient forest air in an oxidation flow reactor." *Atmos. Chem. Phys.* **17**(8): 5331-
1253 5354.
1254 Pankow, J. F. and W. E. Asher (2008). "SIMPOL.1: a simple group contribution method for
1255 predicting vapor pressures and enthalpies of vaporization of multifunctional organic
1256 compounds." *Atmospheric Chemistry and Physics* **8**(10): 2773-2796.
1257 Peischl, J., T. B. Ryerson, J. S. Holloway, D. D. Parrish, M. Trainer, G. J. Frost, K. C. Aikin, S.
1258 S. Brown, W. P. Dubé, H. Stark and F. C. Fehsenfeld (2010). "A top-down analysis of emissions
1259 from selected Texas power plants during TexAQS 2000 and 2006." *Journal of Geophysical*
1260 *Research: Atmospheres* **115**(D16): n/a-n/a.
1261 Pye, H., A. Chan, M. Barkley and J. Seinfeld (2010). "Global modeling of organic aerosol: the
1262 importance of reactive nitrogen (NO_x and NO₃)."
1263 *Atmospheric Chemistry and Physics* **10**(22): 11261-11276.
1264 Pye, H. O. T., D. J. Luecken, L. Xu, C. M. Boyd, N. L. Ng, K. R. Baker, B. R. Ayres, J. O. Bash,
1265 K. Baumann, W. P. L. Carter, E. Edgerton, J. L. Fry, W. T. Hutzell, D. B. Schwede and P. B.
1266 Shepson (2015). "Modeling the Current and Future Roles of Particulate Organic Nitrates in the
1267 Southeastern United States." *Environmental Science & Technology* **49**(24): 14195-14203.
1268 Rollins, A. W., E. C. Browne, K. E. Min, S. E. Pusede, P. J. Wooldridge, D. R. Gentner, A. H.
1269 Goldstein, S. Liu, D. A. Day, L. M. Russell and R. C. Cohen (2012). "Evidence for NO_x Control
1270 over Nighttime SOA Formation." *Science* **337**(6099): 1210.
1271 Rollins, A. W., A. Kiendler-Scharr, J. L. Fry, T. Brauers, S. S. Brown, H.-P. Dorn, W. P. Dube, H.
1272 Fuchs, A. Mensah, T. F. Mentel, F. Rohrer, R. Tillmann, R. Wegener, P. J. Wooldridge and R.
1273 C. Cohen (2009). "Isoprene oxidation by nitrate radical: alkyl nitrate and secondary organic
1274 aerosol yields." *Atmos. Chem. Phys.* **9**: 6685-6703.
1275 Romer, P. S., K. C. Duffey, P. J. Wooldridge, H. M. Allen, B. R. Ayres, S. S. Brown, W. H.
1276 Brune, J. D. Crouse, J. de Gouw, D. C. Draper, P. A. Feiner, J. L. Fry, A. H. Goldstein, A.
1277 Koss, P. K. Misztal, T. B. Nguyen, K. Olson, A. P. Teng, P. O. Wennberg, R. J. Wild, L. Zhang
1278 and R. C. Cohen (2016). "The lifetime of nitrogen oxides in an isoprene-dominated forest."
1279 *Atmos. Chem. Phys.* **16**(12): 7623-7637.
1280 Saha, P. K., A. Khlystov, K. Yahya, Y. Zhang, L. Xu, N. L. Ng and A. P. Grieshop (2017).
1281 "Quantifying the volatility of organic aerosol in the southeastern US." *Atmos. Chem. Phys.* **17**(1):
1282 501-520.
1283 Sato, K., A. Takami, T. Iozaki, T. Hikida, A. Shimono and T. Imamura (2010). "Mass
1284 spectrometric study of secondary organic aerosol formed from the photo-oxidation of aromatic
1285 hydrocarbons." *Atmospheric Environment* **44**(8): 1080-1087.
1286 Schwantes, R. H., A. P. Teng, T. B. Nguyen, M. M. Coggon, J. D. Crouse, J. M. St. Clair, X.
1287 Zhang, K. A. Schilling, J. H. Seinfeld and P. O. Wennberg (2015). "Isoprene NO₃ Oxidation
1288 Products from the RO₂ + HO₂ Pathway." *The Journal of Physical Chemistry A* **119**(40): 10158-
1289 10171.
1290 Spracklen, D. V., J. L. Jimenez, K. S. Carslaw, D. R. Worsnop, M. J. Evans, G. W. Mann, Q.
1291 Zhang, M. R. Canagaratna, J. Allan, H. Coe, G. McFiggans, A. Rap and P. Forster (2011).

1292 "Aerosol mass spectrometer constraint on the global secondary organic aerosol budget." Atmos.
1293 Chem. Phys. **11**(23): 12109-12136.
1294 Surratt, J. D., A. W. H. Chan, N. C. Eddingsaas, M. N. Chan, C. L. Loza, A. J. Kwan, S. P.
1295 Hersey, R. C. Flagan, P. O. Wennberg and J. H. Seinfeld (2010). "Reactive intermediates
1296 revealed in secondary organic aerosol formation from isoprene." Proceedings of the National
1297 Academy of Sciences **107**(15): 6640-6645.
1298 Takegawa, N., T. Miyakawa, K. Kawamura and Y. Kondo (2007). "Contribution of Selected
1299 Dicarboxylic and ω -Oxocarboxylic Acids in Ambient Aerosol to the m/z 44 Signal of an
1300 Aerodyne Aerosol Mass Spectrometer." Aerosol Science and Technology **41**(4): 418-437.
1301 Toon, O. B., H. Maring, J. Dibb, R. Ferrare, D. J. Jacob, E. J. Jensen, Z. J. Luo, G. G. Mace, L.
1302 L. Pan, L. Pfister, K. H. Rosenlof, J. Redemann, J. S. Reid, H. B. Singh, A. M. Thompson, R.
1303 Yokelson, P. Minnis, G. Chen, K. W. Jucks and A. Pszenny (2016). "Planning, implementation,
1304 and scientific goals of the Studies of Emissions and Atmospheric Composition, Clouds and
1305 Climate Coupling by Regional Surveys (SEAC4RS) field mission." Journal of Geophysical
1306 Research: Atmospheres **121**(9): 4967-5009.
1307 Warneke, C., M. Trainer, J. A. de Gouw, D. D. Parrish, D. W. Fahey, A. R. Ravishankara, A. M.
1308 Middlebrook, C. A. Brock, J. M. Roberts, S. S. Brown, J. A. Neuman, B. M. Lerner, D. Lack, D.
1309 Law, G. Hübler, I. Pollack, S. Sjostedt, T. B. Ryerson, J. B. Gilman, J. Liao, J. Holloway, J.
1310 Peischl, J. B. Nowak, K. C. Aikin, K. E. Min, R. A. Washenfelder, M. G. Graus, M. Richardson,
1311 M. Z. Markovic, N. L. Wagner, A. Welti, P. R. Veres, P. Edwards, J. P. Schwarz, T. Gordon, W.
1312 P. Dube, S. A. McKeen, J. Brioude, R. Ahmadov, A. Bougiatioti, J. J. Lin, A. Nenes, G. M.
1313 Wolfe, T. F. Hanisco, B. H. Lee, F. D. Lopez-Hilfiker, J. A. Thornton, F. N. Keutsch, J. Kaiser, J.
1314 Mao and C. D. Hatch (2016). "Instrumentation and measurement strategy for the NOAA SENEX
1315 aircraft campaign as part of the Southeast Atmosphere Study 2013." Atmos. Meas. Tech. **9**(7):
1316 3063-3093.
1317 Wilson, J. C., B. G. Lafleu, H. Hilbert, W. R. Seebaugh, J. Fox, D. W. Gesler, C. A. Brock, B. J.
1318 Huebert and J. Mullen (2004). "Function and Performance of a Low Turbulence Inlet for
1319 Sampling Supermicron Particles from Aircraft Platforms." Aerosol Science and Technology
1320 **38**(8): 790-802.
1321 Worton, D. R., J. D. Surratt, B. W. LaFranchi, A. W. H. Chan, Y. Zhao, R. J. Weber, J.-H. Park,
1322 J. B. Gilman, J. de Gouw, C. Park, G. Schade, M. Beaver, J. M. S. Clair, J. Crouse, P.
1323 Wennberg, G. M. Wolfe, S. Harrold, J. A. Thornton, D. K. Farmer, K. S. Docherty, M. J.
1324 Cubison, J.-L. Jimenez, A. A. Frossard, L. M. Russell, K. Kristensen, M. Glasius, J. Mao, X.
1325 Ren, W. Brune, E. C. Browne, S. E. Pusede, R. C. Cohen, J. H. Seinfeld and A. H. Goldstein
1326 (2013). "Observational Insights into Aerosol Formation from Isoprene." Environmental Science
1327 & Technology **47**(20): 11403-11413.
1328 Xie, Y., F. Paulot, W. P. L. Carter, C. G. Nolte, D. J. Luecken, W. T. Hutzell, P. O. Wennberg, R.
1329 C. Cohen and R. W. Pinder (2013). "Understanding the impact of recent advances in isoprene
1330 photooxidation on simulations of regional air quality." Atmos. Chem. Phys. **13**(16): 8439-8455.
1331 Xu, L., S. Suresh, H. Guo, R. J. Weber and N. L. Ng (2015). "Aerosol characterization over the
1332 southeastern United States using high-resolution aerosol mass spectrometry: spatial and
1333 seasonal variation of aerosol composition and sources with a focus on organic nitrates." Atmos.
1334 Chem. Phys. **15**(13): 7307-7336.
1335 Zhang, H., L. D. Yee, B. H. Lee, M. P. Curtis, D. R. Worton, G. Isaacman-VanWertz, J. H.
1336 Offenberg, M. Lewandowski, T. E. Kleindienst, M. R. Beaver, A. L. Holder, W. A. Lonneman, K.
1337 S. Docherty, M. Jaoui, H. O. T. Pye, W. Hu, D. A. Day, P. Campuzano-Jost, J. L. Jimenez, H.
1338 Guo, R. J. Weber, J. de Gouw, A. R. Koss, E. S. Edgerton, W. Brune, C. Mohr, F. D. Lopez-
1339 Hilfiker, A. Lutz, N. M. Kreisberg, S. R. Spielman, S. V. Hering, K. R. Wilson, J. A. Thornton and
1340 A. H. Goldstein (2018). "Monoterpenes are the largest source of summertime organic aerosol in
1341 the southeastern United States." Proceedings of the National Academy of Sciences **115**(9):
1342 2038.

1343 Zhang, Q., M. R. Alfarra, D. R. Worsnop, J. D. Allan, H. Coe, M. R. Canagaratna and J. L.
1344 Jimenez (2005). "Deconvolution and Quantification of Hydrocarbon-like and Oxygenated
1345 Organic Aerosols Based on Aerosol Mass Spectrometry." Environmental Science & Technology
1346 **39**(13): 4938-4952.
1347 Zhang, Q., J. L. Jimenez, M. R. Canagaratna, J. D. Allan, H. Coe, I. Ulbrich, M. R. Alfarra, A.
1348 Takami, A. M. Middlebrook, Y. L. Sun, K. Dzepina, E. Dunlea, K. Docherty, P. F. DeCarlo, D.
1349 Salcedo, T. Onasch, J. T. Jayne, T. Miyoshi, A. Shimono, S. Hatakeyama, N. Takegawa, Y.
1350 Kondo, J. Schneider, F. Drewnick, S. Borrmann, S. Weimer, K. Demerjian, P. Williams, K.
1351 Bower, R. Bahreini, L. Cottrell, R. J. Griffin, J. Rautiainen, J. Y. Sun, Y. M. Zhang and D. R.
1352 Worsnop (2007). "Ubiquity and dominance of oxygenated species in organic aerosols in
1353 anthropogenically-influenced Northern Hemisphere midlatitudes." Geophysical Research Letters
1354 **34**(13): L13801.
1355 Zhang, Q., C. O. Stanier, M. R. Canagaratna, J. T. Jayne, D. R. Worsnop, S. N. Pandis and J.
1356 L. Jimenez (2004). "Insights into the Chemistry of New Particle Formation and Growth Events in
1357 Pittsburgh Based on Aerosol Mass Spectrometry." Environmental Science & Technology **38**(18):
1358 4797-4809.
1359 Zheng, Y., N. Unger, A. Hodzic, L. Emmons, C. Knote, S. Tilmes, J. F. Lamarque and P. Yu
1360 (2015). "Limited effect of anthropogenic nitrogen oxides on secondary organic aerosol
1361 formation." Atmos. Chem. Phys. **15**(23): 13487-13506.
1362
1363
1364

1365 **Supplemental Information**

1366 In the main text, we noted a discrepancy between overall average aerosol volume estimates
1367 based on size measurements vs. AMS for the flight analyzed here (see Figure S1). We checked
1368 to see if this bias was also present in the individual plumes studied here by calculating the
1369 volume changes from the sizing instruments and the derived volume changes from the
1370 AMS+rBC mass. There is quite a bit of scatter in the volume enhancements, with most of the
1371 points falling along the same line as the data for this flight. It is unclear why the two types of
1372 volume measurements disagree more for this flight. Therefore, the bias in volume changes
1373 introduces additional uncertainty in the magnitude of the plume enhancements.
1374



1375 **Figure S1.** Aerosol volume measured using the total aerosol mass from the AMS plus refractory
1376 black carbon (rBC) and mass-weighted densities versus the aerosol volume measured by
1377 optical size with the UHSAS after correcting for AMS lens transmission. The procedure for
1378 calculating the mass-weighted density is described by [Bahreini et al. \(2009\)](#). On average, the
1379 measured aerosol volume from composition is roughly equal to the measured aerosol volume
1380 from size for the entire SENEX study (left hand panel) and is higher than one for the flight
1381 analyzed here (July 2, 2013, right hand panel).
1382
1383

1384 **Corrections for AMS UMR nitrate data and applicability to pRONO₂ estimation**

1385
1386 Nitrate in the AMS is quantified in unit mass resolution mode (UMR) as the sum of the estimated
1387 NO⁺ at *m/z* 30 and NO₂⁺ at *m/z* 46, with a correction factor to account for the smaller ions (N⁺
1388 and HNO₃⁺, mostly) produced from nitrate (Allan et al., 2004). The default AMS UMR
1389 quantification algorithm (documented in the AMS “fragmentation table”) estimates NO⁺ as the
1390 total signal at *m/z* 30 minus a small (2.2% of OA at *m/z* 29, “Org29” in AMS parlance)
1391 subtraction to account for organic interferences and an isotopic correction for naturally-occurring
1392 ¹⁵N₂ from nitrogen in air. The default UMR fragmentation table was developed for mixed ambient
1393 aerosols, in particular in urban studies, and it is the responsibility of each AMS user to correct it
1394 as needed for each study. In environments with high biogenic contributions to total OA, and/or
1395 low total nitrate concentrations, the contribution of the CH₂O⁺ ion can be much larger than the

Juliane Fry 5/26/2018 6:45 PM

Deleted: Bahreini

Juliane Fry 5/26/2018 6:46 PM

Deleted: [65]

1398 default subtraction at m/z 30. Similarly, the CH_2O_2^+ ion at m/z 46 becomes non-negligible, and
1399 hence nitrate reported from AMS data with UMR resolution will frequently be overestimated in
1400 these situations. The poor performance of the default AMS correction is likely due to the initial
1401 focus on urban OA with high nitrate fractions when deriving those corrections (Allan et al., 2004,
1402 Zhang et al., 2004).

1403
1404 Here we derive a set of corrections based on an aircraft high-resolution (HR) dataset acquired
1405 with the University of Colorado HR-AMS (Dunlea et al., 2009) on the NASA DC-8 during the
1406 SEAC⁴RS campaign (Toon et al., 2016). SEAC⁴RS took place with a strong emphasis on the
1407 SEUS 6 weeks after the SENEX flight analyzed in this manuscript. Based on an initial screening
1408 of the correlations of the CH_2O^+ and CH_2O_2^+ ions with UMR signals, 10 potential UMR m/z
1409 between m/z 29 and m/z 53 were selected as viable for deriving suitable corrections. Further
1410 analysis using three specific SEAC⁴RS flights (RF11 on 30 Aug 30th, 2013, RF16 on Sep 11th,
1411 2013 and RF18 on Sep 16th, 2013) that covered a wide range of OA composition with both
1412 strong biogenic contributions and fresh and aged biomass plumes showed that only four m/z
1413 (29, 42, 43 and 45) had good enough S/N and robust enough correlations to be used as
1414 corrections. Table S1 summarizes the correction coefficients obtained in this analysis, and
1415 Figure S2 shows the ability of matching the actual NO^+ and NO_2^+ signals (as obtained from
1416 high-resolution analysis of these flights) with the corrected UMR procedure. These corrections
1417 are applied as:

$$\begin{aligned} \text{UMR NO} &= \text{Signal}(m/z30) - a_i * \text{Signal}(\text{Variable}_i) \\ \text{UMR NO}_2 &= \text{Signal}(m/z 46) - b_i * \text{Signal}(\text{Variable}_i) \end{aligned}$$

1421
1422 with the coefficients a_i and b_i as reported in Table S1. It should be noted that in all cases the
1423 contributions of C^{18}O^+ to m/z 30 need to be subtracted first before applying the correction (which
1424 is constrained to the organic CO_2^+ signal, measured at m/z 44, by the naturally-occurring
1425 isotopic ratio and assuming that OA produces $\text{CO}^+ = \text{CO}_2^+$ (Zhang et al., 2005, Takegawa et al.,
1426 2007). Likewise, the contribution of $^{13}\text{CO}^+$ to Org29 needs to be subtracted first. It is hence very
1427 important for this analysis that the corrections to the AMS frag table to suitably estimate the
1428 contribution of gas phase CO_2^+ to total UMR m/z 44 as well as the baseline correction for m/z 29
1429 be properly applied first (Allan et al., 2004). Finally, also note that the corrections using m/z 29
1430 and 43 are rather based on Org29 and Org43, which are standard AMS products that take the
1431 OA relative ionization efficiency (RIE) into account.

1432
1433 For the SEAC⁴RS dataset, the corrections amounted to on average subtracting 55% from UMR
1434 m/z 30 and 33% from UMR m/z 46. Despite this large subtraction, the corrected data correlates
1435 very well with the HR AMS results, with less than 5% deviation in the regression slope between
1436 the two datasets.

1437
1438 Although all of the corrections in Table S1 were valid for the SEAC⁴RS data set, for the flight
1439 analyzed here we chose Org29 to correct m/z 30 and mz 45 correction to correct m/z 46
1440 because they were the closest organic signals to the UMR nitrate peaks with organic
1441 interferences and may be more valid for other field studies where different types of OA are

1442 sampled. After these UMR signals were corrected and the appropriate RIEs and CE were
1443 applied, the nitrate mass concentrations in the final data archive for the flight analyzed here
1444 were reduced by 0-0.24 $\mu\text{g sm}^{-3}$, averaging 0.11 $\mu\text{g sm}^{-3}$ or 32%. The corresponding increase in
1445 OA due to the organic interferences in the UMR nitrate had linear dependence on the reported
1446 OA mass concentrations ($r^2 = 0.89$) with a slope of 1.3%.

1447

1448 To estimate the fraction of nitrate that is organic nitrate (pRONO₂) the use of the NO₂⁺/NO⁺ ratio
1449 with an empirically determined pRONO₂ calibration ratio has been successfully used previously
1450 with HR-AMS data (Farmer et al., 2010, Fry et al., 2013, Ayres et al., 2015, Fisher et al., 2016,
1451 Lee et al., 2016, Day et al., 2017, Palm et al., 2017). Figure S2 summarizes how well the ratio of
1452 the corrected UMR *m/z* 30 and 46 signals correlate with the NO₂⁺ and NO⁺ (and ratios)
1453 determined using HR data. As expected, there is considerable scatter at very low nitrate
1454 concentrations (which is a considerable part of the dataset, as the time series shows, since the
1455 free troposphere was sampled extensively). However, for the predicted pRONO₂ (which is
1456 mass-weighted), most of this scatter disappears, and for concentrations above 0.1 $\mu\text{g sm}^{-3}$ of
1457 nitrate there is good agreement between the HR results and the UMR-corrected pRONO₂,
1458 regardless of the correction chosen. For lower concentrations the scatter is considerable larger,
1459 with the Org29 correction providing the best overall agreement. Based on the variability in this
1460 dataset for this correction (Org29), we estimate the uncertainty in pRONO₂ fraction
1461 apportionment using UMR to be about 30%, in addition to an estimated uncertainty for the
1462 apportionment method using HR of 20%. From the comparison of UMR-corrected total nitrate
1463 to HR nitrate (not shown), we estimate an additional error of 5% for total nitrate error using
1464 these corrections.

1465

1466 As mentioned in the main text, the empirically determined pRONO₂ calibration ratio used for the
1467 flight data analyzed here was the ratio of NO₂⁺/NO⁺ from the ammonium nitrate calibration
1468 aerosols divided by 2.8. This factor was determined as the average of several literature studies
1469 (Fry et al., 2009, Rollins et al., 2009, Farmer et al., 2010, Sato et al., 2010, Fry et al., 2011,
1470 Boyd et al., 2015) and applied according to the "ratio of ratios" method (Fry et al., 2013). The
1471 ammonium nitrate NO₂⁺/NO⁺ ratio was obtained from the two calibrations on 30 June and 7 July
1472 that bracketed the flight on 2 July, as described above. This ratio averaged 0.490. Hence, the
1473 organic nitrate NO₂⁺/NO⁺ ratio was estimated to be 0.175. The ratio of NO₂⁺/NO⁺ from the flight
1474 data was then used with the pRONO₂ and ammonium nitrate NO₂⁺/NO⁺ calibration ratios to
1475 estimate the fraction of the total corrected nitrate mass concentrations that was organic
1476 (pRONO₂) or inorganic (nitrate associated with ammonium or NH₄NO₃). Propagating the 30%
1477 UMR vs HR uncertainty and 20% apportionment (see above) error on top of the 34% AMS total
1478 nitrate measurement uncertainty results in $\pm 50\%$ uncertainties in the derived organic nitrate
1479 mass concentrations (and similar for NH₄NO₃; however it will depend on the relative
1480 contributions of pRONO₂ and NH₄NO₃ to total nitrate since the absolute concentration errors
1481 associated with pRONO₂ - NH₄NO₃ apportionment should be similar [64]).

1482

Juliane Fry 5/26/2018 9:58 PM

Deleted: (Day et al., 2017).

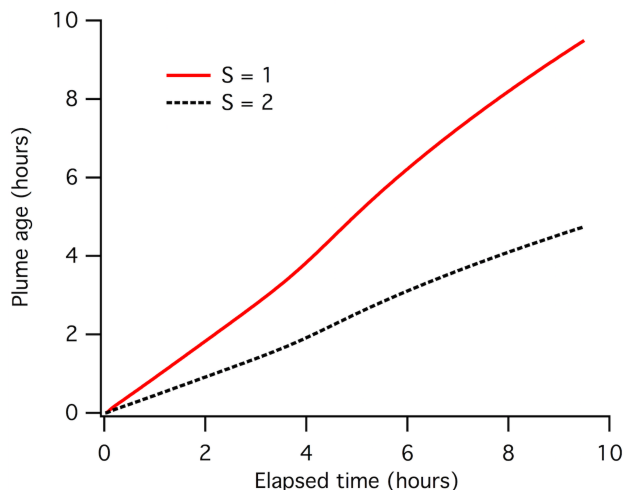
Juliane Fry 5/26/2018 10:16 PM

Formatted: Normal

Juliane Fry 5/26/2018 10:11 PM

Deleted: (Boyd et al., 2015)

1504



1505

1506

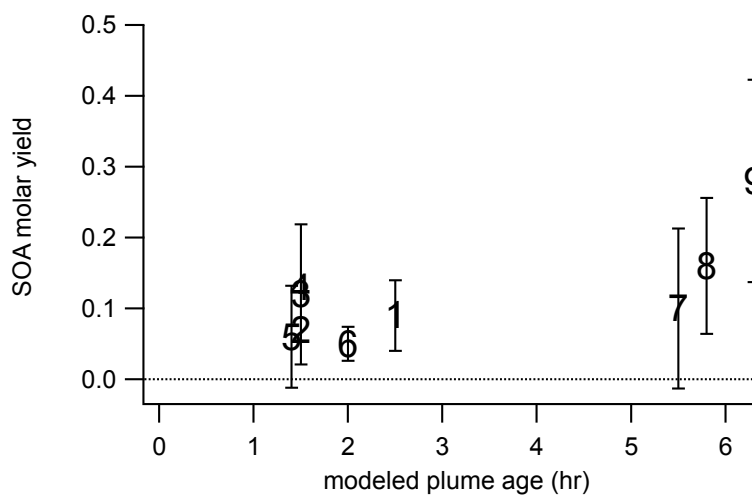
1507

1508

1509

1510

Figure S3. Calculated plume age vs. elapsed time in a box model run for a single representative night. Plume ages on the y-axis are calculated based on Equation 1 in the main text but using model NO_2 and O_3 data. Time since sunset on the x-axis is the model elapsed time (i.e., run time of the model during darkness).



1511

1512

1513

1514

1515

Figure S4. SOA molar yield is positively correlated with estimated plume age. This SOA molar yield is based on Eq. 3, with error bars determined by propagation of observed variability in pRONO_2 and isoprene, where multiple point averaging was possible. Markers correspond to

1516 plume numbers.). Based on the box model described in more detail below, the first-generation
1517 isoprene products peak at a approximately 4 hours plume age and then begin to decay.

1518

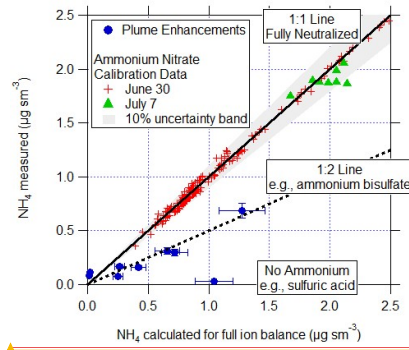
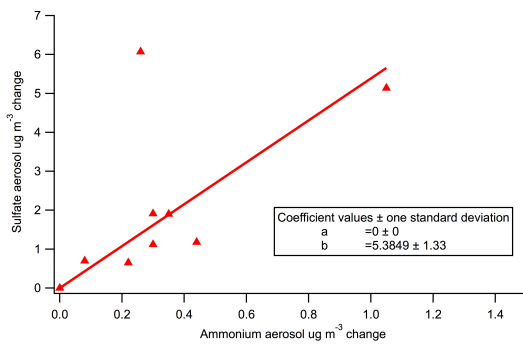
1519 **Table S2.** Peak ambient (wet) aerosol surface area during each plume used in the yield
1520 analysis (plume numbers 1 – 9), and for the two longer urban plumes transected at the end of
1521 the flight.

plume number	7/2/13 plume time (UTC)	Peak aerosol surface area ($\mu\text{m}^2 \text{cm}^{-3}$)
1	2:18	280
2	2:20	370
3	2:21	470
4	3:03	340
5	3:55	800
6	4:34	470
7	4:37	370
8	4:39	420
9	5:04	490
Urban plume	5:36	340
Urban plume	6:37	300

1522

1523

1524



Juliane Fry 6/1/2018 8:36 AM
Formatted: Normal1

Unknown
Formatted: Font:Font color: Blue

Juliane Fry 6/1/2018 8:36 AM
Formatted: Font:(Default) Arial, 11 pt, Font color: Black

1525
1526
1527
1528
1529
1530
1531
1532
1533
1534
1535
1536
1537
1538
1539
1540
1541

Figure S5. (a) In-plume change in sulfate mass concentration vs. change in ammonium aerosol mass concentration is generally well correlated, with a slope of 5.4. The masses of the cations and anions would give an ion balance for pure $(\text{NH}_4)_2\text{SO}_4$ of $\text{MW}(\text{SO}_4)/(\text{2 x MW}(\text{NH}_4)) = 2.7$, and for $(\text{NH}_4)\text{HSO}_4$ of $\text{MW}(\text{SO}_4)/(\text{MW}(\text{NH}_4)) = 5.4$. Hence, this slope provides support for a mix of these two ammonium sulfate salts, with sometimes exclusively $(\text{NH}_4)\text{HSO}_4$. This is consistent with incomplete neutralization of the sulfate mass by ammonium. The one clear outlier (sulfate increase of $6 \mu\text{g m}^{-3}$ for Plume #5) suggests excess sulfate, rendering ammonium or other inorganic nitrate formation even less likely. Points with ammonium aerosol below $0.1 \mu\text{g m}^{-3}$ are within the variability of that measurement; their omission does not change the slope. (b) Measured vs. calculated (ion balanced) NH_4 for calibration data and plume enhancements. This also shows that plumes are acidic than ammonium sulfate, ruling out the possibility of inorganic nitrate formation.

Juliane Fry 6/1/2018 8:34 AM
Formatted: Subscript

1542 **Additional AMS and auxiliary data from plumes**

1543

1544 **Table S3.** Additional information for the list of plumes used in this NO₃ + isoprene SOA yield
 1545 analysis, for which key yield-related data is presented in Table 1. For each plume, the delta-
 1546 values listed indicate the difference between in-plume and outside-plume background in
 1547 average observed concentration. After each plume number, the numbers of points averaged for
 1548 isoprene and AMS, respectively, are listed. Plume numbers annotated with * indicate brief
 1549 plumes for which only single-point measurements of in-plume aerosol composition were
 1550 possible. Also shown are the plume changes in isoprene used in the present analysis (Δ_{isop} ,
 1551 the difference between in-plume and background isoprene concentration, reproduced from
 1552 Table 1), alongside for comparison the Δ_{isop} determined as the difference between in-plume
 1553 isoprene and the modeled sunset (initial) concentration of isoprene present at that location
 1554 outside of the plume, determined using an iterative box model (Edwards et al., 2017). The
 1555 similarity between these two values for most points suggests that the isoprene just outside of
 1556 each plume transect was largely unperturbed from the sunset initial value.

plume number [#isop/#AMS]	7/2/13 plume time (UTC)	$\Delta_{ORG,aero}$ ($\mu\text{g m}^{-3}$)	$\Delta_{NH_4,aero}$ ($\mu\text{g m}^{-3}$)	$\Delta_{SO_4,aero}$ ($\mu\text{g m}^{-3}$)	Temp (C)	%RH	Δ_{isop} (pptv)	Δ_{isop} from model (pptv)
Typical variability ($\mu\text{g m}^{-3}$):		0.75	0.1	0.5				
1 [2/3]	2:18	0.35	0	0	23.6	66.5	-335	-327
2 [*]	2:20	0.89	0.3	1.91	23.6	65	-404	-453
3 [4/5]	2:21	1.25	1.05	5.14	23.6	65.2	-228	-337
4 [*]	3:03	0.16	0.08	0.7	21.2	68.1	-453	-391
5 [3/4]	3:55	0.32	0.26	6.07	21.9	65.5	-255	-376
6 [2/2]	4:34	0.57	0.3	1.12	19.9	74.6	-713	-233
7 [5/6]	4:37	1.05	0.22	0.65	19.7	76.2	-298	-221
8 [2/3]	4:39	1.26	0.44	1.18	18.3	82.2	-443	-353
9 [7/8]	5:04	1.45	0.35	1.9	17.2	84.8	-293	-434

1557

1558

1559

1560 **Box model calculations**

Juliane Fry 6/1/2018 8:26 AM
Formatted ... [10]

Juliane Fry 5/26/2018 8:10 PM
Formatted ... [11]

Juliane Fry 5/26/2018 8:10 PM
Formatted ... [12]

Juliane Fry 5/26/2018 8:10 PM
Formatted ... [13]

Juliane Fry 6/1/2018 8:25 AM
Formatted ... [14]

Juliane Fry 6/1/2018 8:25 AM
Formatted ... [15]

Juliane Fry 6/1/2018 8:26 AM
Formatted ... [16]

Juliane Fry 5/26/2018 6:54 PM
Formatted Table ... [17]

Juliane Fry 5/26/2018 8:07 PM
Formatted ... [19]

Juliane Fry 5/26/2018 7:59 PM
Formatted ... [18]

Juliane Fry 5/26/2018 8:07 PM
Formatted ... [21]

Juliane Fry 5/26/2018 7:59 PM
Formatted ... [20]

Juliane Fry 5/26/2018 8:07 PM
Formatted ... [23]

Juliane Fry 5/26/2018 7:59 PM
Formatted ... [22]

Juliane Fry 5/26/2018 8:07 PM
Formatted ... [25]

Juliane Fry 5/26/2018 7:59 PM
Formatted ... [24]

Juliane Fry 5/26/2018 8:07 PM
Formatted ... [27]

Juliane Fry 5/26/2018 7:59 PM
Formatted ... [26]

Juliane Fry 5/26/2018 8:07 PM
Formatted ... [29]

Juliane Fry 5/26/2018 7:59 PM
Formatted ... [28]

Juliane Fry 5/26/2018 8:07 PM
Formatted ... [31]

Juliane Fry 5/26/2018 7:59 PM
Formatted ... [30]

Juliane Fry 5/26/2018 8:07 PM
Formatted ... [33]

Juliane Fry 5/26/2018 7:59 PM
Formatted ... [32]

Juliane Fry 5/26/2018 8:07 PM
Formatted ... [35]

Juliane Fry 5/26/2018 7:59 PM
Formatted ... [34]

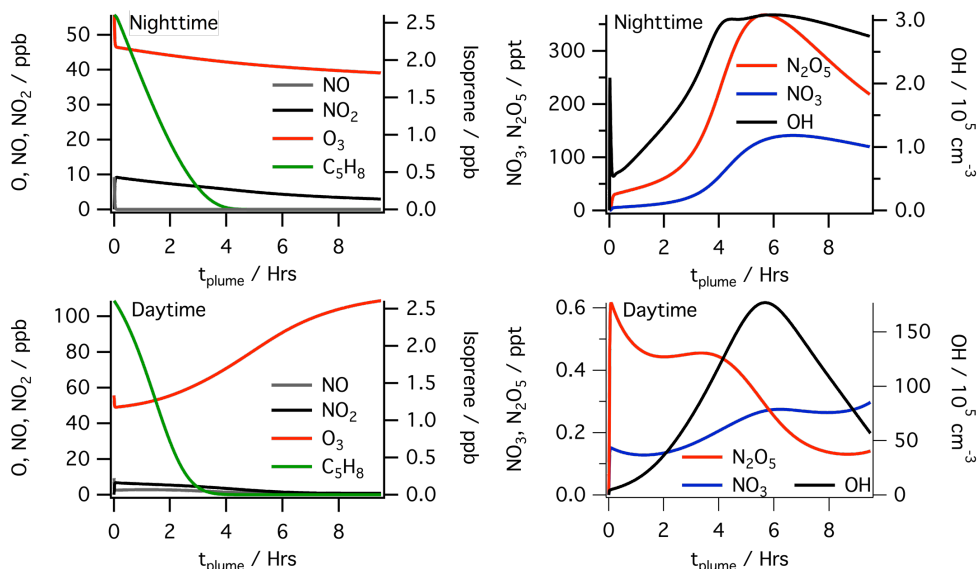
1561 Box model simulations were performed using the Dynamically Simple Model of Atmospheric
 1562 Chemical Complexity (DSMACC, http://wiki.seas.harvard.edu/geos-chem/index.php/DSMACC_chemical_box_model), containing the Master Chemical Mechanism
 1563 v3.3.1 chemistry scheme (<http://mcm.leeds.ac.uk/MCM/>). The model approach is similar to that
 1564 described in detail in Edwards et al. 2017, and the accompanying supplement, with the model
 1565 run over a 9.5 hour night to simulate the nocturnal residual layer. For the nocturnal simulation
 1566 used in this work (for both the plume lifetime calculation and the peroxy radical lifetime analysis
 1567 in Sect. 4.3) the model was initialized with concentrations of the constraining species
 1568 representative of the SENEX observations (Table S4). As the model is simulating power plant
 1569 plume evolution from point of emission, a starting NO mixing ratio of 10 ppb was used to
 1570 constrain NO_x, and the chemistry scheme was subsequently allowed to partition the reactive
 1571 nitrogen. The top panels in Figure S7 show the evolution of key species during this nocturnal
 1572 simulation.
 1573

1574 **Table S4:** Species constrained (MCM v3.3.1 names) during model simulations and constraining
 1575 values. Constraint column indicates if species concentrations were held at the constrained value
 1576 throughout the simulation (Fixed) or allowed to vary after initialization (Initial).

Species	Mixing ratio	Units	Constraint
NO	9.28	ppb	Initial
O3	55.72	ppb	Initial
CO	134.00	ppb	Fixed
CH4	1920.00	ppb	Fixed
C5H8	2606.80	ppt	Initial
APINENE	38.87	ppt	Initial
BPINENE	195.50	ppt	Initial
LIMONENE	12.42	ppt	Initial
MACR	454.13	ppt	Initial
MVK	1006.00	ppt	Initial
IC4H10	47.00	ppt	Fixed
NC4H10	128.00	ppt	Fixed
C2H6	1199.00	ppt	Fixed
C2H4	117.00	ppt	Fixed
C2H2	145.00	ppt	Fixed
NC6H14	20.00	ppt	Fixed
IC5H12	120.00	ppt	Fixed
NC5H12	76.00	ppt	Fixed
C3H8	344.00	ppt	Fixed
C3H6	26.00	ppt	Fixed
CH3COCH3	2556.00	ppt	Fixed
BENZENE	35.90	ppt	Fixed
C2H5OH	2239.00	ppt	Fixed
MEK	309.00	ppt	Fixed
CH3OH	5560.00	ppt	Fixed

1577 The daytime simulation used for comparison in Sect. 4.3 of the main manuscript (lower panels
 1578 of Figure S7) uses the same initialization as the nocturnal simulation; with the only difference
 1579 being the model is run during the daytime. Photolysis rates are calculated using TUV
 1580 (<https://www2.acom.ucar.edu/modeling/tropospheric-ultraviolet-and-visible-tuv-radiation-model>).
 1581 The daytime simulation does not accurately simulate daytime mixing ratios of species such as
 1582 O₃ representative of SENEX observations. However, the intent of this simulation is to compare
 1583 model daytime peroxy radical fate and lifetime with the nocturnal simulation. The presence of

1584 intense convective mixing in the daytime planetary boundary layer of the Southeast US makes
1585 accurately modeling these concentrations difficult with a zero dimensional model.
1586



1587
1588 **Fig. S6.** Model calculated NO, NO₂, O₃, and isoprene (left) and NO₃, N₂O₅ and OH (right for the
1589 nocturnal (top) and daytime (bottom) simulations shown in Sect. 4.3.

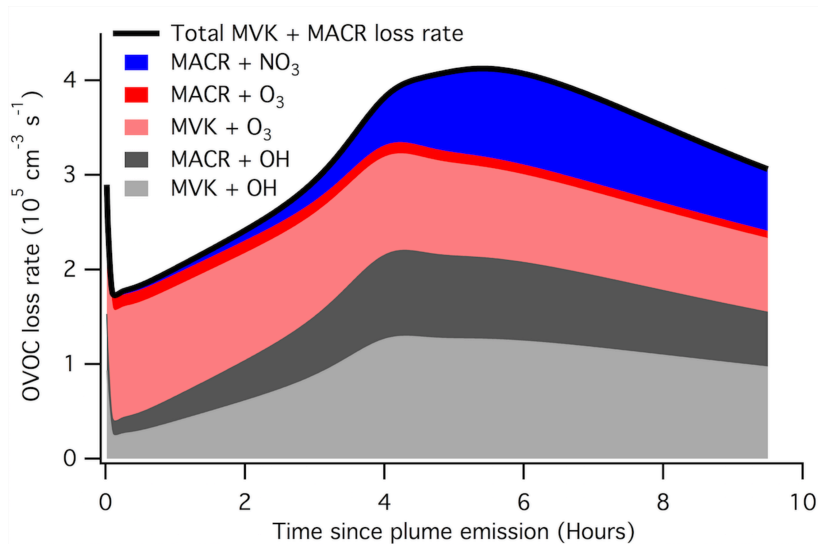
1590

1591 **Additional considerations investigated via RO₂ fate box modeling**

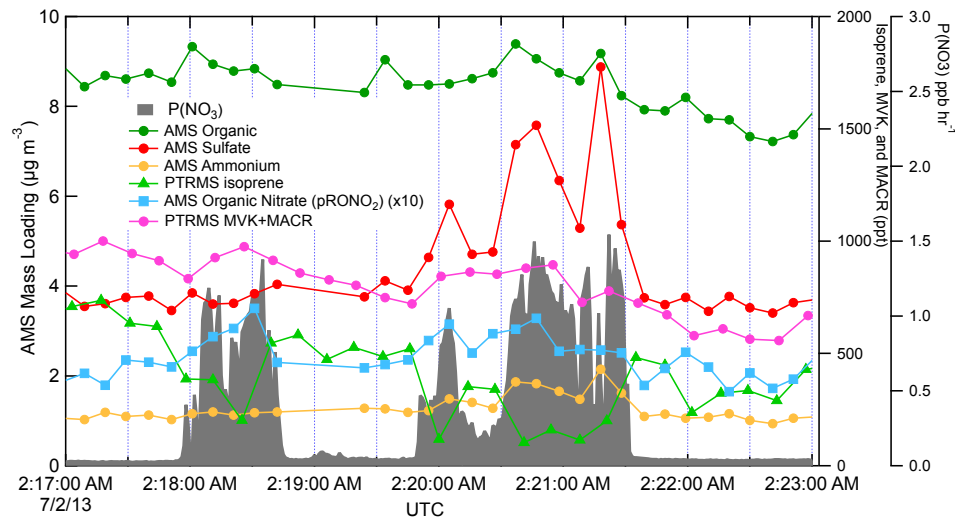
1592

1593 Based on the potentially larger than previously estimated contribution of RO₂+RO₂ reactions at
1594 night, we considered a related possible source of a high bias in the determined SOA yields. If
1595 NO₃ reaction with the major daytime isoprene oxidation products MVK and/or MACR produces
1596 RO₂ radicals that can cross-react with NO₃ + isoprene products to produce condensable
1597 products, this would be a mechanism of recruiting isoprene-derived organic mass into the
1598 aerosol, but that original isoprene oxidation would not be counted in the denominator of the yield
1599 calculation, since its interaction with NO₃ began as MACR or MVK. In the box model, substantial
1600 MVK and MACR are available in the plume at nighttime, but only MACR reacts with NO₃, and a
1601 maximum fraction of one-quarter of MVK+MACR losses go to reaction with NO₃ overnight (see
1602 Figure S8). In addition, in our power plant plume observations, MVK+MACR are not observed to
1603 be appreciably depleted by the large NO₃ injection, further suggesting that this chemistry is not
1604 a substantial additional source of SOA (see Figure S9).

1605



1606
 1607 **Figure S7.** Calculated (via MCM) loss rate contributions for the daytime isoprene products
 1608 methyl vinyl ketone (MVK) and methacrolein (MACR) in the simulated nighttime plume used in
 1609 the text. Only MACR reacts with NO_3 , and the contribution of this process to total losses (green
 1610 stack) is relatively minor.



1611
 1612 **Figure S8.** MVK and MACR are not titrated on the timescale of these yield estimates in power
 1613 plant plumes.
 1614

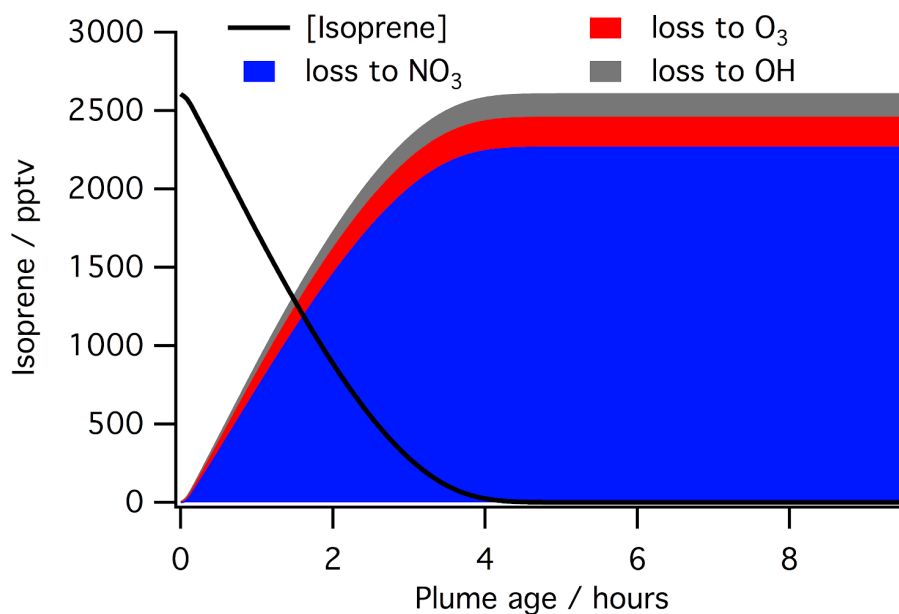


Figure S9. Model simulation of typical in-plume consumption of isoprene (black line), and stacked plot showing the contributions to this from the NO₃, O₃, and OH. Modeled plume was emitted at sunset, so this represents nocturnal processing under power plant plume conditions.

Unknown
Formatted: Font:

Juliane Fry 6/1/2018 8:30 AM
Formatted: Font color: Auto

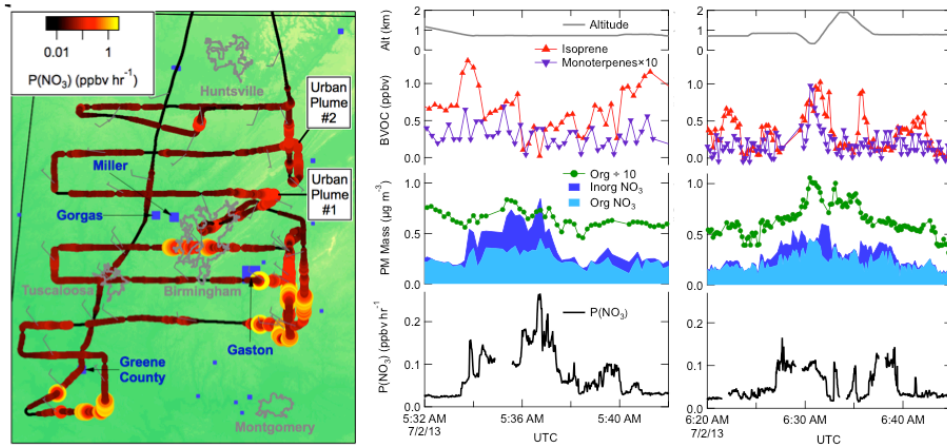
1615
1616
1617
1618
1619
1620

Two urban plume case studies

1621
1622
1623
1624
1625
1626
1627
1628
1629
1630
1631
1632
1633
1634
1635
1636
1637
1638

In addition to the nine power plant plumes analyzed above to determine the NO₃ + isoprene SOA molar yield, towards the end of the July 2 flight, the Birmingham urban plume was intercepted twice (around 5:36 am and 6:37 am UTC, Fig. 8). These downwind urban plumes are among the most aged plumes (estimated at 5.2 and 5.8 hours, respectively), but are also substantially more diffuse than the narrow power plant plume intercepts and have lower peak $P(\text{NO}_3)$. Nevertheless, we note that these two plumes contain periods of apparent anti-correlation of isoprene and organic nitrate aerosol time series and high apparent SOA molar yields (23%, 19%) and mass yields (62%, 51%), if calculated by the same method as above and omitting the period of vertical profiling in the second plume. Potentially complicating these urban SOA yield determinations is the fact that the inorganic fraction of nitrate was much larger than in the power plant plumes (see Fig. 8). The background isoprene is also somewhat lower in these urban plumes, potentially shifting the NO₃/N₂O₅ fate to reactions other than NO₃ + isoprene (see Fig. S4 in Edwards et al. (Edwards et al., 2017)). The aerosol surface area is not noticeably higher in these urban plumes, which one might expect to lead to a larger contribution of N₂O₅ uptake and hydrolysis. In the more complex mix of gases characteristic of an urban plume, we hesitate to attribute these apparent yields exclusively to the NO₃ + isoprene reaction.

1639



1640

1641

1642

1643

1644

1645

1646

1647

Figure S10. Flight map and time series of two urban plume intercepts, showing anticorrelation of organic nitrate and isoprene. These more diffuse plumes, with lower $P(\text{NO}_3)$ and larger inorganic nitrate contribution, make yield determination more uncertain, so we do not include them in the overall yield determination. However, using the same methodology as for the power plant plumes would give similarly high yields for these very aged plumes.